SH
11
A2
F53
FISH

U.S. Department
of Commerce

Volume 122
Number 3
July 2024

Fishery Bulletin

U.S. Department of Commerce

Gina M. Raimondo
Secretary

National Oceanic and Atmospheric Administration

Richard W. Spinrad
Administrator

National Marine Fisheries Service

Janet Coit
Assistant Administrator
for Fisheries

Fishery Bulletin

Scientific Editor
José I. Castro
National Marine Fisheries Service, NOAA
263 13th Avenue South
Saint Petersburg, Florida 33701

Managing Editor
Kathryn Dennis
Scientific Publications Office
National Marine Fisheries Service, NOAA
1845 Wasp Boulevard, Building 176
Honolulu, Hawaii 96818

Associate Editor
Cara Mayo
Scientific Publications Office
National Marine Fisheries Service, NOAA
7600 Sand Point Way NE
Seattle, Washington 98115-0070

Editorial Board

Henry L. Bart Jr.	Tulane University, New Orleans, Louisiana
Katherine E. Bemis	National Systematics Laboratory, Washington, DC
Matthew D. Campbell	National Marine Fisheries Service, Pascagoula, Mississippi
William B. Driggers III	National Marine Fisheries Service, Pascagoula, Mississippi
Gretchen L. Grammer	South Australian Research and Development Institute, Adelaide, Australia
Eric R. Hoffmayer	National Marine Fisheries Service, Pascagoula, Mississippi
Richard Langton	National Marine Fisheries Service, Walpole, Maine (retired)
J. Fernando Márquez-Farías	Universidad Autónoma de Sinaloa, Mazatlán, México
Richard S. McBride	National Marine Fisheries Service, Woods Hole, Massachusetts
Richard L. Merrick	National Marine Fisheries Service, Falmouth, Massachusetts (retired)
Richard D. Methot	National Marine Fisheries Service, Seattle, Washington
Lisa J. Natanson	National Marine Fisheries Service, Narragansett, Rhode Island (retired)
Mark S. Peterson	University of Southern Mississippi, Ocean Springs, Mississippi
André E. Punt	University of Washington, Seattle, Washington
Joseph M. Quattro	University of South Carolina, Columbia, South Carolina
John F. Walter III	National Marine Fisheries Service, Miami, Florida

Fishery Bulletin website: https://spo.nmfs.noaa.gov/fb.htm

Fishery Bulletin (ISSN 0090-0656) is published quarterly by the Scientific Publications Office, National Marine Fisheries Service, NOAA, 7600 Sand Point Way NE, Seattle, WA 98115-0070.

Although the contents of this publication have not been copyrighted and may be reprinted entirely, reference to source is appreciated.

The Secretary of Commerce has determined that the publication of this periodical is necessary according to law for the transaction of public business of this Department. Use of funds for printing of this periodical has been approved by the Director of the Office of Management and Budget.

For Sale by the Superintendent of Documents, U.S. Government Publishing Office, Washington, DC 20401. Subscription price per year: $32.00 domestic and $44.80 foreign. Cost per single issue: $19.00 domestic and $26.60 foreign. **See back for order form.**

Fishery Bulletin carries original research reports on investigations in fishery science, engineering, and economics. It began as the Bulletin of the United States Fish Commission in 1881; it became the Bulletin of the Bureau of Fisheries in 1904 and the *Fishery Bulletin* of the U.S. Fish and Wildlife Service in 1941. Separates were issued as documents through volume 46; the last document was no. 1103. Beginning with volume 47 in 1931 and continuing through volume 62 in 1963, each separate appeared as a numbered bulletin. A new system began in 1963, with volume 63, in which papers are bound together in a single issue. Beginning with volume 70, number 1, January 1972, *Fishery Bulletin* became a periodical, issued quarterly. In this form, it is available by subscription from the Superintendent of Documents, U.S. Government Publishing Office, Washington, DC 20401. It is also available free in limited numbers to libraries, research institutions, and state and federal agencies and in exchange for other scientific publications.

U.S. Department of Commerce
Seattle, Washington

Volume 122
Number 3
July 2024

Fishery Bulletin

Contents

Articles

63–75 Kojiro Hara, Keisuke Furumitsu, and Atsuko Yamaguchi
Age, growth parameters, and reproductive characteristics of the sharpspine skate (*Okamejei acutispina*) in the East China Sea

76–88 Gregg R. Poulakis, Jennifer T. Wyffels, P. Eric Fortman, Andrew K. Wooley, Lukas B. Heath, Dylan M. Yakich, and Patrick W. Wilson
Morphology, composition, and deterioration of the embryonic rostral sheath of the smalltooth sawfish (*Pristis pectinata*)

89–118 Yana Yu. Bolshakova and Artem M. Prokofiev
An identification guide to the larvae of lanternfishes (Teleostei: Myctophidae) from the Subtropical Convergence: subfamilies Lampanyctinae and Notolychninae

119–128 Kaila Fritch, Grant Waltz, Melissa Monk, Ellie Brauer, Zachary Kucinski, Chandler Skinner-Horne, and Dean Wendt
Collecting age and length data from recovered carcasses of filleted rockfish: a new data source for examination of life history characteristics

129–132 Guidelines for authors

The National Marine Fisheries Service (NMFS) does not approve, recommend, or endorse any proprietary product or proprietary material mentioned in this publication. No reference shall be made to NMFS, or to this publication furnished by NMFS, in any advertising or sales promotion that would indicate or imply that NMFS approves, recommends, or endorses any proprietary product or proprietary material mentioned herein or that has as its purpose an intent to cause directly or indirectly the advertised product to be used or purchased because of this NMFS publication.

The NMFS Scientific Publications Office is not responsible for the contents of the articles.

SMITHSONIAN
OCT 02 2024
LIBRARIES

National Marine Fisheries Service
NOAA

Fishery Bulletin
established in 1881

Spencer F. Baird
First U.S. Commissioner
of Fisheries and founder
of *Fishery Bulletin*

Age, growth parameters, and reproductive characteristics of the sharpspine skate (*Okamejei acutispina*) in the East China Sea

Kojiro Hara
Keisuke Furumitsu
Atsuko Yamaguchi (contact author)

Email address for contact author: y-atsuko@nagasaki-u.ac.jp

Laboratory of Marine Zoology
Graduate School of Fisheries and Environmental Sciences
Nagasaki University
1-14 Bunkyo-machi
Nagasaki 852-8521, Japan

Abstract—The sharpspine skate (*Okamejei acutispina*) is a commercially exploited skate species in the East China Sea, and it is suspected that the population of this species in this region has declined due to fishing pressure and other factors. Nonetheless, information on its life history, which is essential for population assessment and management, is limited. We estimated its age, growth, maturity, and egg-laying season on the basis of data for 331 specimens captured in the East China Sea. Age was determined by counting translucent bands on vertebral centrum sections. Maximum total length (TL) and age were 448 mm and 10 years for females and 444 mm and 9 years for males. Among the 3 growth models applied to length-at-age data, the von Bertalanffy growth function provided the best fit for both sexes (females: theoretical asymptotic length [L_∞]=428 mm, growth coefficient [k]=0.30, and theoretical time a zero length [t_0]=−1.04 years; males: L_∞=422 mm, k=0.31, and t_0=−1.04 years). Size and age at 50% maturity were 380 mm TL and 4.60 years for females and 357 mm TL and 4.21 years for males. The monthly seasonal reproductive data, including egg case occurrence and oocyte maximum diameter, indicate a prolonged egg-laying season. Our findings indicate that the life history of the sharpspine skate in the East China Sea is characterized by a shorter lifespan, faster growth, and earlier age at maturity than many other skates globally.

The sharpspine skate (*Okamejei acutispina*), a small skate belonging to the family Rajidae, inhabits sandy-muddy bottoms at depths of 20–175 m in the Northwest Pacific Ocean, from the waters of Japan south of the Niigata and Wakayama Prefectures to the East China Sea and waters of Taiwan (Yamada et al., 2007; Hatooka et al., 2013; Last et al., 2016).

In the East China Sea, located in both temperate and subtropical zones and bounded by China, South Korea, and Japan, the sharpspine skate is a predominant skate species, along with the polkadot skate (*Dipturus chinensis*), and is mainly found on the continental shelf edge (26–33°N) (Yamada et al., 2007; Hara et al., 2016). Data from a bottom-trawl survey conducted on the continental shelf of the central (approximately 126°30′E, 29°30′N) and northern (127°30′–128°00′E, 31°00′–32°30′N) East China Sea reveal that all skate specimens collected in the central waters were identified as sharpspine skate and that, in the northern waters, the sharpspine skate was the second-most collected skate species after the polkadot skate, accounting for 23% and 14% of all specimens by number and weight, respectively (Hara et al., 2016).

Skate species (Rajiformes) are captured (either as a targeted species or as bycatch) by commercial bottom trawlers of the countries that surround the East China Sea, in the sea and in adjacent waters, for human consumption (Baeck et al., 2011; Hara et al., 2014; Rigby et al., 2021). Commercial bottom trawlers from Japan directly target skates, and captured animals are then primarily processed into dried skate wings. Smaller skate species are generally of less economic value than larger ones; however, in this region, small-to-medium-sized skate species (up to 350–700 mm in total length [TL]), which are suitable for processing into dried skate wings, have considerable economic value and are targeted by bottom trawlers that operate from Japan (Hara et al., 2014). Consequently, in the East China Sea, the sharpspine skate is one of the main skate species targeted by bottom trawlers of Japan, in addition to the polkadot skate (Hara et al., 2014), and in other areas of the distribution of this species, the sharpspine skate is landed as a bycatch species (Rigby et al., 2021).

The continuous overexploitation by surrounding countries in the East China Sea over the past several decades

Manuscript submitted 12 January 2024.
Manuscript accepted 16 April 2024.
Fish. Bull. 122:63–75 (2024).
Online publication date: 9 May 2024.
doi: 10.7755/FB.122.3.1

The views and opinions expressed or implied in this article are those of the author (or authors) and do not necessarily reflect the position of the National Marine Fisheries Service, NOAA.

has led to a notable decline in the abundance of many demersal fish species (Yamada et al., 2007; Yamamoto and Nagasawa, 2015). Species-level catch data for skates have not been reported in Japan; however, for a reported category called *skates and rays*, annual landings by commercial bottom trawlers of Japan in the East China Sea have declined. In particular, there was a marked decline that began in the mid-1980s, from 3207 metric tons (t) in 1985 to 133 t in 2006 (data for 1993–2006 available at website; data for the full period from the 1980s to 2006 available in printed reports, MAFF[1]). Unfortunately, landings in subsequent years are unknown because, since 2007, catches of skates and rays have been included in the aggregated *other fish* category in government statistics. Although the decrease from the 1980s to 2006 in the annual catch of skates and rays appears to be consistent with the decreasing number of bottom trawlers from Japan operating in the region, results from an experimental trawl survey indicate a decline in skate populations, including those of the sharpspine skate (Yamada et al., 2007). Hence, the Ministry of the Environment, Japan, categorized the sharpspine skate as *near threatened* in 2017 (MEJ, 2017). Furthermore, in the IUCN Red List (Rigby et al., 2021), it is listed as *vulnerable*, on the basis of an estimated population reduction of 30–49% over the past 31 years due to fishing pressure.

Despite concerns about declining populations in the East China Sea, information on the life history of the sharpspine skate is extremely limited. Furthermore, published studies on its biology and ecology are scarce, even more than those on the polkadot skate, about which our recent studies have been published (Hara et al., 2018a, 2018b). In a previous study (Joung et al., 2011), the age and growth parameters of the sharpspine skate in the coastal waters of Taiwan, the southern limit of its range, were estimated; however, young of the year were not included in the estimation. Moreover, no published study has provided a detailed description of the overall life history characteristics of this species. To address this knowledge gap, we investigated, using specimens collected from the East China Sea, off southwestern Japan, the life history characteristics of the sharpspine skate, information about which is critical for accurate assessment of population status and conservation (Cailliet and Goldman, 2004). Specifically, we determined the age, growth parameters, and reproductive characteristics of the sharpspine skate, including its size and age at sexual maturity and egg-laying season.

Materials and methods

Sample collection and measurements

A total of 331 sharpspine skate (161 females and 170 males) were captured from April 2009 through November 2022 at depths of approximately 100–200 m in the central and northern East China Sea, off southwestern Japan (approximately between 27°30′N, 125°50′E and 32°20′N, 128°00′E). Skates were caught with bottom-trawl nets deployed from the commercial fishing vessels of the Yamada Suisan Co. Ltd.[2] (Nagasaki City, Japan) and the training ship of Nagasaki University (Hara et al., 2016, 2018a, 2018b). The TL (to the nearest 1 mm), disc width (DW, to the nearest 1 mm), body weight (BW, to the nearest 0.01 g), and sex of each individual were recorded in the laboratory. Although TL is a commonly used metric for measuring body size in skate life history studies, DW was used as a metric of size in a previous study on the age and growth of the sharpspine skate (Joung et al., 2011). Therefore, in our latest study that we describe herein, we employed DW as a metric, in addition to TL, for the purpose of comparison with size data from Joung et al. (2011).

A chi-square test was conducted to test whether the sex ratio was significantly different from 1:1. The relationship between TL and BW was calculated by using KyPlot, vers. 6.0 (KyensLab Inc., Tokyo, Japan). Analysis of covariance (ANCOVA), also done with KyPlot, was used to test for differences between the sexes in the relationship between TL and BW (both $\log_{10}$-transformed). Clasper length (to the nearest 0.01 mm), the distance from the posterior part of the cloaca to the tip of the clasper; oviducal gland width (to the nearest 0.01 mm); and the weights of the testes and ovaries (to the nearest 0.01 g) were recorded. Maturity stages were assigned on the basis of the scale of Hara et al. (2018a). The maximum diameter of oocytes (to the nearest 0.01 mm) in mature females was measured, and the presence or absence of egg cases in oviducts was recorded.

Age determination and growth estimation

For age determination, approximately 10 large vertebrae were extracted from the posterior portion of the abdominal cavity of specimen and immersed in 70% ethanol for 1–2 weeks. Each vertebral centrum was sectioned, following the procedure described by Hara et al. (2018a), with whetstones (#400–3000; Kai Corp. and Kai Industries Co. Ltd., Tokyo, Japan) (Fig. 1). The vertebral sections were air-dried for approximately 12 h, immersed in 100% ethanol, examined under a dissecting microscope by using reflected light (20× magnification), and then photographed by using a Nikon DS-Fi1 camera (Nikon Instruments Inc., Tokyo, Japan) attached to the microscope.

Age was determined by counting the translucent bands on the corpus calcareum (each band pair comprises a broad opaque band and a narrow translucent band). In this study, only fully completed translucent bands were counted as growth bands, and the translucent zones that were in the process of forming at the vertebral margins

---

[1] MAFF (Ministry of Agriculture, Forestry and Fisheries). 1980–2006. Annual statistics on fishery and aquaculture production. [In Japanese.] [Available from Prod. Mark. Consum. Stat. Div., MAFF. 1-2-1 Kasumigaseki, Chiyoda-ku, Tokyo 100-8950, Japan.]

[2] Mention of trade names or commercial companies is for identification purposes only and does not imply endorsement by the National Marine Fisheries Service, NOAA.

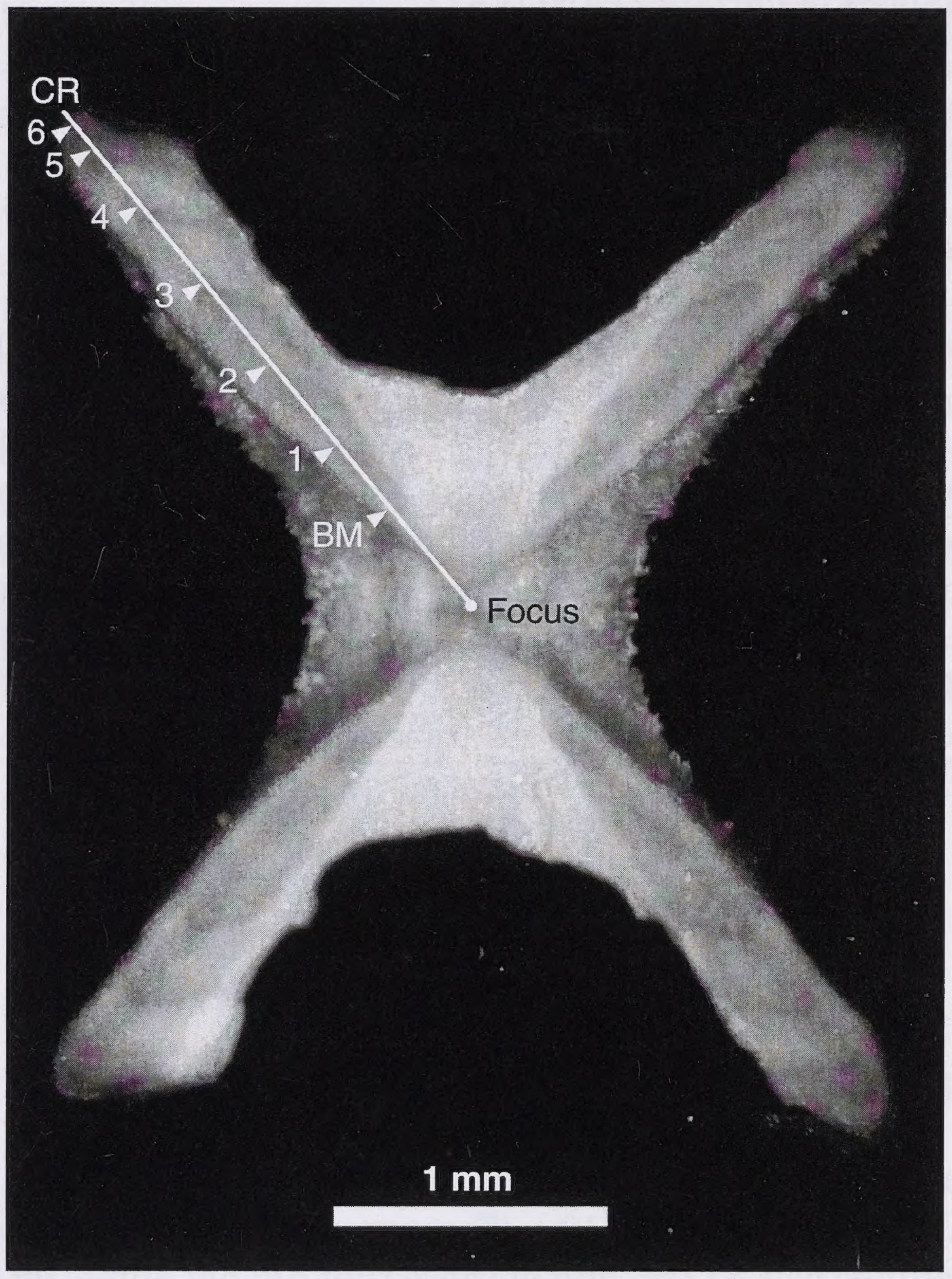

Figure 1

Photograph of the vertebral section from a female sharpspine skate (*Okamejei acutispina*) captured in the northern East China Sea on 20 August 2012. Arrows indicate the translucent bands (1–6). The estimated age of this specimen is 6 years, and its measured total length was 395 mm. CR=centrum radius; BM=birthmark.

(translucent margin) were not included in the age counts. Additionally, for each vertebral centrum, the first distinct band corresponding to a change of angle in the corpus calcareum was considered the birthmark and was not included in age determination (Sulikowski et al., 2007). Bands were counted twice by the same reader, without prior knowledge of specimen TL or sex. In cases for which the first and second counts differed, a third count was conducted. When the third count was consistent with either of the previous 2 counts, it was accepted; otherwise, the specimen was discarded. The reproducibility of the band count (age estimates) was evaluated by using average percentage error (APE) and Chang's coefficient of variation (CV) (Beamish and Fournier, 1981; Chang, 1982).

Centrum radius (CR) was measured from the focus to the distal margin. Distances from the focus to the translucent bands were measured at points along the margin of the corpus calcareum. Measured values of TL and DW were plotted against CR values, and an ANCOVA was performed on the $\log_{10}$-transformed data set to test for significant differences between sexes in the relationship between CR and TL and between CR and DW. The allometric function derived using the nonlinear least-squares procedure in KyPlot was used to describe the relationships between CR and TL and between CR and DW:

$$TL \text{ or } DW = uCR^{v}, \tag{1}$$

where u and v = constants.

To evaluate the periodicity of translucent band formation, marginal increment ratio (MIR) and edge analyses were performed. The MIR was calculated according to Hara et al. (2018a) as follows:

$$MIR = (CR - r_i) / (r_i - r_{i-1}), \tag{2}$$

where r_i = the radius of the last complete translucent band; and
r_{i-1} = the radius of the next-to-last complete translucent band.

Mean MIR was plotted against month, and the Kruskal–Wallis test (performed with KyPlot) was used to identify significant differences among months. Edge analysis was done on each vertebral section by determining whether the outer edge was translucent or opaque. The percentage of vertebrae with opaque or translucent margins was calculated monthly for all thin sections (Kume et al., 2008). Differences among months in the percentage of vertebrae with translucent margins were assessed by using Fisher's exact test (Fisher, 1922).

Back-calculation analysis was performed by using the body proportional hypothesis, a nonlinear method described by Francis (1990), because the samples lacked neonate individuals. For each individual, the TL and DW when the nth transparent band was formed (L_n) were back-calculated as follows:

$$L_n = (r_n / CR_c)^{v} L_c, \tag{3}$$

where r_n = the radius of the nth transparent band;
CR_c = the centrum radius at capture;
L_c = the specimen TL or DW at capture; and
v = a constant of the allometric CR–TL or CR–DW relationship.

To analyze the growth pattern, von Bertalanffy, Gompertz, and logistic growth models were fitted to back-calculated length-at-age data for each sex by using KyPlot, in which a quasi-Newton method is employed for nonlinear least-squares parameter estimation. Mature females with egg cases were observed throughout the sampling period, indicating a prolonged egg-laying season. Furthermore, the duration of embryonic development in the egg case is poorly known for this species. Therefore, we did not assign a theoretical birth date when estimating growth parameters of sharpspine skate to avoid the potential introduction of error and further uncertainty.

The von Bertalanffy, Gompertz, and logistic growth models were fitted by using Equations 4–6, respectively:

$$L_t = L_\infty(1 - \exp[-k(t - t_0)]); \tag{4}$$

$$L_t = L_\infty \exp(-\exp[-k(t - I)]); \text{ and} \tag{5}$$

$$L_t = \frac{L_\infty}{1+\exp\left(-k\left[t-I\right]\right)}, \tag{6}$$

where L_t = the calculated TL or DW at age t (in years);
L_∞ = the theoretical asymptotic length;
k = the growth coefficient;
t_0 = the theoretical time at zero length; and
I = the age at the curve's inflection point.

The goodness of fit of these 3 growth models was compared by using Akaike's information criterion (AIC) (Akaike, 1974). For the best-fit model, a likelihood-ratio test (Kimura, 1980) was performed to determine whether there was a significant difference in growth between sexes.

The maximum observed age based on vertebral-centrum analysis serves as an initial estimate of longevity, although this value may be underestimated if the population has been commercially exploited (Sulikowski et al., 2007). Therefore, theoretical longevity was estimated on the basis of the age at which 95% of L_∞ was reached, by using the growth coefficients from the von Bertalanffy, Gompertz, and logistic growth models in the following equation (Ricker, 1979):

$$5 \times \ln(2) \times k^{-1}. \tag{7}$$

Size and age at sexual maturity

Size at 50% maturity was estimated for each sex separately, by fitting a logistic model to both the maturity and length data through nonlinear least-squares parameter estimation in KyPlot (Furumitsu et al., 2019). The following logistic model was used:

$$Y = (1 + \exp[a + bX])^{-1}, \tag{7}$$

where Y = the proportion of mature individuals in each 10-mm size interval;
X = the TL (in millimeters); and
a and b = the empirical parameters.

Size at 50% maturity was calculated as $-ba^{-1}$. Age at 50% maturity was estimated directly for each sex from the age and maturity data of all aged individuals by using these methods.

Egg-laying season

The gonadosomatic index (GSI) for each mature individual was calculated by using the following formula:

$$GSI = \frac{Testis\ or\ ovary\ weight}{BW} \times 100. \tag{8}$$

To assess the reproductive cycle, monthly variation in mean GSI values was examined for each sex. The egg-laying season was estimated by examining the monthly variation in mean maximum diameter of oocytes and in the frequency of females with egg cases. Differences among months in the percentage of mature females with egg cases in their oviducts were assessed by using Fisher's exact test. Monthly differences in GSI values and in mean oocyte maximum diameter were tested by using one-way analysis of variance (ANOVA).

Results

Morphological measurements

Females (sample size [n]=161) ranged in size from 158 to 448 mm TL and from 115 to 319 mm DW, and males (n=170) ranged from 167 to 444 mm TL and from 134 to 295 mm DW. The distribution of total lengths of females and males is provided in Table 1. The overall sex ratio was not significantly different from 1:1 (chi-square test: χ^2=0.25, P>0.05). The relationship between TL and BW differed significantly between sexes (ANCOVA: F=30.5, P<0.001); therefore, this relationship was estimated separately for each sex as follows:

$$\text{Females: } BW = 6.06 \times 10^{-6} TL^{3.03} \text{ (coefficient of determination } [r^2]=0.93\text{); and} \tag{9}$$

$$\text{Males: } BW = 2.23 \times 10^{-5} TL^{2.79}\ (r^2=0.93). \tag{10}$$

Age determination and growth estimation

The vertebrae from all 331 specimens were readable (APE=1.88%, CV=2.61%). The agreement between the 2 readings was 81.0%, and of those that did not agree, 95.2% differed by one band. Neither the relationship between CR and TL (ANCOVA: F=2.76, P>0.05) nor that between CR and DW (ANCOVA: F=1.65, P>0.05) was significantly different between the sexes. Therefore, the relationships were described for the pooled sexes as follows:

$$TL = 227CR^{0.67}\ (r^2=0.94)\text{; and} \tag{11}$$

$$DW = 160CR^{0.66}\ (r^2=0.92). \tag{12}$$

The strong correlations between CR and TL and between CR and DW indicate that centrum growth was proportional to body growth.

Table 1

Length distribution for female (sample size [n]=161) and male (n=170) sharpspine skates (*Okamejei acutispina*) sampled from the East China Sea between April 2009 and September 2022.

Total length class (mm)	*n*		
	Females	Males	Total
151–200	5	3	8
201–250	5	8	13
251–300	16	19	35
301–350	15	26	41
351–400	60	86	146
401–450	60	28	88
Total	161	170	331

The mean MIR differed significantly between months, with a distinct seasonal trend (Kruskal–Wallis test: χ^2=78.1, P<0.001). Specifically, the mean MIR value was highest in May and lowest in October (Fig. 2A). Edge analysis revealed that between March and August translucent margins appeared on the vertebral centra examined in this study, with the highest percentage of vertebrae with these margins observed in May (Fig. 2B); there was a significant difference in the frequency of translucent margins in different months (Fisher's exact test: P<0.001). Although no samples were available for July and for the period between December and February, a clear annual band formation pattern emerged, with translucent bands assumed to form once a year (i.e., from spring through summer).

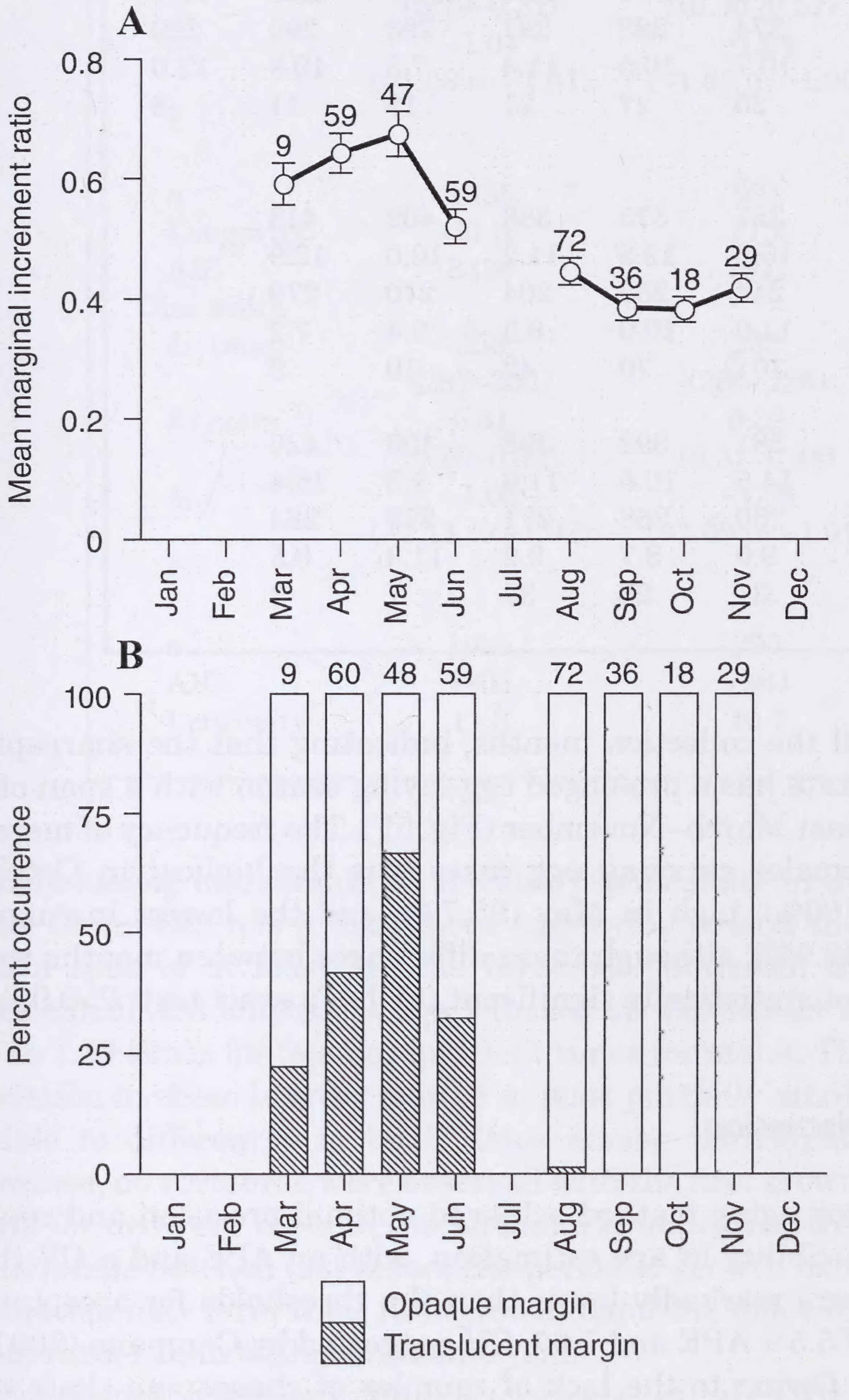

Figure 2

Monthly changes in (**A**) mean marginal increment ratio and (**B**) percent occurrence of opaque and translucent margins in the vertebral centra of sharpspine skates (*Okamejei acutispina*) sampled between April 2009 and November 2022 in the East China Sea. The error bars in panel A indicate standard errors of the mean. Numbers above circles and bars in panels A and B indicate sample sizes.

The mean back-calculated and observed lengths for each age class are presented in Table 2. For both sexes, the mean back-calculated lengths were close to the mean observed lengths at age for the class with ages ≥1 year. Meanwhile, the back-calculated lengths at birth (at age 0) were 45–67 mm smaller in TL and 33–54 mm smaller in DW than the observed lengths of young-of-the-year individuals; these size differences are attributed to the absence of neonates in our sample. The length at birth (based on TL) obtained through back-calculation analysis was 95–132 mm (mean: 113 mm) for females and 93–131 mm (mean: 114 mm) for males, values that are close to the previously reported TL of approximately 110 mm (Last et al., 2016). The back-calculated length (based on TL) at formation of the first growth band was 171–233 mm (mean: 201 mm) for females and 162–233 mm (mean: 202 mm) for males; Lee's phenomenon (Ricker, 1975) was not evident.

The growth parameters of the von Bertalanffy, Gompertz, and logistic growth models estimated from back-calculated length-at-age data are presented in Table 3. Among these growth models, the von Bertalanffy growth function had the lowest AIC for both sexes and was chosen as the best-fit model, regardless of whether TL or DW was used as the size metric (Table 3). The likelihood-ratio test revealed that there were significant differences in growth patterns between the sexes, when either TL (χ^2=13.2, df=3, P<0.01) or DW (χ^2=253.2, df=3, P<0.001) was used as the size metric. Results from likelihood-ratio tests for each parameter indicate significant differences between the sexes for all parameters, regardless of whether TL (L_∞: χ^2=7.1, df=1, P<0.01; k: χ^2=10.3, df=1, P<0.01; and t_0: χ^2=13.0, df=1, P<0.001) or DW (L_∞: χ^2=112.3, df=1, P<0.001; k: χ^2=241.5, df=1, P<0.001; and t_0: χ^2=252.7, df=1, P<0.001) was used as the size metric.

The von Bertalanffy growth function revealed that both sexes reached >80% of L_∞ at 5 years of age (Fig. 3). The observed maximum age was 10 years (TL: 402–448 mm; DW: 280–319 mm) for females and 9 years (TL: 412–444 mm; DW: 262–295 mm) for males. The theoretical longevity predicted by using the von Bertalanffy growth function was 11.5 years for females and 11.2 years for males, based on TL, and it was 11.3 years for females and 10.7 years for males, based on DW, estimates that are slightly higher than the maximum observed age. In contrast, the predictions of theoretical longevity from the Gompertz and logistic growth models were markedly lower than the maximum observed age for both sexes (Table 3).

Size and age at sexual maturity

Oviducal gland width increased abruptly when TL was approximately 320 mm, a pattern consistent with the observations of premature females, and oviducal gland growth slowed after sexual maturity (Fig. 4A). Clasper length increased abruptly in males with TLs >330 mm and slowed after sexual maturity (Fig. 4B).

The smallest sexually mature female and male were 366 and 355 mm TL, respectively. All females with TLs >389 mm and males with TLs >390 mm were mature. Size

Table 2

Mean back-calculated and observed total length (in millimeters) and disc width (in millimeters) at each age for female and male sharpspine skates (*Okamejei acutispina*) captured from April 2009 through November 2022 in the East China Sea. SD=standard deviation; *n*=sample size.

	Age (years)										
Sex and size measurement	0	1	2	3	4	5	6	7	8	9	10
Female											
Back-calculated											
Total length	113	201	256	298	332	358	377	391	398	408	420
SD	6.1	12.7	14.0	15.0	15.9	16.8	17.0	15.9	13.4	12.0	11.9
Disc width	82	144	182	212	235	254	267	275	282	286	295
SD	4.7	9.4	10.8	11.8	12.3	13.4	13.1	11.8	10.6	10.6	10.8
n	161	160	152	136	124	100	80	53	32	19	8
Observed											
Total length	158	202	270	327	362	386	398	412	410	414	426
SD		14.4	14.5	19.3	14.6	11.5	14.1	11.4	13.9	12.8	13.7
Disc width	115	143	190	232	255	274	283	287	293	290	299
SD		9.5	10.8	17.9	12.3	10.7	10.5	11.4	7.3	10.8	12.0
n	1	8	16	12	24	20	27	21	13	11	8
Male											
Back-calculated											
Total length	114	202	257	298	332	357	375	388	402	418	
SD	5.9	11.5	13.3	14.3	15.6	15.3	12.8	11.2	10.0	12.9	
Disc width	80	141	178	205	227	244	255	264	270	279	
SD	4.2	8.2	9.5	10.2	11.2	11.0	10.0	9.3	9.4	7.2	
n	170	169	161	144	125	101	70	42	10	3	
Observed											
Total length	181	219	269	317	354	381	392	398	406	426	
SD		28.1	17.0	17.2	16.4	14.5	10.6	11.6	9.3	16.4	
Disc width	134	155	190	221	244	260	268	271	273	284	
SD		20.6	13.2	12.1	11.0	9.0	8.7	9.2	11.3	9.5	
n	1	8	17	19	24	31	28	32	7	3	

at 50% sexual maturity was 380 mm TL for females and 357 mm TL for males (Fig. 4C).

The youngest mature individuals of both sexes were 4 years old. For both sexes, all individuals with assigned ages of 6 years or older were sexually mature. The age at 50% sexual maturity was 4.60 years for females and 4.21 years for males (Fig. 4D).

Egg-laying season

Mature females and males appeared in all months sampled (Fig. 5, A and B). There were no significant differences in GSI values among months for either females (one-way ANOVA: *F*=1.26, *P*>0.05) or males (one-way ANOVA: *F*=1.80, *P*>0.05) (Fig. 5, C and D). Maximum diameter of oocytes was not significantly different among months (one-way ANOVA: *F*=1.37, *P*>0.05), and all the mature females had yellow vitellogenic oocytes ≥15 mm in diameter (Fig. 5E).

Of the 98 mature females, 54 skates (55.1%) were carrying egg cases in their oviducts. Of these females, 33 individuals had an egg case in both the right and left oviducts, and 21 individuals had an egg case in only one of the oviducts. Mature females with egg cases were observed in all the collection months, indicating that the sharpspine skate has a prolonged egg-laying season with a span of at least March–November (Fig. 5F). The frequency of mature females carrying egg cases was the highest in October (100%), high in May (85.7%), and the lowest in August (42.9%), although these differences between months were not statistically significant (Fisher's exact test: *P*>0.05).

Discussion

Our aging method achieved optimal precision and reproducibility in age estimation, with an APE and a CV that were markedly lower than the thresholds for acceptance of 5.5% APE and 7.6% CV suggested by Campana (2001).

Owing to the lack of samples of sharpspine skate collected in July and in the period December–February, we were unable to fully validate the annual band formation of sharpspine skate in the East China Sea. However, the clear periodicity of translucent band formation detected through both the MIR and edge analyses indicates that a single translucent band is likely to form annually between spring and summer. Hence, the time required from hatching to the formation of the first growth band may vary

Table 3

Comparison of estimated growth parameters and goodness of fit for the von Bertalanffy, Gompertz, and logistic growth models fitted to back-calculated length-at-age data for female and male sharpspine skates (*Okamejei acutispina*) sampled from April 2009 through November 2022 in the East China Sea. The parameters are theoretical asymptotic length (L_∞), with length in total length or disc width; growth coefficient (k); theoretical time at zero length (t_0); and age at the curve inflection point (I). The 95% confidence intervals for parameter estimates are provided in parentheses. Theoretical longevity was estimated as the age at which 95% of L_∞ was reached: $5\times\ln(2)\times k^{-1}$. Akaike's information criterion (AIC) values were used to compare the goodness of fit of the 3 growth models. The sample sizes (n) for back-calculated length-at-age data are also provided.

	von Bertalanffy		Gompertz		Logistic	
Parameter	Females	Males	Females	Males	Females	Males
Total length						
L_∞ (mm)	428	422	405	396	394	383
	(423–432)	(418–427)	(402–408)	(392–399)	(391–397)	(380–386)
k (years^{-1})	0.30	0.31	0.47	0.50	0.65	0.69
	(0.29–0.31)	(0.30–0.32)	(0.46–0.49)	(0.49–0.51)	(0.63–0.67)	(0.68–0.71)
t_0	−1.04	−1.04				
	(−1.08 to −1.01)	(−1.07 to −1.00)				
I			0.40	0.35	1.15	1.04
			(0.37–0.43)	(0.32–0.37)	(1.11–1.18)	(1.01–1.07)
n	1025	995	1025	995	1025	995
Longevity	11.5	11.2	7.3	6.9	5.3	5.0
AIC	8336	7911	8501	8087	8713	8299
Disc width						
L_∞ (mm)	300	283	285	267	278	259
	(297–303)	(280–286)	(283–287)	(265–270)	(275–280)	(257–261)
k (years^{-1})	0.31	0.32	0.48	0.51	0.65	0.70
	(0.30–0.32)	(0.31–0.34)	(0.46–0.49)	(0.50–0.53)	(0.63–0.67)	(0.68–0.72)
t_0	−1.06	−1.05				
	(−1.11 to −1.02)	(−1.09 to −1.01)				
I			0.35	0.27	1.09	0.95
			(0.32–0.38)	(0.25–0.30)	(1.06–1.13)	(0.92–0.98)
n	1025	995	1025	995	1025	995
AIC	7801	7264	7930	7409	8104	7593
Longevity	11.3	10.7	7.3	6.8	5.3	5.0

widely among individuals, as the sharpspine skate in the East China Sea has a continuous egg-laying season that has a span of at least March–November. Moreover, the back-calculated lengths at age 1 (based on TL) varied by up to 1.39 times for females and 1.41 times for males. The variation in these lengths may be at least partially attributable to differences in birth dates among individuals. However, no vertebrae were observed with the first growth band formed very close to the birthmark, indicating that individuals hatched just before the period of growth band formation may form their first growth band the following year, rather than within the same year.

Consistent with our findings, Joung et al. (2011) reported that, for sharpspine skate from the coastal waters of Taiwan, translucent margins were most frequently observed in May. Therefore, the results of both studies indicate a similar timing for formation of translucent bands for this species in both the East China Sea and Taiwan. Similarly, Yamaguchi et al. (1998) found that, for the star-spotted smooth-hound (*Mustelus manazo*), the timing of band formation did not differ among 5 geographically distant areas in Japan and Taiwan; they proposed that growth band formation may not be caused by reproduction and water temperature but may be influenced by factors other than a change in location.

The von Bertalanffy growth function has traditionally been used in modeling fish growth, including for elasmobranch species (Cailliet et al., 2006). However, the results of an increasing number of studies indicate that the Gompertz or logistic growth models provide better fits for length-at-age data than the von Bertalanffy growth function, especially for skates and rays (Jacobsen and Bennett, 2011; Porcu et al., 2020; Bellodi et al., 2021). Joung et al. (2011) showed that the logistic growth model is the best fit for describing the growth patterns of sharpspine skate in Taiwan. In our study, however, on the basis of AIC values, the von Bertalanffy growth function provided the best fit for describing the growth pattern of sharpspine skate in the East China Sea. For both sexes, the von Bertalanffy growth function predicted an L_∞ that approximates the observed maximum length, whereas the predictions of the Gompertz and logistic growth models were much smaller.

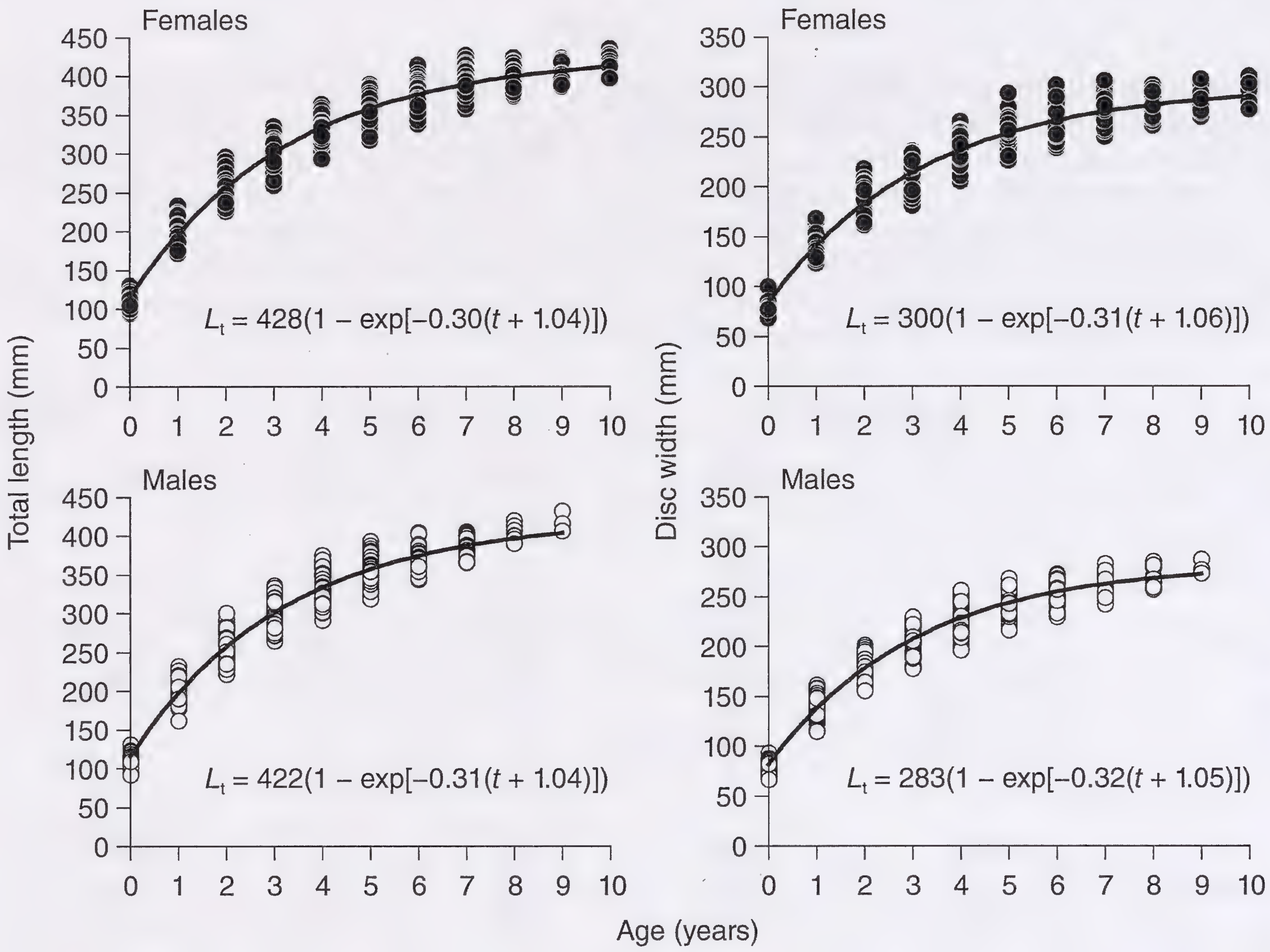

Figure 3

von Bertalanffy growth curves fitted to back-calculated length-at-age data for female and male sharpspine skates (*Okamejei acutispina*). Data used in the growth model are back-calculated total lengths and disc widths from specimens captured from April 2009 through November 2022 in the East China Sea. The equation for calculated length at age t (L_t) is given under each curve.

Additionally, the theoretical longevity derived from the k values estimated with the Gompertz and logistic growth models was much less than the observed maximum age for females and males, and therefore, was not biologically realistic. In summary, the von Bertalanffy growth function provided the most biologically reasonable parameter estimates for both sexes.

Goodness of fit for growth models can be influenced by several factors, including data quality, sample size, and dispersion of data across size classes (Cailliet et al., 2006). The logistic growth model may provide a better fit than the von Bertalanffy growth function if the length distribution is skewed toward larger sizes (Bellodi et al., 2022). Although the samples both in our study presented herein and in that by Joung et al. (2011) were biased toward larger (or older) individuals, our use of back-calculation effectively increased the number of length-at-age data points for younger (smaller) individuals for the growth models. This increase in data points for younger individuals might have contributed to the discrepancy in the best-fit model between this study and that of Joung et al. (2011). The use of back-calculation in our study may also have contributed to the description of the biologically reasonable growth pattern of the sharpspine skate, given that the length at age 0 from the von Bertalanffy growth function (116 mm TL for females and 115 mm TL for males) approximated the previously reported length at birth, despite the lack of neonates in our sample.

The maximum size in DW of sharpspine skate in Taiwan was 338 mm for females and 289 mm for males (Joung et al., 2011), indicating that females from the East China Sea attain a slightly smaller size than those from Taiwan and that males attain sizes that are similar between locations. The maximum ages observed in our study were 10 years for females and 9 years for males; each of these ages is 1 year younger than the maximum age reported for each sex of this species in Taiwan (Joung et al., 2011).

For all 3 growth models, the growth rates (k values) were markedly higher in our study than in that by Joung et al. (2011); for the von Bertalanffy growth function fitted to DW data, k was 0.31 for females and 0.32 for males in our study but 0.15 for females and 0.17 for males in that by Joung et al. (2011). Indeed, for nearly all age groups, the DW at age estimated from the von Bertalanffy growth function was larger in our study than in that by Joung et al. (2011) for both sexes. Geographic variation in estimates of age and growth parameters has often been reported for elasmobranchs, including several skate species (Yamaguchi et al., 1998; Frisk and Miller, 2006; Licandeo and Cerna, 2007; Bellodi et al., 2022). These geographic variations may be caused by several factors, including differences in environmental conditions, food availability, and fishing-related

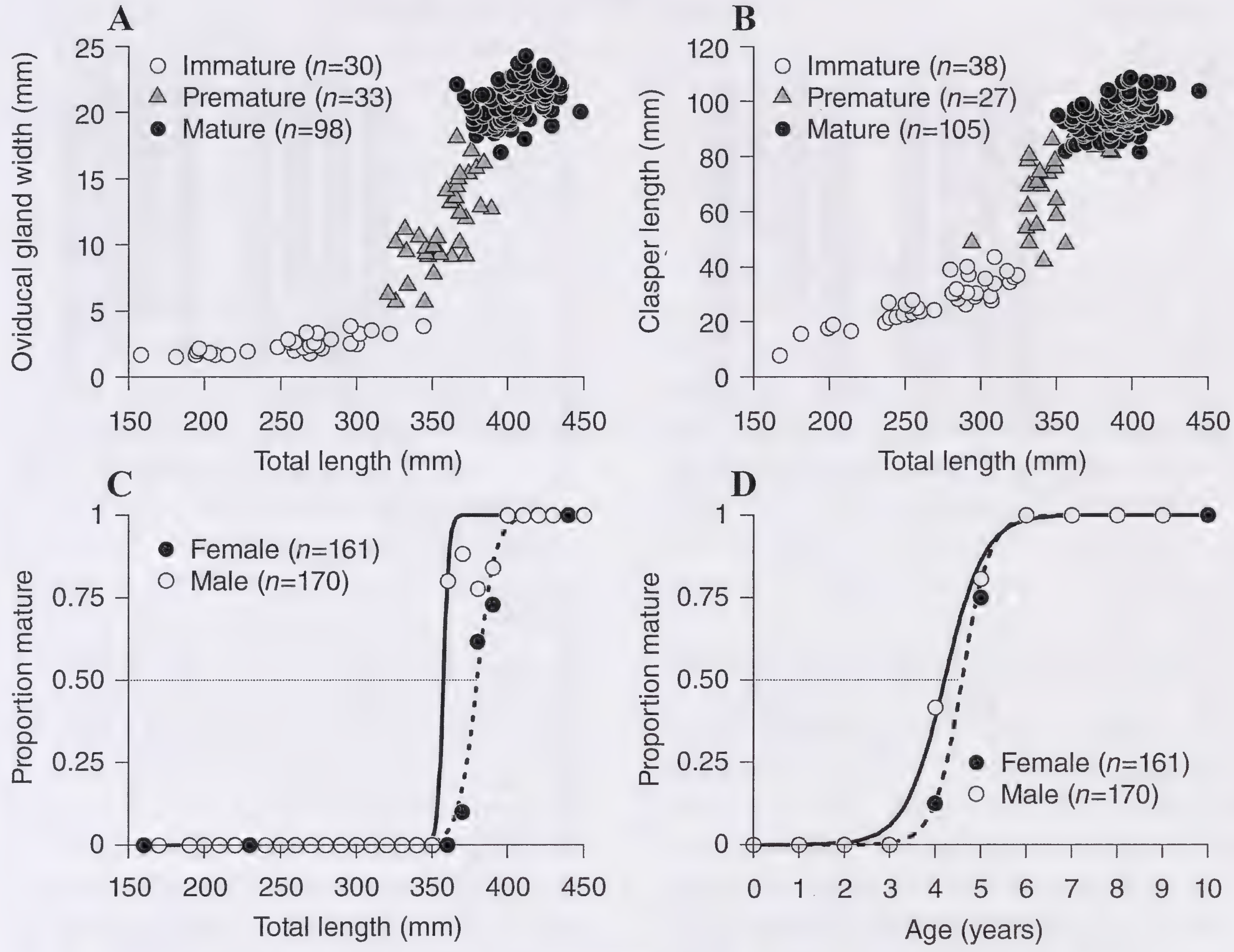

Figure 4

Maturation of female and male sharpspine skates (*Okamejei acutispina*) sampled between April 2009 and November 2022 in the East China Sea. The top panels show the relationship between total length and (**A**) oviducal gland width for females or (**B**) clasper length for males. The bottom panels show the (**C**) size and (**D**) age at maturity for females (dashed line) and males (solid line). The horizontal dotted line in each bottom panel indicates the size at 50% maturity. *n*=sample size.

mortality and could reflect the existence of separate stocks (Yamaguchi, 2002). Alternatively, such variations may also be due to other factors, such as sample bias and differences in readers, reading precision, preparation techniques, and growth modeling approaches (Cailliet et al., 1990; Carbonara et al., 2020). Therefore, evaluating whether the large differences between the East China Sea and Taiwan in observed growth patterns truly reflect geographic differences or result from methodological issues requires involving the same readers making comparisons using the same methods to minimize error, as was demonstrated by Yamaguchi et al. (1998).

Based on life history data (Caltabellotta et al., 2019) and the range of life history variation (Frisk, 2010; Ebert et al., 2017) for 28 skate species, the maximum observed age varies greatly among species, from 6 years for the Rio skate (*Rioraja agassizii*) to 37 years for the whitebrow skate (*Bathyraja minispinosa*). Frisk (2010) calculated the mean observed maximum age of skates, using data from 14 skate species available at the time, as 17.5 years for females and 17.3 years for males. In our study, the maximum observed ages for both sexes of sharpspine skate were relatively low, similar to those reported by Joung et al. (2011), although they were within the range reported for skates. The maximum observed age has also been reported to be relatively low for several other small-sized skates, including the roundel skate (*Rostroraja texana*), the brown ray (*Raja miraletus*), and the speckled ray (*Raja polystigma*), with maximum observed ages ranging from 9 to11 years for females and from 7 to 8 years for males (Sulikowski et al., 2007; Kadri et al., 2012; Porcu et al., 2020). Because the sharpspine skate is among the smallest skate species for which age and growth data are available, the results of our study and of that by Joung et al. (2011) are consistent with the general trend that smaller skate species reach a lower maximum age than larger species (Sulikowski et al., 2007).

For both sexes of sharpspine skate in the East China Sea, *k* was considerably higher than the mean *k* value for skates (1.20 for females and 1.40 for males) calculated by Frisk (2010) on the basis of published estimates for parameters of the von Bertalanffy growth function. The growth rates derived with the von Bertalanffy growth function for skate species range from 0.02 for the whitebrow skate to 0.34 for the Sydney skate (*Dentiraja australis*), with very few species (such as the sharpspine skate in this study) exceeding 0.30 (Gallagher et al., 2005; Frisk, 2010; Ebert et al., 2017; Reis and Figueira, 2020). Estimates made

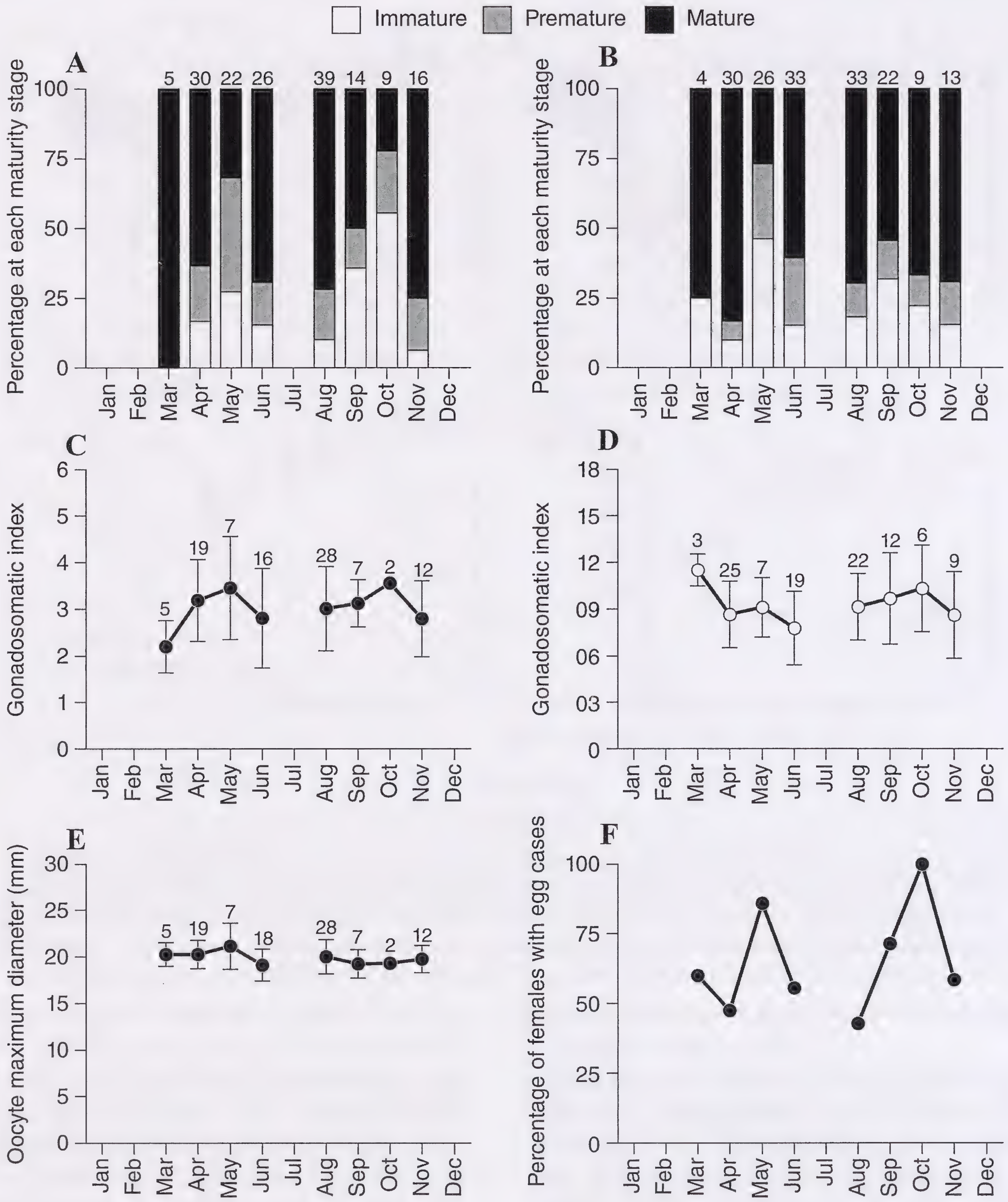

Figure 5

Monthly reproductive parameters for female and male sharpspine skates (*Okamejei acutispina*) captured during April 2009–November 2022 in the East China Sea. The top panels show the percentage of (**A**) females and (**B**) males at each of 3 maturity stages in each month. The middle panels provide the mean gonadosomatic index values for mature (**C**) females and (**D**) males. The bottom panels show (**E**) the mean maximum diameter of oocytes for mature females and (**F**) the percentage of mature females with egg cases. Error bars in panels C–E indicate standard deviations, and numbers above stacked bars and error bars indicate sample sizes.

with the von Bertalanffy growth function in our study indicate that both sexes of sharpspine skate in the East China Sea grow rapidly up to 5 years of age, reaching approximately 360 mm TL, after which point growth slows. These findings reveal that sharpspine skate in the East China Sea grow faster than those in Taiwan and most other skate species for which age and growth data are available, with the greater part of the growth occurring during the first half of their life.

In our study, estimated size at 50% maturity was 84.8% and 80.0% of the maximum observed length for this species for females and males, respectively, falling within the typical range (75–90%) reported for skates (Ebert et al., 2008). Although the maximum observed lengths were nearly the same for both sexes, the size at 50% maturity was approximately 25 mm TL larger for females than for males, indicating slight sexual dimorphism in size at maturity. Female elasmobranchs typically mature at a larger size than males. Nonetheless, in skates, the occurrence of sexual dimorphism in size at maturity varies among species. For instance, for the roundel skate (Sulikowski et al., 2007), brown ray (Kadri et al., 2012), and white skate (*Rostroraja alba*) (Ebert et al., 2008), females mature at a slightly larger size than males, consistent with our latest findings for the sharpspine skate. For the bigthorn skate (*Rajella barnardi*), in contrast, the sexes mature at approximately the same size (Ebert et al., 2008). Moreover, for some species, such as the zipper sandskate (*Psammobatis extenta*) (Braccini and Chiaramonte, 2005) and the African softnose skate (*Bathyraja smithii*) (Ebert et al., 2008), males mature at a slightly larger size than females.

For both sexes in our study, the youngest mature sharpspine skate was estimated to be 4 years old, and the age at 50% maturity corresponded to 46.0% of the maximum observed age for females and 46.8% of this age for males. Among the elasmobranchs, which are generally slow to mature, skates tend to mature particularly slowly (Frisk, 2010; Hara et al., 2018a). According to Frisk (2010), the mean age at 50% maturity for skate species is 10.1 years for females and 9.1 years for males, that is, approximately 64% of the maximum age for females and approximately 60% of this age for males. Therefore, sharpspine skate in the East China Sea appear to have a lower age at maturity than many other skate species, maturing very early in its life span.

In the East China Sea, the sharpspine skate occurs sympatrically with several other skate species, such as the polkadot skate, the bigeye skate (*Okamejei meerdervoortii*), and the acutenose skate (*Dipturus tengu*) (Hara et al., 2016), but their species-specific biological information is very limited, with comparable life history data available only for the polkadot skate (Hara et al., 2018a). Sharpspine skate in our latest study had a maximum age 5 years lower for females and 4 years lower for males, compared with that of the polkadot skate, and growth rates of sharpspine skate were much higher for both sexes than for those of the polkadot skate (0.30 versus 0.10 for females and 0.31 versus 0.11 for males) (Hara et al., 2018a). In addition, the 50% age at maturity of female and male sharpspine skate was approximately half that of polkadot skate (Hara et al., 2018a). Given that these species coexist and presumably occupy similar ecological niches and are fished together, the population dynamics of the sharpspine skate and the polkadot skate likely interact. Therefore, it is appropriate to assess the population status and establish fisheries management for each species separately.

Prior to this study, there was a lack of reliable information on the egg-laying season of the sharpspine skate. The lack of samples for the period December–February and for July prevented us from determining the full extent of its egg-laying cycle. However, on the basis of our results, we do have evidence that the egg-laying season of this species spans at least from March through November, as there was no significant difference in the maximum diameter of oocytes in different months and mature females with egg cases were found in all the months sampled. Because measuring egg-laying rates in the wild for oviparous elasmobranchs like skates is challenging (Frisk, 2010), the annual fecundity could not be estimated in this study. Overall, more than half of the mature females were carrying egg cases, indicating that they repeatedly lay egg cases at short intervals. The frequency of females with egg cases was high in May and November but was not significantly different among months.

We were unable to draw strong conclusions regarding egg-laying seasonality because, for some months (especially in November), few mature females were obtained. However, given the lack of a significant difference in monthly GSI values for mature females, the 2 peaks that were observed in the percentage of females with egg cases may not reflect egg-laying seasonality. Year-round egg-laying, with or without seasonal peaks, has been reported for many skate species, such as the thorny skate (*Amblyraja radiata*), little skate (*Leucoraja erinacea*), brown ray, and polkadot skate (Sulikowski et al., 2005; Palm et al., 2011; Kadri et al., 2012; Hara et al., 2018a). Additional sampling in December–February, in July, and in the months when few mature females were collected is needed to fully determine the annual egg-laying cycle of the sharpspine skate and to verify whether this species also lays egg cases throughout the year.

The similarity among months in the GSI for mature males indicates that males of this species may be capable of reproducing continuously. In male elasmobranchs, however, temporal variation in GSI values does not always synchronize with spermatogenesis (Sulikowski et al., 2005). Furthermore, the females of some skate species can store sperm in the oviducal glands (Luer and Gilbert, 1985; Soto-López et al., 2021). Therefore, histological examination of male testes is necessary to fully elucidate the reproductive cycle of the sharpspine skate.

Conclusions

The results of this study provide comprehensive information on the life history characteristics of the sharpspine skate in the East China Sea. Our findings reveal that, although the sharpspine skate in the East China Sea has a prolonged egg-laying season, as is typical for skates, it is short-lived, grows faster, and matures much earlier than many other skate species, including the sympatric polkadot skate. These unique life history traits of the sharpspine skate in the East China Sea have important implications for its population assessment and sustainable management as a fishery resource, and they highlight the need for species-specific life history investigations and population monitoring for skates in this region, many of which are targeted by bottom trawlers. Finally, because the growth pattern of sharpspine skate in the East China Sea estimated in this study is substantially different from that of the same species in Taiwan, further study is recommended to verify the existence of geographic differences in life history traits and the possible existence of distinct regional populations.

Resumen

La raya picuda (*Okamejei acutispina*) es una especie de raya explotada comercialmente en el Mar Oriental de China, y se sospecha que la población de esta especie en esta región ha disminuido debido a la presión pesquera y a otros factores. Sin embargo, la información sobre su ciclo vital, esencial para la evaluación y manejo de la población, es limitada. Estimamos la edad, crecimiento, madurez y su época de desove a partir de los datos de 331 ejemplares capturados en el Mar Oriental de China. La edad se determinó contando las bandas translúcidas en las secciones del centro vertebral. La máxima longitud total (LT) y edad fue 448 mm y 10 años para hembras y 444 mm y 9 años para machos. Entre los 3 modelos de crecimiento aplicados a los datos de longitud a la edad, la función de crecimiento de von Bertalanffy proporcionó el mejor ajuste para ambos sexos (hembras: longitud asintótica teórica [L_∞]=428 mm, coeficiente de crecimiento [k]=0.30 y tiempo teórico a longitud cero [t_0]=−1.04 años; machos: L_∞=422 mm, k=0.31 y t_0=−1.04 años). La talla y la edad al 50% de madurez fueron 380 mm LT y 4.60 años para las hembras y 357 mm LT y 4.21 años para los machos. Los datos reproductivos estacionales mensuales, incluyendo la aparición de huevos y el diámetro máximo del oocitos, indican una prolongada temporada de desove. Nuestros hallazgos indican que la historia de vida de la raya de espina afilada en el Mar Oriental de China se caracteriza por una vida más corta, un crecimiento más rápido y una edad de madurez menor que la de muchas otras rayas del mundo.

Acknowledgments

We are grateful to T. Ozaki and S. Takase (Yamada Suisan Co. Ltd.) and the officers and crew of the Nagasaki University training ship for their help with sample collection. This study was financially supported by a Grant-in-Aid for Scientific Research (B) (19H02977, 23H02237) from the Japan Society for the Promotion of Science and by the Environment Research and Technology Development Fund (1-2203) of the Environmental Restoration and Conservation Agency of Japan.

Literature cited

Akaike, H.
1974. A new look at the statistical model identification. IEEE Trans. Autom. Control 19:716–723.

Baeck, G. W., C.-I. Park, H. C. Choi, S.-H. Huh, and J. M. Park.
2011. Feeding habits of ocellate spot skate, *Okamejei kenojei* (Müller & Henle, 1841), in coastal waters of Taean, Korea. J. Appl. Ichthyol. 27:1079–1085.

Beamish, R. J., and D. A. Fournier.
1981. A method for comparing the precision of a set of age determinations. Can. J. Fish. Aquat. Sci. 38:982–983.

Bellodi, A., A. Mulas, P. Carbonara, A. Cau, D. Cuccu, M. F. Marongiu, V. Mura, P. Pesci, W. Zupa, C. Porcu, et al.
2021. New insights into life-history traits of Mediterranean electric rays (Torpediniformes: Torpedinidae) as a contribution to their conservation. Zoology 146:125922.

Bellodi, A., A. Massaro, W. Zupa, M. Donnaloia, M. C. Follesa, A. Ligas, A. Mulas, M. Palmisano, and P. Carbonara.
2022. Assessing thornback ray growth pattern in different areas of Western-Central Mediterranean Sea through a Multimodel Inference analysis. J. Sea Res. 179:102141.

Braccini, J. M., and G. E. Chiaramonte.
2005. Reproductive biology of *Psammobatis extenta*. J. Fish Biol. 61:272–288.

Cailliet, G. M., and K. J. Goldman.
2004. Age determination and validation in chondrichthyan fishes. *In* Biology of sharks and their relatives (J. Carrier, J. A. Musick, and M. Heithaus, eds.), p. 399–447. CRC Press, Boca Raton, FL.

Cailliet, G. M., K. G. Yudin, S. Tanaka, and T. Taniuchi.
1990. Growth characteristics of two populations of *Mustelus manazo* from Japan based upon cross-readings of vertebral bands. *In* Elasmobranchs as living resources: advances in the biology, ecology, systematics, and the status of the fisheries (H. L. Pratt, Jr., S. H. Gruber, and T. Taniuchi, eds.), p. 167–176. NOAA Tech. Rep. NMFS 90.

Cailliet, G. M., W. D. Smith, H. F. Mollet, and K. J. Goldman.
2006. Age and growth studies of chondrichthyan fishes: the need for consistency in terminology, verification, validation, and growth function fitting. Environ. Biol. Fishes 77:211–228.

Caltabellotta, F. P., F. M. Silva, F. S. Motta, and O. B. F. Gadig.
2019. Age and growth of the threatened endemic skate *Rioraja agassizii* (Chondrichthyes, Arhynchobatidae) in the western South Atlantic. Mar. Freshw. Res. 70:84–92.

Campana, S. E.
2001. Accuracy, precision and quality control in age determination, including a review of the use and abuse of age validation methods. J. Fish Biol. 59:197–242.

Carbonara, P., A. Bellodi, M. Palmisano, A. Mulas, C. Porcu, W. Zupa, M. Donnaloia, R. Carlucci, L. Sion, and M. C. Follesa.
2020. Growth and age validation of the thornback ray (*Raja clavata* Linnaeus, 1758) in the South Adriatic Sea (central Mediterranean). Front. Mar. Sci. 7:586094.

Chang, W. Y. B.
1982. A statistical method for evaluating the reproducibility of age determination. Can. J. Fish. Aquat. Sci. 39:1208–1210.

Ebert, D. A., L. J. V. Compagno, and P. D. Cowley.
2008. Aspects of the reproductive biology of skates (Chondrichthyes: Rajiformes: Rajoidei) from southern Africa. ICES J. Mar. Sci. 65:81–102.

Ebert, D. A., J. S. Bigman, and J. M. Lawson.
2017. Biodiversity, life history, and conservation of northeastern Pacific chondrichthyans. *In* Northeast Pacific shark biology, research and conservation, part A. Advances in Marine Biology, vol. 77 (S. E. Larson, and D. Lowry, eds.), p. 9–78. Acad. Press, London.

Fisher, R. A.
1922. On the interpretation of χ^2 from contingency tables, and the calculation of P. J. R. Stat. Soc. 85:87–94.

Francis, R. I. C. C.
1990. Back-calculation of fish length: a critical review. J. Fish Biol. 36:883–902.

Frisk, M. G.
2010. Life history strategies of batoids. *In* Sharks and their relatives 2: biodiversity, adaptive physiology, and conservation (J. C. Carrier, J. A. Musick, and M. Heithaus, eds.), p. 283–316. CRC Press, Boca Raton, FL.

Frisk, M. G., and T. J. Miller.
2006. Age, growth, and latitudinal patterns of two Rajidae species in the northwestern Atlantic: little skate (*Leucoraja erinacea*) and winter skate (*Leucoraja ocellata*). Can. J. Fish. Aquat. Sci. 63:1078–1091.

Furumitsu, K., J. T. Wyffels, and A. Yamaguchi.
2019. Reproduction and embryonic development of the red stingray *Hemitrygon akajei* from Ariake Bay, Japan. Ichthyol. Res. 66:419–436.

Gallagher, M. J., C. P. Nolan, and F. Jeal.
2005. Age, growth and maturity of the commercial ray species from the Irish Sea. J. Northwest Atl. Fish. Sci. 35:47–66.

Hara, K., K. Furumitsu, and A. Yamaguchi.
2014. Record of a Korean skate, *Hongeo koreana* (Jeong and Nakabo, 1997) from off the Goto Islands. Rep. Japan. Soc. Elasmobranch Stud. 50:21–26. [In Japanese.]

Hara, K., K. Furumitsu, T. Aoshima, Y. Morii, N. Yamawaki, N. Kusumoto, H. Kanehara, and A. Yamaguchi.
2016. Species composition of skates (Rajiformes: Rajoidei) collected in the East China Sea, during the cruise of the T/S *Nagasaki-Maru*. Rep. Japan. Soc. Elasmobranch Stud. 52:5–11. [In Japanese.]

Hara, K., K. Furumitsu, T. Aoshima, H. Kanehara, and A. Yamaguchi.
2018a. Age, growth, and age at sexual maturity of the commercially landed skate species, *Dipturus chinensis* (Basilewsky, 1855), in the northern East China Sea. J. Appl. Ichthyol. 34:66–72.

Hara, K., K. Furumitsu, and A. Yamaguchi.
2018b. Dietary habits of the polkadot skate *Dipturus chinensis* in the East China Sea. Ichthyol. Res. 65:363–373.

Hatooka, K., U. Yamada, M. Aizawa, A. Yamaguchi, and N. Yagishita.
2013. Rajidae. *In* Fishes of Japan with pictorial keys to the species, 3rd ed. (T. Nakabo, ed.), p. 205–216. Tokai Univ. Press, Hadano, Japan. [In Japanese.]

Jacobsen, I. P., and M. B. Bennett.
2011. Life history of the blackspotted whipray *Himantura astra*. J. Fish Biol. 78:1249–1268.

Joung, S.-J., P.-H. Lee, K.-M. Liu, and Y.-Y. Liao.
2011. Estimates of life history parameters of the sharpspine skate, *Okamejei acutispina*, in the northeastern waters of Taiwan. Fish. Res. 108:258–267.

Kadri, H., S. Marouani, B. Saïdi, M. N. Bradai, M. Ghorbel, A. Bouaïn, and E. Morize.
2012. Age, growth and reproduction of *Raja miraletus* (Linnaeus, 1758) (Chondrichthyes: Rajidae) of the Gulf of Gabès (Tunisia, central Mediterranean Sea). Mar. Biol. Res. 8:388–396.

Kimura, D. K.
1980. Likelihood methods for the von Bertalanffy growth curve. Fish. Bull. 77:765–776.

Kume, G., K. Furumitsu, and A. Yamaguchi.
2008. Age, growth and age at sexual maturity of fan ray *Platyrhina sinensis* (Batoidea: Platyrhinidae) in Ariake Bay, Japan. Fish. Sci. 74:736–742.

Last, P., G. Naylor, B. Séret, W. White, M. Stehmann, and M. de Carvalho (eds.).
2016. Rays of the world, 790 p. CSIRO Publ., Clayton South, Australia.

Licandeo, R., and F. T. Cerna.
2007. Geographic variation in life-history traits of the endemic kite skate *Dipturus chilensis* (Batoidea: Rajidae), along its distribution in the fjords and channels of southern Chile. J. Fish Biol. 71:421–440.

Luer, C. A., and P. W. Gilbert.
1985. Mating behavior, egg deposition, incubation period, and hatching in the clearnose skate, *Raja eglanteria*. Environ. Biol. Fishes 13:161–171.

MEJ (Ministry of the Environment, Japan).
2017. Red list of threatened marine fishes in Japan, 6 p. Minist. Environ., Jpn., Tokyo, Japan. [In Japanese.] [Available from website, accessed February 2024.]

Palm, B. D., D. M. Koester, W. B. Driggers III, and J. A. Sulikowski.
2011. Seasonal variation in fecundity, egg case viability, gestation, and neonate size for little skates, *Leucoraja erinacea*, in the Gulf of Maine. Environ. Biol. Fishes 92:585–589.

Porcu, C., A. Bellodi, A. Cau, R. Cannas, M. F. Marongiu, A. Mulas, and M. C. Follesa.
2020. Uncommon biological patterns of a little known endemic Mediterranean skate, *Raja polystigma* (Risso, 1810). Reg. Stud. Mar. Sci. 34:101065.

Reis, M., and W. F. Figueira.
2020. Age, growth and reproductive biology of two endemic demersal bycatch elasmobranchs: *Trygonorrhina fasciata* and *Dentiraja australis* (Chondrichthyes: Rhinopristiformes, Rajiformes) from Eastern Australia. Zoologia 37:1–12.

Ricker, W. E.
1975. Computation and interpretation of biological statistics of fish populations. Bull. Fish. Res. Board Can. 191, 382 p.
1979. Growth rates and models. *In* Fish physiology, vol. 8 (W. S. Hoar, D. J. Randall, and J. R. Brett, eds.), p. 677–743. Acad. Press, New York.

Rigby, C. L., N. K. Dulvy, D. Derrick, Y. V. Dyldin, K. Herman, H. Ishihara, C.-H. Jeong, Y. Semba, S. Tanaka, I. V. Volvenko, et al.
2021. *Okamejei acutispina*. The IUCN Red List of Threatened Species 2021:e.T161636A124519140. [Available from website, accessed September 2022.]

Soto-López, K., R. I. Ochoa-Báez, F. Galván-Magaña, and M. C. Oddone.
2021. Reproductive biology of the rasptail skate *Rostroraja velezi* (Rajiformes: Rajidae). J. Fish Biol. 98:791–802.

Sulikowski, J. A., J. Kneebone, S. Elzey, J. Jurek, P. D. Danley, W. H. Howell, and P. C. W. Tsang.
2005. The reproductive cycle of the thorny skate (*Amblyraja radiata*) in the western Gulf of Maine. Fish. Bull. 103:536–543.

Sulikowski, J. A., S. B. Irvine, K. C. DeValerio, and J. K. Carlson.
2007. Age, growth and maturity of the roundel skate, *Raja texana*, from the Gulf of Mexico, USA. Mar. Freshw. Res. 58:41–53.

Yamada, U., M. Tokimura, H. Horikawa, and T. Nakabo.
2007. Fishes and fisheries of the East China and Yellow Seas, 1340 p. Tokai Univ. Press, Hadano, Japan. [In Japanese.]

Yamaguchi, A.
2002. On the sharks as fishery resources and aspects of their life histories. Aquabiology 24:401–408. [In Japanese.]

Yamaguchi, A., T. Taniuchi, and M. Shimizu.
1998. Geographic variation in growth of the starspotted dogfish *Mustelus manazo* from five localities in Japan and Taiwan. Fish. Sci. 64:732–739.

Yamamoto, K., and K. Nagasawa.
2015. Temporal changes in demersal fish assemblage structure in the East China Sea and the Yellow Sea. Nippon Suisan Gakkaishi 81:429–437. [In Japanese.]

National Marine
Fisheries Service
NOAA

Fishery Bulletin
established in 1881

Spencer F. Baird
First U.S. Commissioner
of Fisheries and founder
of *Fishery Bulletin*

Morphology, composition, and deterioration of the embryonic rostral sheath of the smalltooth sawfish (*Pristis pectinata*)

Gregg R. Poulakis (contact author)[1]
Jennifer T. Wyffels[2,3]
P. Eric Fortman[4]
Andrew K. Wooley[1]
Lukas B. Heath[1]
Dylan M. Yakich[1]
Patrick W. Wilson[4]

Email address for contact author: gregg.poulakis@myfwc.com

[1] Charlotte Harbor Field Laboratory
Fish and Wildlife Research Institute
Florida Fish and Wildlife Conservation Commission
585 Prineville Street
Port Charlotte, Florida 33954

[2] Center for Bioinformatics and Computational Biology
University of Delaware
590 Avenue 1743
Newark, Delaware 19713

[3] Ripley's Aquariums
7576 Kingspointe Parkway
Suite 188
Orlando, Florida 32819

[4] Fish and Wildlife Research Institute
Florida Fish and Wildlife Conservation Commission
100 Eighth Avenue SE
St. Petersburg, Florida 33701

Abstract—Elongated rostra evolved in diverse animal groups as adaptations for feeding, defense, sensory perception, and reproduction. Sawfish rostra have tooth-like dermal denticles, referred to as *rostral teeth*, along their lateral margins. Embryos have a sheath, or covering, for the calcified rostral teeth during gestation, and it persists until after parturition. Little is known about the morphology and composition of the sheath. During 18 years of tagging juvenile smalltooth sawfish (*Pristis pectinata*), sheaths were documented for 36 neonates with stretch total lengths of 581–812 mm, and samples were collected from 6 specimens for laboratory evaluation. The multilayered, skin-like sheath, which cannot be easily removed manually, has a vascularized inner layer of connective tissue composed primarily of fibrous proteins (e.g., collagen, reticulin, and keratin) surrounded by an outer layer of columnar and spherical epithelial cells overlying a basement membrane. The columnar cells contain condensed chromatin and differentiate into the outermost spherical cells that contain carbohydrates. After birth, the sheath is shed evenly over 4 d, through sloughing and apoptosis, fully exposing the rostral teeth. The sheath is an ephemeral embryonic organ that protects the female and the embryos from injury during gestation and birth.

Manuscript submitted 17 November 2023.
Manuscript accepted 7 May 2024.
Fish. Bull. 122:76–88 (2024).
Online publication date: 28 May 2024.
doi: 10.7755/FB.122.3.2

The views and opinions expressed or implied in this article are those of the author (or authors) and do not necessarily reflect the position of the National Marine Fisheries Service, NOAA.

Relationships between form and function have been the subject of many morphological and evolutionary studies (e.g., Dean et al., 2007; Kolmann et al., 2014). For example, elongated rostra have appeared in diverse animal groups as adaptations for feeding, defense (especially if rigid and armored), sensory perception, and reproduction (e.g., Breder, 1952; Thorson, 1976; Williams, 1984; Kells and Carpenter, 2011). Examples of chondrichthyan taxa that have elongated rostra include sharks (e.g., *Apristurus* spp.; *Deania* spp.; goblin shark, *Mitsukurina owstoni*; and *Pristiophorus* spp.), rays (e.g., *Pristis* spp.; *Aptychotrema* spp.; sixgill stingray, *Hexatrygon bickelli*; and Sclerorhynchoidea), skates (e.g., *Dipturus* spp.), and chimaeras (e.g., *Harriotta* spp. and *Rhinochimaera* spp.) (Last and Stevens, 2009; Castro, 2011; Welten et al., 2015).

Sawfish species (family Pristidae) and sawshark species (family Pristiophoridae) have among the most extreme examples of elongated rostra. Rostra of sawfish compose up to 25% of the total body length, and both sawfishes and sawsharks have tooth-like scales referred to as *rostral teeth* along the lateral margins of their rostra (Bigelow and Schroeder, 1953; Miller, 1974, 1995; Last and Stevens, 2009). These groups are thought to have evolved their rostra independently (Slaughter and Springer, 1968), indicating that broad or shared advantages of rostrum elongation span the deepwater habitats of sawsharks and the shallow-water habitats of sawfishes (Last and Stevens, 2009; Poulakis et al., 2011).

Sawfishes and sawsharks, as well as other chondrichthyans (e.g., stingrays and dogfishes), have evolved ephemeral embryonic coverings, often called sheaths, to encapsulate sharp body parts, such as spines and rostral teeth, during gestation (Whitley, 1940; Gudger, 1951; Babel, 1967). The gross morphology and microscopic anatomy of these sheaths has not been investigated, and for sawfishes, the coverings have been described as "transparent cartilaginous tissue" (Southwell, 1910), a "membrane" (Hussakof, 1912; Setna and Sarangdhar, 1948), and "gelatinous" (Abel and Grubbs, 2020). Although they apparently refer to the sheath as both "skin" and an unspecified "narrow band," Bigelow and Schroeder (1953) indicated that the rostral teeth of sawfish embryos are "entirely enclosed in the skin until birth, while a narrow band along each margin of the saw is naked, both below and above." Contrary to the description by Bigelow and Schroeder (1953) of rostral teeth as soft until birth, rostral teeth form and calcify early in gestation and the sheath forms around the entire tooth-bearing portion of the rostrum (Miller, 1995). The sheath prevents the rostral teeth of embryos from damaging 1) siblings and the uterus during gestation and 2) the female's cloaca during parturition (Setna and Sarangdhar, 1948). The purpose of this paper is to describe the macroscopic and microscopic morphology of the embryonic rostral sheath of the smalltooth sawfish (*Pristis pectinata*), including its organization, composition, and shedding process.

Materials and methods

Sample collection

Neonate smalltooth sawfish, defined as newborns having partial or complete rostral sheaths or being in the length range for size at birth, were caught in Florida between 2004 and 2022 primarily as part of ongoing, fishery-independent sampling in the Charlotte Harbor estuarine system and as opportunistic captures elsewhere in the southern half of the state (e.g., in the Indian River Lagoon). This research was conducted under endangered species research permit numbers 1475, 15802, 21043, and 25864 issued to the Florida Fish and Wildlife Conservation Commission.

Sampling was carried out during the day, primarily with gill nets that had panels of 102-mm (4-in) and 152-mm (6-in) stretch monofilament mesh. Some individuals were caught in seines, in cast nets, or by hand. Detailed gear descriptions and sampling protocols can be found in Scharer et al. (2017).

Prior to being released alive, neonates observed with partial or complete rostral sheaths were measured (in stretch total length [STL] in millimeters) and photographed. Small (2–4 mm long by 2–4 mm wide) samples of sheath tissue were collected when at least half the sheath remained. Samples were taken between the rostral teeth and placed in 95% ethanol or 10% neutral buffered formalin in the field.

Sample processing

Histology, scanning electron microscopy (SEM), micro-computed tomography, and elemental analysis were used to characterize the microscopic morphology, composition, and deterioration of the sheath and its association with the rostrum.

For histology, ethanol- and formalin-fixed samples were embedded in glycol methacrylate (JB-4 Embedding Kit[1], Polysciences Inc., Warrington, PA) at the Fish and Wildlife Research Institute in St. Petersburg, Florida. Most samples that included scales were decalcified through pretreatment with 90% formic acid for 5 d or 10% ethylenediaminetetraacetic acid for 3 weeks before embedding. Samples were sectioned at 4 µm by using a standard microtome and were stained with standard hematoxylin and eosin, with periodic acid Schiff's hematoxylin and metanil yellow (PASMY) to identify carbohydrates and mucus (Quintero-Hunter et al., 1991), with Masson's trichrome dye for collagen- and keratin-like tissue components (Sheehan and Hrapchak, 1987), and with a silver-based reticulin stain to highlight structural tissue and basement membranes (Quagio-Grassiotto[2]). Slides were retained.

At the University of Delaware, SEM was used to document surface features and degradation of the sheath. For visualizing sheath deterioration and rostral scales, a frozen rostrum from a dead neonate (reported to us by a member of the public) was thawed and scanned by using a SkyScan 1276 micro-computed tomography scanner (Bruker Corp., Billerica, MA) at a nominal resolution of 21.2 µm with a 0.25-mm thick aluminum filter and an applied X-ray tube voltage of 50 kV. Camera pixel binning was applied by combining each 2-by-2 grid of pixels into 1 pixel. The scan orbit was 180° with a rotation step of 0.9°. Reconstruction was performed with a modified Feldkamp algorithm by using the SkyScan NRecon software and NReconServer, vers. 1.7.4.2 (Bruker Corp.). Beam hardening correction was applied. With the same rostrum used for micro-computed tomography, energy-dispersive X-ray spectroscopy was performed by using an INCAx-act detector (Oxford Instruments, Abingdon, UK) attached to a Hitachi S-4700 field-emission scanning electron microscope (Hitachi Ltd., Tokyo, Japan) for elemental analysis to determine if neonates possessed a rostrum with uniformly calcified scales at birth.

Results

Live neonate smalltooth sawfish (sample size [n]=141) were caught primarily in southwest Florida between 2004 and 2022. Complete or partial embryonic rostral sheaths were observed on 36 individuals (range: 581–812 mm STL; mean: 733 mm STL), and multiple samples were collected from 6 individuals for laboratory analysis.

---

[1] Mention of trade names or commercial companies is for identification purposes only and does not imply endorsement by the National Marine Fisheries Service, NOAA, or the Florida Fish and Wildlife Conservation Commission.

[2] Quagio-Grassiotto, I. 2014. Unpubl. data. Dep. Morphol., Inst. Biosci., Sao Paulo State Univ.-UNESP, Botucatu, São Paulo, 18618-689 Brazil.

Macroscopic morphology

The sheath, partial or complete, was firmly connected to the rostrum and could not be easily removed manually. The sheath covered the underlying calcified rostral teeth and rostral scales (Fig. 1, A and B; Fig. 2). The sheath also contains some scales near the rostrum (Fig. 3). Notably, during a parturition event, we observed the birth of a neonate with the tips (<1 mm) of its rostral teeth already exposed. The other neonate observed from the same event had a complete sheath (i.e., rostral teeth completely covered). Normally, the sheath receded evenly across the

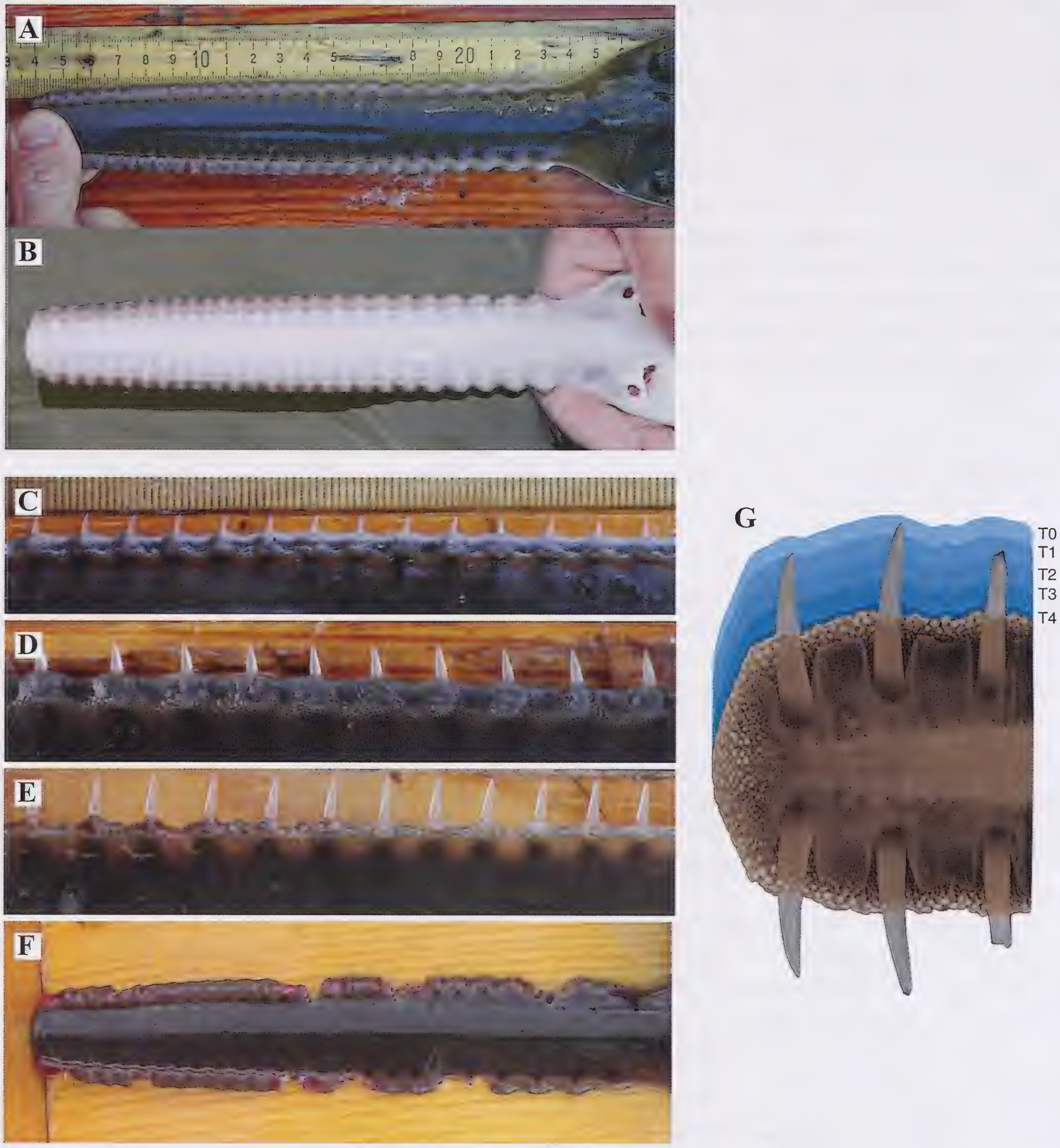

Figure 1

Photographs and an illustration showing the typical progression of deterioration of the embryonic rostral sheath of neonate smalltooth sawfish (*Pristis pectinata*) after parturition. The (**A**) dorsal and (**B**) ventral views of the complete rostral sheaths of specimens caught shortly after birth show that no teeth are exposed at this stage (labeled as T0 in panel G). The sheath usually recedes evenly across the entire rostrum, exposing more and more of the rostral teeth over time with (**C**) about 1 mm shed (stage T1) after 1 h of observation and (**D**) about 2 mm shed (stage T2) after 1 d. (**E**) After approximately 4 d, only a thin layer of remnant sheath is visible along the entire edge of the rostrum (stage T4). (**F**) Only 1 individual shed its sheath unevenly, with some teeth exposed before others. We hypothesize that this damage occurred because this individual began using the rostrum regularly before the sheath deteriorated much. The damage did not occur during capture because this fish was caught by hand. (**G**) This visualization shows the sequence of rostral sheath degradation.

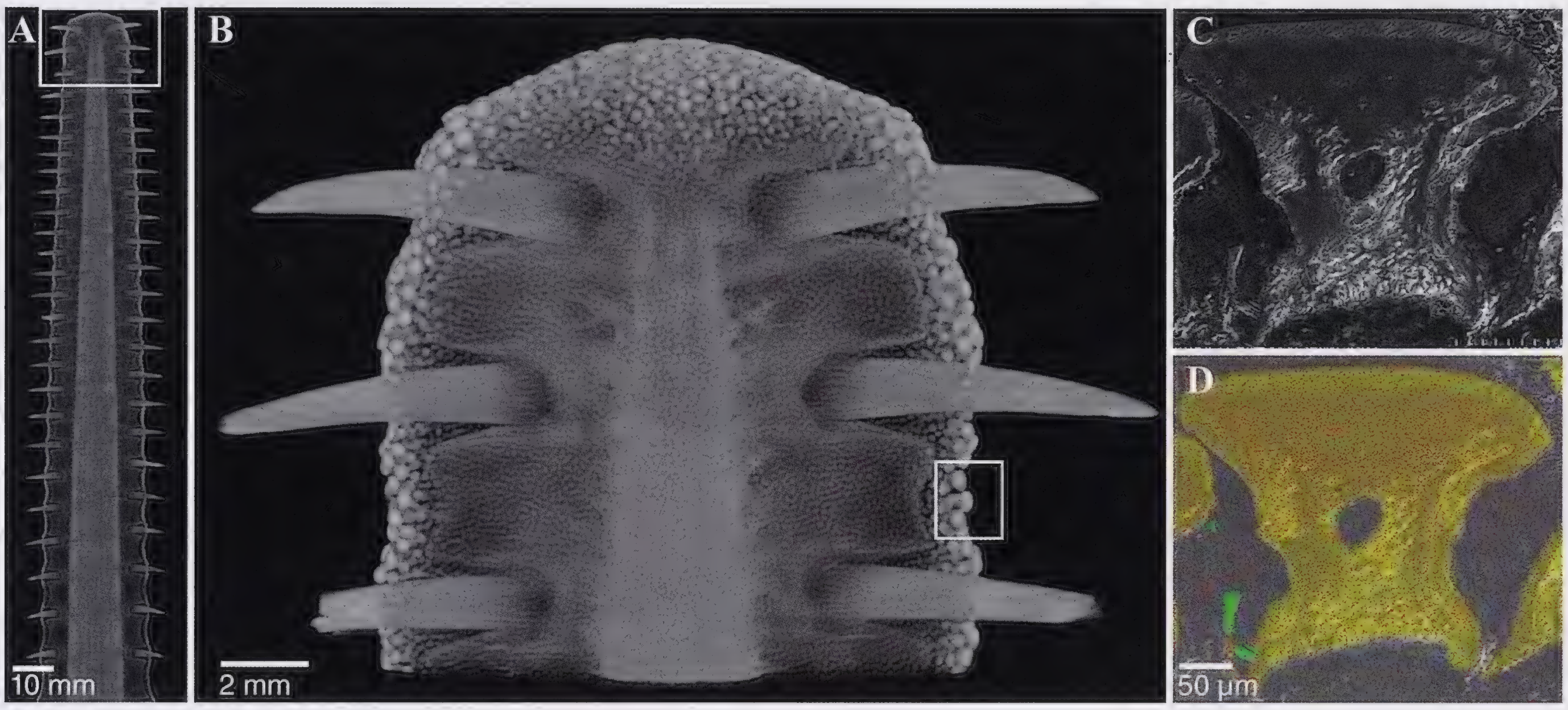

Figure 2

(**A**) A micro-computed tomography scan of a complete rostrum of a neonate smalltooth sawfish (*Pristis pectinata*) and (**B**) a close-up view of the tip of the rostrum from part of that scan (indicated by the box outlined in white in panel A) showing rostral scales, which are largest at the edges and tip of the rostrum. The 3D rendering applied to the scan makes the uniformly calcified rostral scales on the rostrum more conspicuous. Images from (**C**) scanning electron microscopy and (**D**) elemental analysis of cross sections of a rostral scale, from the region indicated by the box outlined in white in panel B, show deposition of calcium (green) and phosphorous (red) throughout the scale. The 50-µm scale bar in panel D also applies to panel C.

entire length of the rostrum (Fig. 1, C–E). However, on one occasion, an individual with a damaged sheath was observed (Fig. 1F).

One neonate was captured with a complete rostral sheath (i.e., sheath 5 mm wide, with no rostral teeth exposed; see the photographs of the full sheath in Figure 1, A and B, and the visualization of this stage [T0] in Figure 1G) and was observed on 4 successive occasions over 4 d, so that we could follow the progression of exposure of the rostral teeth. After 1 h of observation (at a water depth of 0.6 m and in surface and bottom temperatures of 30.0°C and 28.6°C and surface and bottom salinities of 16.7 and 17.5), 1 mm of the outermost sheath had been shed (stage T1 in Figure 1G). Then 2 mm of the sheath had shed after 1 d (stage T2 in Figure 1G), and 3 mm of it had shed (i.e., 60% of all individual rostral teeth were exposed) after 2 d (stage T3 in Figure 1G; in waters with temperatures of 22.3–30.0°C and salinities of 16.7–18.0 over those 2 d). After 2 more days (i.e., 4 d postpartum), only a thin layer of sheath remained at the base of the rostral teeth along the margin of the entire rostrum (stage T4 in Figure 1G).

Microscopic morphology and composition

Examination of cross sections revealed that the sheath is skin-like and composed of 2 main layers: a relatively thin outer layer of epithelial cells and a thicker inner layer composed of collagen-, reticulin-, and keratin-like connective tissues (Figs. 3–5). The 2 main layers are separated by a basement membrane spanning the entire cylindrical perimeter of the sheath.

Outer layer The outer layer of the sheath is composed of spherical and columnar epithelial cells. The spherical cells overlie the tips of the rostral teeth and penetrate between the scales on the rostrum (Figs. 4–6). Near the rostrum–sheath interface, groups of outer sheath cells surround the rostral scales, contributing to firm connectivity of the sheath to the rostrum (Fig. 6B).

Spherical cells are PASMY-positive (i.e., they contain carbohydrates) and are in direct contact with the environment. The diameter of the cells in the outermost half of the spherical cell layer (~8 cells thick) is approximately twice that of the interior spherical cells (Fig. 5B). Approximately half the cytoplasm of the outermost spherical cells is PASMY-positive and contains nuclei and glycoproteins, and the other half is PASMY-negative (i.e., they do not contain carbohydrates) (Fig. 5D). These cells also display cytoskeletal support with microfilaments (Fig. 5C). The outermost cells are hypothesized to maintain isolation of the tips of the rostral teeth during gestation by being constantly replaced and to begin gradually sloughing off after birth, evenly exposing more area of the rostral teeth.

Below the PASMY-positive spherical cells are columnar cells overlying a basement membrane. The columnar cells have darkly stained nuclei with condensed

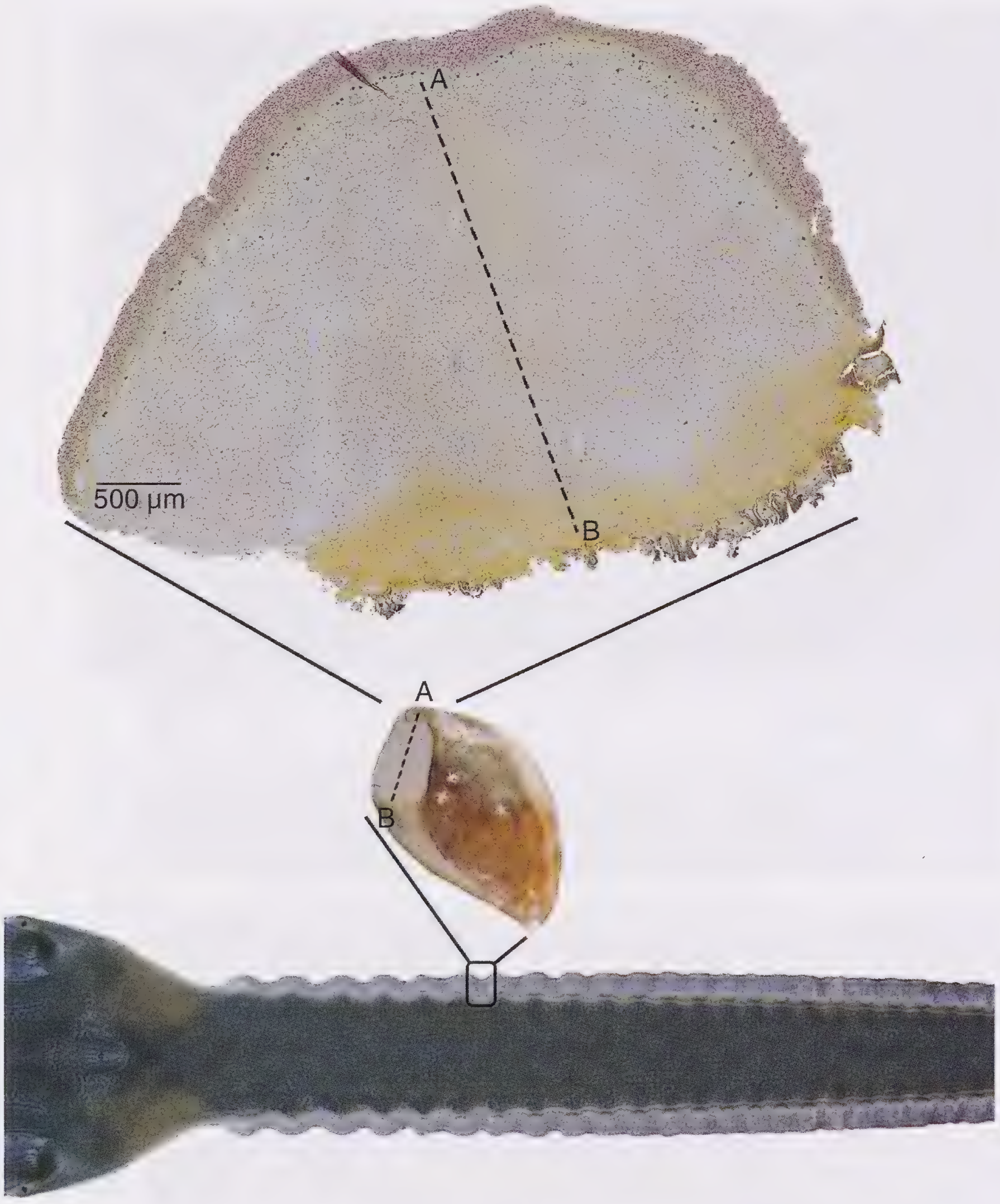

Figure 3

Cross section (top image) of a sample of an embryonic rostral sheath (middle image) taken between rostral teeth (the box outlined in black in the bottom image) of a neonate smalltooth sawfish (*Pristis pectinata*). Circular scales are visible on the outside of the gross sheath sample (middle image) and in the bottom margin of the histology (dark brown areas in the top image). The cross section shows the general orientation of the sheath and its components and was stained with periodic acid Schiff's hematoxylin and metanil yellow. Samples were taken from multiple locations along the rostrum for analysis.

chromatin and are PASMY-negative (Fig. 5, E and F). The columnar cells are hypothesized to be derived from stem cells adjacent to the basement membrane that maintain the cellular composition of the entire outer layer of epithelial cells (Fig. 5E).

Inner layer Below the basement membrane lies an inner layer of connective tissues containing fibrocytes, melanocytes, and blood vessels (Figs. 6–8). The connective tissues increase in density nearest the rostrum (Figs. 4C and 6A), where bases of the outermost rostral scales, some of which are likely shed with the sheath (see Figure 3), are embedded in interwoven collagen- and keratin-like connective tissues (Fig. 6, E and F). Fibrocytes were observed throughout the inner layer, often near collagen-like connective tissue (Fig. 7). Melanocytes were found in both layers of the sheath but were concentrated at the margin of the inner layer near the basement membrane (Fig. 8).

Degradation and surface features The sheath is hypothesized to be shed through a combination of sloughing, during which the outer layer contacts the environment, and apoptosis. Morphological evidence of apoptosis (e.g., pyknosis or karyorrhexis) was observed in nuclei of the deteriorating sheath cells (Fig. 9). Broader signs of degradation, such as gaps in the basement membrane and the presence of eosinophils, were also noted.

The SEM revealed an uneven texture of the spherical epithelial cells on the sheath surface as they were losing connectivity and integrity (Fig. 10, A and B). In addition, surface pores (Fig. 10, C and D), rostral scales (Fig. 10E), and degradation of the junction between scales and abutting cells of the sheath were observed (Fig. 10F).

Discussion

Elongated rostra have evolved in different animal groups, including fishes (Breder, 1952; Bigelow and Schroeder, 1953; Wueringer et al., 2012). We hypothesize that the embryonic rostral sheath of sawfishes evolved to protect females while gravid and during parturition. However, because there is no parental care, the sheath deteriorates within 4 d, as the neonates begin using their toothed rostrum to feed. Therefore, few neonates have been caught with any remnants of sheath during almost 2 decades of fishery-independent surveys.

The smalltooth sawfish feeds primarily on other fishes (Poulakis et al., 2017; Hancock et al., 2019), capturing prey by quickly swinging the rostrum side to side (Wueringer et al., 2012). Quick deterioration of the sheath and exposure of the rostral teeth benefits neonates by allowing them to begin feeding soon after birth. Maternally derived resources have been shown to aid neonatal hammerhead sharks (*Sphyrna* spp.) by increasing survivorship during the first weeks after birth (Lyons et al., 2020). Whether sawfish rely on similar provisions is unknown. However, sheath-retaining neonates were

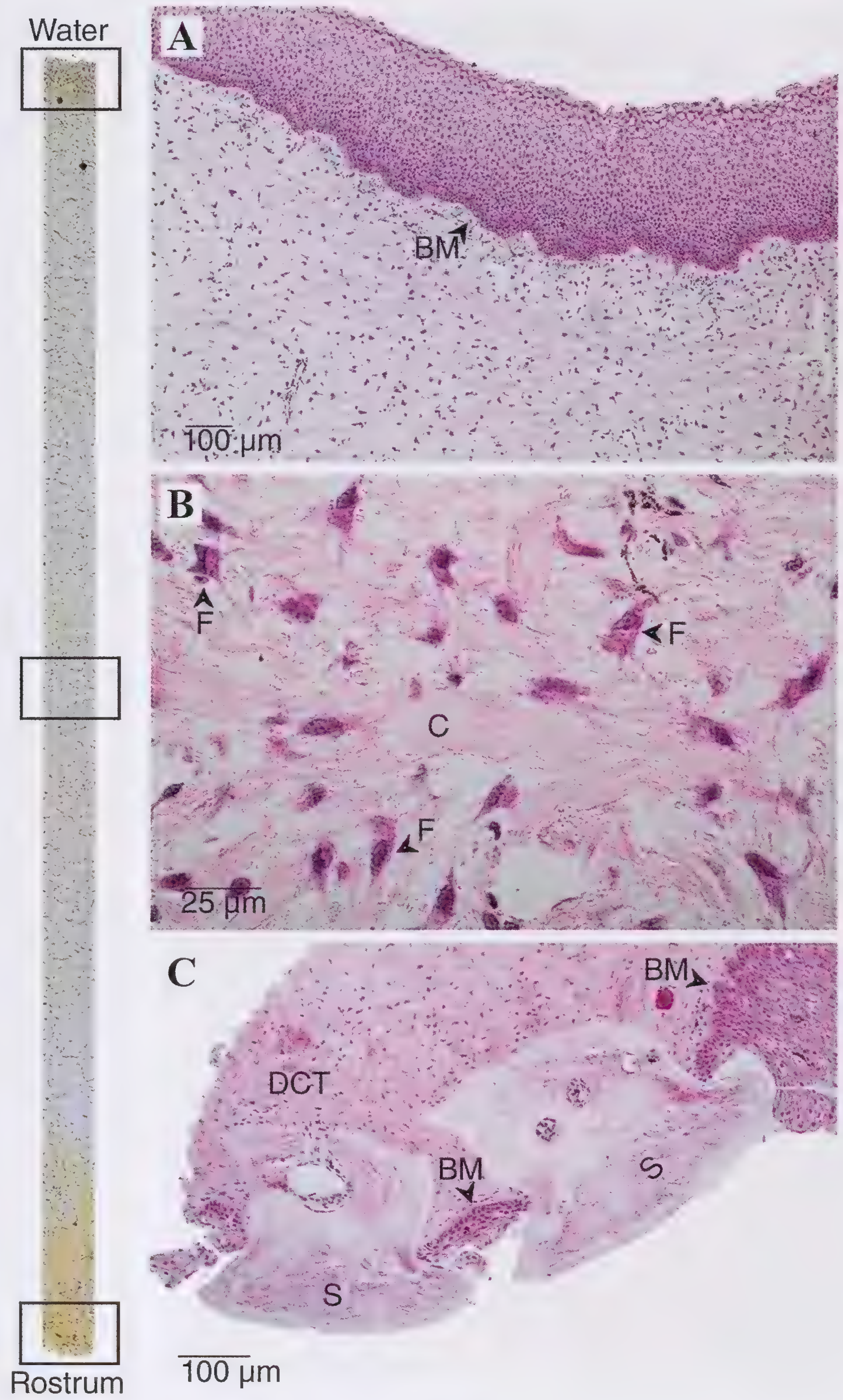

Figure 4

Cross sections of the embryonic rostral sheaths of neonate smalltooth sawfish (*Pristis pectinata*) showing the morphology of the (**A**) outermost, (**B**) central, and (**C**) innermost areas. The boxes outlined in black and adjacent to the micrographs are meant to aid orientation and correspond to the general area of the sheath from which each micrograph came. The morphological features shown include the basement membrane (BM), fibrocytes (F), collagen-like fibers (C), dense connective tissue (DCT), and scales (S). These cross sections were stained with standard hematoxylin and eosin.

captured in productive estuarine nursery areas with ample food supplies; therefore, a few days are unlikely to be detrimental to early survivorship, especially if some residual maternal resources, such as an internal yolk sac, are available.

Rostral teeth and scales presumably form and calcify early in gestation (Miller, 1995). For this reason, the sheath likely evolved with a robust, firm connection to the rostrum to maximize its durability during a 1-year gestation period (Brame et al., 2019). On the basis of these data, we describe the sheath and its connection to the rostrum as a continuum between the sheath and the rostrum rather than as each being a discrete entity. This approach allowed us to describe the morphology and composition of the sheath and to show a theoretical sequence of sheath deterioration and exposure of the rostral components, despite the limitations of studying a species that is listed as endangered under the U.S. Endangered Species Act (Federal Register, 2003) and as critically endangered on the IUCN Red List of Threatened Species (Carlson et al., 2022) (e.g., low sample size and inability to sample through the sheath deep into the rostra of live specimens). Still, questions remain. For example, we were not able to fully elucidate all aspects of the connectivity of the sheath to the rostrum because there is skin on the rostrum and the sheath also appears to be skin, indicating a "double skin" morphology. In addition, the sheath contains some scales (see Figure 3) that are likely lost as the sheath fully deteriorates because of the intimate association between the sheath and rostral scales.

Notably, during a parturition event in the field, we observed the birth of 2 neonates, an individual with a complete sheath and another with the tips of its rostral teeth already exposed, indicating that the sheath sometimes begins to recede in utero. This observation supports our contention that these 2 neonates were not born prematurely.

On one occasion, a rostrum with a damaged sheath was observed (see Figure 1F). We hypothesize that this damage occurred because this individual began using the rostrum regularly before the sheath deteriorated much. The damage did not occur during capture because this fish was caught by hand.

We observed deterioration and sloughing of the rostral sheath of one neonate smalltooth sawfish. This individual was first caught (and tagged) in the Peace River, Florida, where neonates tend to remain (Scharer et al., 2017); therefore, we returned to the area to acoustically relocate the individual. Observations made during a series of recaptures corroborate our hypothesis that the sheath normally recedes evenly across the entire length of the rostrum and allowed us to refine the shedding time. Previous observations of an individual recaptured after 10 d have been used to conservatively estimate a shedding time of within 2 weeks (Poulakis et al., 2011), but our latest research has shortened that estimate. On the basis of the observation time series and observations from other captured neonates, we hypothesize that the last layer of sheath to deteriorate corresponds to the dense connective tissue layer at the junction between the rostrum and sheath (see Figures 4C and 6A).

The protected status of the smalltooth sawfish makes obtaining specimens and resolving interpretation uncertainties inherently difficult because there are no regular sources of specimens, such as recreational or commercial fisheries. In this study, one of the most difficult things to describe was the association between the

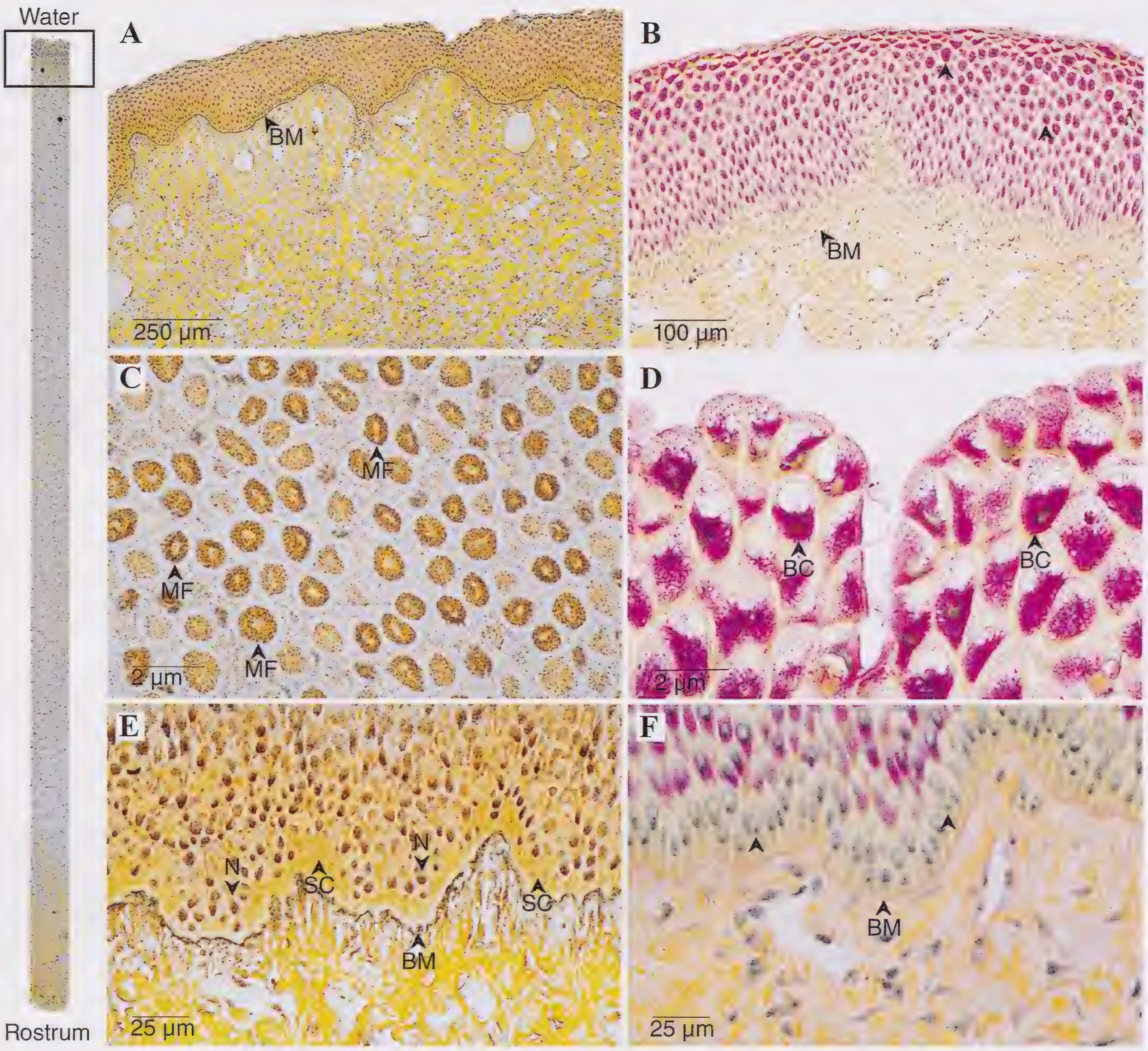

Figure 5

Cross sections of the outer layer of the embryonic rostral sheaths of neonate smalltooth sawfish (*Pristis pectinata*). The cross sections were stained with a silver-based reticulin stain (left panels) to highlight structural tissue and basement membranes and periodic acid Schiff's hematoxylin and metanil yellow (PASMY, right panels) to identify carbohydrates. (**A**) This micrograph shows the outermost portion of the sheath above a basement membrane (BM) and the cells within it. (**B**) This micrograph shows the spherical epithelial cells above the BM that are in direct contact with the environment; the magenta color indicates that cells are PASMY-positive (i.e., they contain carbohydrates). The innermost epithelial cells in the yellow area above the BM are columnar and PASMY-negative. About half the spherical cell layer (~8 cells thick), closest to the water, are about twice the diameter of the more interior spherical cells (compare the diameters of cells at unlabeled arrowheads). (**C**) This micrograph shows spherical cells that have cytoskeletal support with microfilaments (MF). (**D**) In this close-up view of the outermost spherical cells shown in panel B, about half the area of cytoplasm of these cells is PASMY-positive, contains the nuclei, and contains glycoproteins, and the other half is PASMY-negative (BC). (**E**) The columnar epithelial cells in this micrograph contain densely and darkly stained nuclei (N). The columnar cells are hypothesized to be derived from stem cells (SC) adjacent to the basement membrane and appear to create and maintain the entire outer layer of the sheath. (**F**) This micrograph provides a close-up view of the innermost epithelial cells (indicated with unlabeled arrowheads) and their columnar shape in the outer layer of the sheath (yellow area) shown in panel B. The box outlined in black and adjacent to the micrographs is meant to aid orientation and corresponds to the general area of the sheath from which each micrograph came.

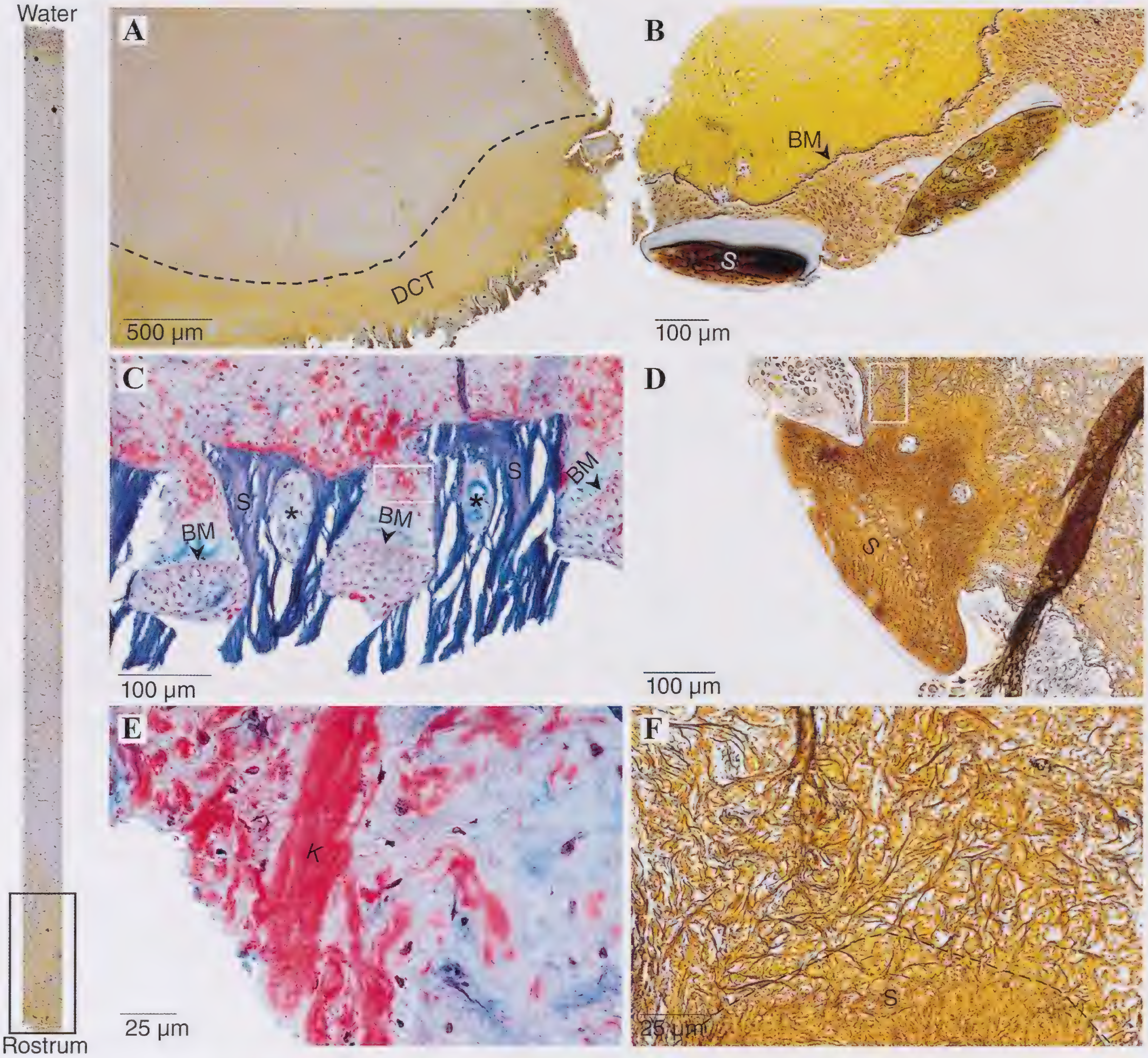

Figure 6

Cross sections of the innermost layer of the embryonic rostral sheaths of neonate smalltooth sawfish (*Pristis pectinata*). (**A**) This micrograph shows the layer of dense connective tissue (DCT, below the dashed line) near the scales (which are dark brown along the margin) of the rostrum. (**B**) In this micrograph, the basement membrane (BM), which produces the outer layer of the sheath, is continuous and exists behind the rostral scales (S). Note how groups of spherical cells in the outer layer curve around the largest scale, helping to secure the sheath to the rostrum. (**C**) The BM appears between the scales in this micrograph, which also shows the locations of pulp cavities of scales (*). The scales were not decalcified in this early sample. The box outlined in white indicates the approximate area shown in panel E. (**D**) The scale in this micrograph is embedded in interwoven collagen- and keratin-like connective tissues. The box outlined in white indicates the approximate area shown in panel F. The dark area on the right side of the micrograph is folded tissue. (**E**) This micrograph provides a close-up view of the presence of keratin (K) in the area outlined in panel C. (**F**) In this micrograph, the partial scale (indicated with the dashed line) at the bottom of the panel blends in with the interwoven tissues of the DCT layer. The cross section in panel A was stained with periodic acid Schiff's hematoxylin and metanil yellow, the cross sections in panels C and E were stained with Masson's trichrome dye, and the cross sections in panels B, D, and F were stained with a silver-based reticulin stain. The box outlined in black and adjacent to the micrographs is meant to aid orientation and corresponds to the general area of the sheath from which each micrograph came. Collectively, aspects of the outer and inner layers of the sheath establish a firm connection between the sheath and the rostrum. The sheath is not easily separated from the rostrum and cannot be removed manually.

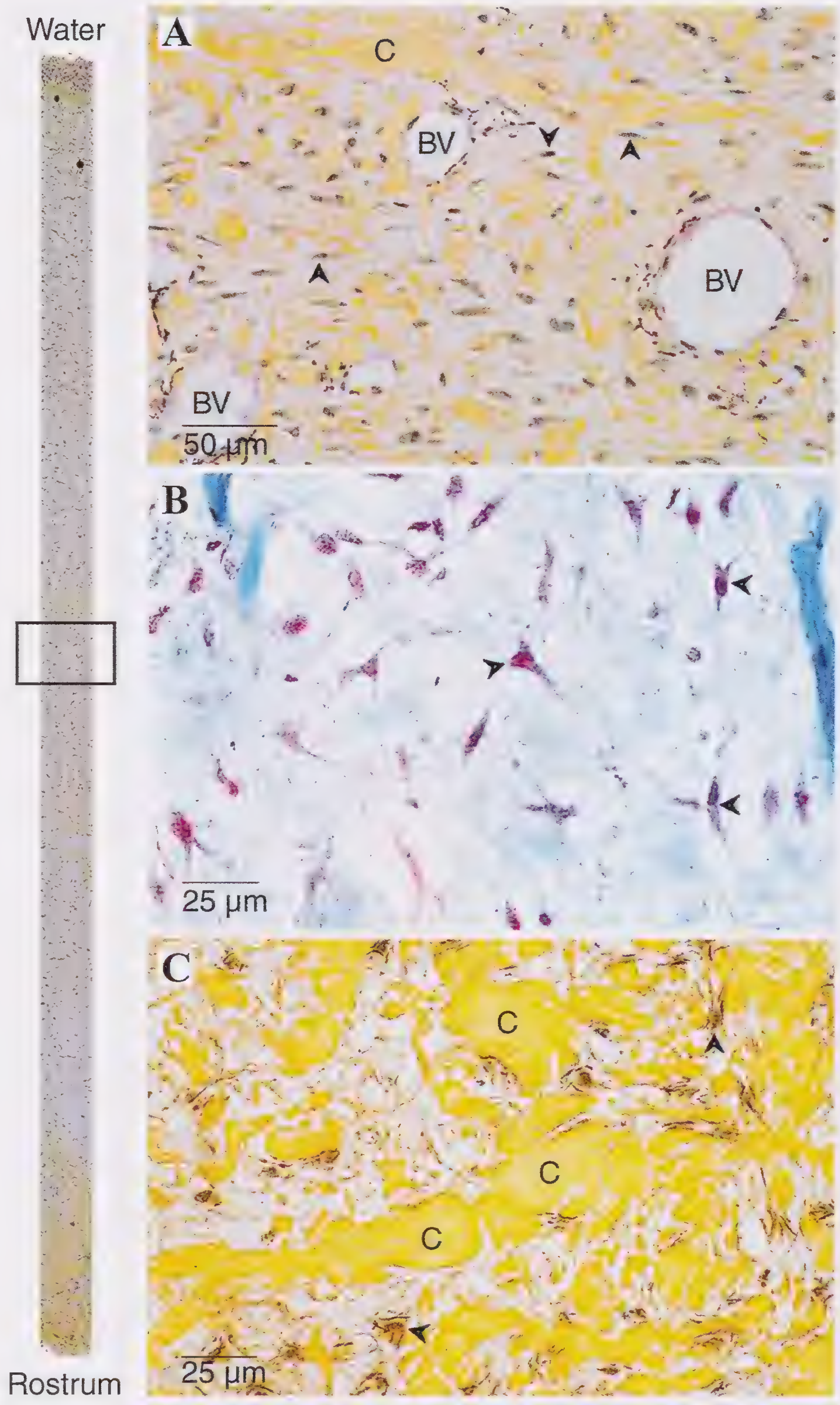

Figure 7

Cross sections of the central, inner structural tissue layer of the embryonic rostral sheaths of neonate smalltooth sawfish (*Pristis pectinata*) stained with (**A**) periodic acid Schiff's hematoxylin and metanil yellow, (**B**) Masson's trichrome dye, and (**C**) a silver-based reticulin stain. The micrographs show collagen-like fibers (C) and fibrocytes (indicated with unlabeled arrowheads) interspersed with blood vessels (BV). The box outlined in black and adjacent to the micrographs is meant to aid orientation and corresponds to the general area of the sheath from which each micrograph came. The fibrocytes can also be seen in a cross section stained with standard hematoxylin and eosin in Figure 4B.

sheath and the rostrum—where does each begin and end? In the future, if dead gravid females are obtained, and if the embryos can be adequately preserved, examining cross sections of the sheath that extend into the rostrum may help answer this question. Similarly, if the endogenous origin of the sheath can be determined, perhaps the hypothesis of a double skin morphology could be resolved also.

Conclusions

The intact, embryonic rostral sheath of sawfishes is not easily removed manually, a finding that is inconsistent with terminology used in previous descriptions. For example, to describe a structure as "gelatinous" or a simple "membrane" (see Southwell, 1910; Hussakof, 1912; Setna and Sarangdhar, 1948; Abel and Grubbs, 2020) implies fragility and weak attachments to the underlying tissue. Given its morphology, the embryonic sheath of the smalltooth sawfish is a skin-like, ephemeral embryonic organ with specialized structure rather than a discrete layer of surrounding tissue or secretions. Whether analogous chondrichthyan embryonic sheaths of tail spines of rays (e.g., *Hypanus* spp.; *Rhinoptera* spp.; round stingray, *Urobatis halleri*; Babel, 1967; senior author, unpubl. data), dorsal-fin spines of dogfishes (e.g., spiny dogfish, *Squalus acanthias*; roughskin dogfish, *Cirrhigaleus asper*; velvet belly lanternshark, *Etmopterus spinax*; Whitley, 1940; Gudger, 1951; Castro[3]), or oral teeth of neonates in this class (e.g., bull shark, *Carcharhinus leucas*; A. Wooley, personal observ.) have similar morphologies is unknown. Their study and comparison to the embryonic rostral sheath of the smalltooth sawfish would inform our understanding of their form and function.

Resumen

Los rostros alargados evolucionaron en diversos grupos de animales como adaptaciones para la alimentación, la defensa, la percepción sensorial y la reproducción. Los rostros de los peces sierra tienen a lo largo de sus márgenes laterales, dentículos dérmicos, denominados dientes rostrales. Los embriones tienen una cubierta o envoltura para los dientes rostrales calcificados durante la gestación, que persiste hasta después del parto. Se sabe poco sobre la morfología y composición de la cubierta. Durante 18 años de marcado de juveniles de pez sierra peine (*Pristis pectinata*), se documentaron las cubiertas de 36 neonatos con longitudes totales estiradas de 581-812 mm, y se recogieron muestras de 6 especímenes para su evaluación en laboratorio. La cubierta multicapa, similar a la piel, la cual no puede extraerse manualmente con facilidad, tiene una capa interna vascularizada de tejido conectivo compuesta principalmente de proteínas fibrosas (ej. colágeno, reticulina y queratina) rodeada por una capa externa de células epiteliales columnares y esféricas que recubren una membrana basal. Las células columnares contienen cromatina condensada y se diferencian en las células esféricas más externas que contienen carbohidratos. Tras el nacimiento, la cubierta se desprende uniformemente a lo largo de 4 días, mediante descamación y apoptosis, exponiendo completamente los dientes rostrales. La cubierta es un

---

[3] Castro, J. I. 2023. Personal commun. Southeast Fish. Sci. Cent., Natl. Mar. Fish. Serv., NOAA, 263 13th Ave. South, St. Petersburg, FL 33701.

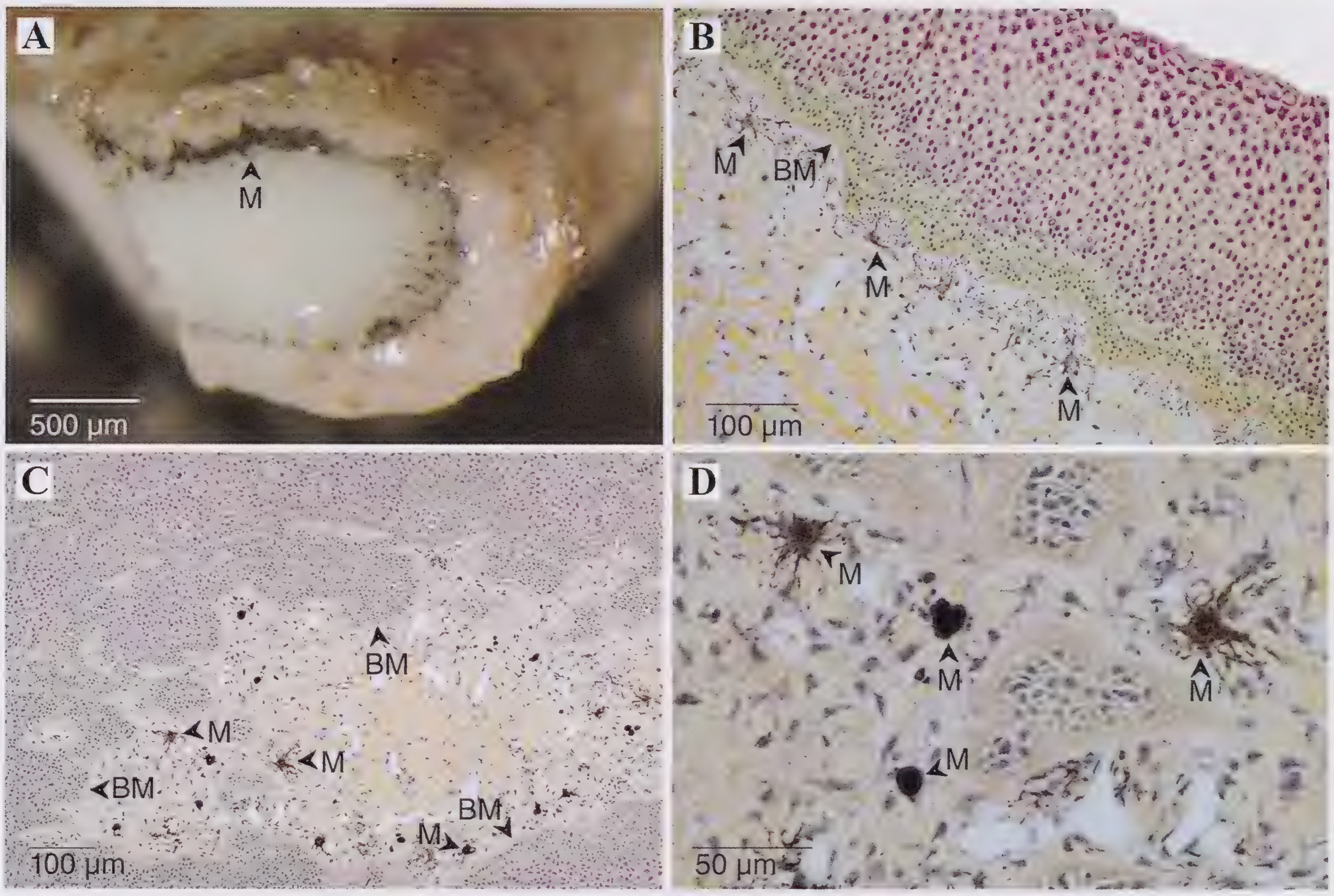

Figure 8

(**A**) Photograph and (**B–D**) histological sections of the embryonic rostral sheaths of neonate smalltooth sawfish (*Pristis pectinata*). The cross sections in panels B and D and the tangential section in panel C show the prevalence of melanocytes (M) in the inner connective tissue layer, just below the basement membrane (BM). The histological sections were stained with periodic acid Schiff's hematoxylin and metanil yellow.

órgano embrionario efímero que protege a la hembra y los embriones de lesiones durante la gestación y el nacimiento.

Acknowledgments

We thank N. Perry and S. Modla for their assistance with sample processing. Expertise was provided by M. Boggs with micro-computed tomography and by D. Powel with energy-dispersive X-ray spectroscopy. We thank D. Adams, M. Bakenhaster, H. Grier, S. Kajiura, Y. Kiryu, L. Parenti, and 2 anonymous reviewers for assistance interpreting micrographs and improving earlier versions of the manuscript. This research was supported primarily by funding from the National Marine Fisheries Service through Section 6 (Cooperation with the States) of the U.S. Endangered Species Act under the following grant awards to the Florida Fish and Wildlife Conservation Commission: NA06NMF4720032, NA10NMF4720032, NA13NMF4720047, NA16NMF4720062, NA19NMF4720108, and NA22NMF4720102. Microscopy and tomography access at the University of Delaware was supported by grants from the National Institute of General Medical Sciences, National Institute of Health (NIH-NIGMS: P20 GM103446), the NIGMS and NIH-NIGMS Centers of Biomedical Research Excellence (P20 GM139760), and the state of Delaware.

Literature cited

Abel, D. C., and R. D. Grubbs.
2020. Shark biology and conservation: essentials for educators, students, and enthusiasts, 430 p. Johns Hopkins Univ. Press, Baltimore, MD.

Babel, J. S.
1967. Reproduction, life history, and ecology of the round stingray, *Urolophus halleri* Cooper. Calif. Dep. Fish Game, Fish Bull. 137, 104 p.

Bigelow, H. B., and W. C. Schroeder.
1953. Fishes of the western North Atlantic. Part 2: sawfishes, guitarfishes, skates and rays, chimaeroids, 588 p. Sears Found. Mar. Res., Yale Univ., New Haven, CT.

Brame, A. B., T. R. Wiley, J. K. Carlson, S. V. Fordham, R. D. Grubbs, J. Osborne, R. M. Scharer, D. M. Bethea, and G. R. Poulakis.
2019. Biology, ecology, and status of the smalltooth sawfish *Pristis pectinata* in the USA. Endanger. Species Res. 39:9–23.

Breder, C. M., Jr.
1952. On the utility of the saw of the sawfish. Copeia 1952:90–91.

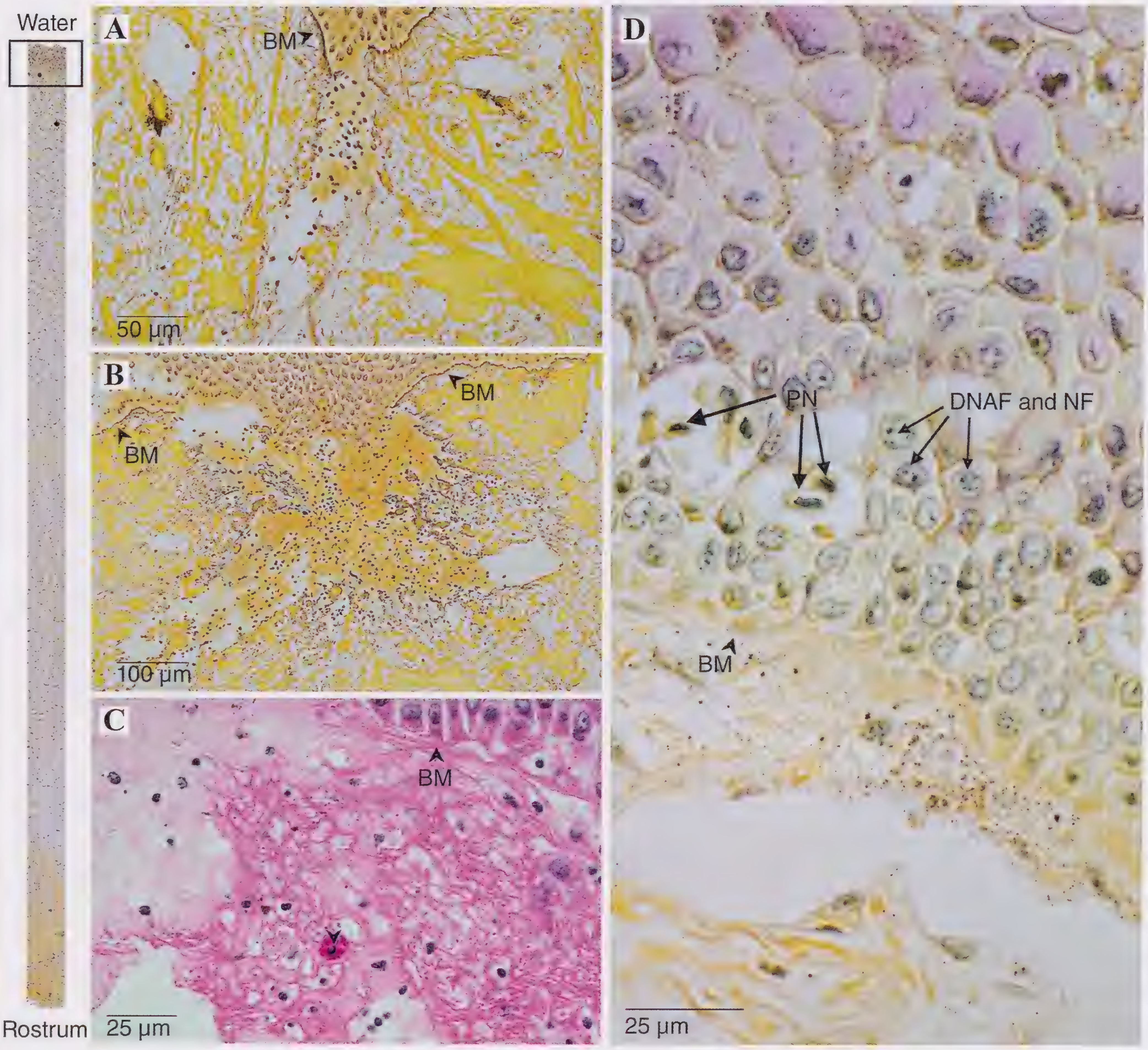

Figure 9

Cross sections of degraded portions of the embryonic rostral sheaths of neonate smalltooth sawfish (*Pristis pectinata*). (**A** and **B**) The integrity of the outer and inner layers of the sheath is disturbed in these micrographs, a result of the failed coherence of the basement membrane (BM) caused by the apoptosis that occurs during sheath degradation. (**C**) This micrograph shows an eosinophil (indicated with the unlabeled arrowhead). (**D**) In this micrograph, signs of apoptosis, including pyknotic nuclei (PN), DNA fragmentation (DNAF), and nuclear fading (NF), are apparent. The box outlined in black and adjacent to the micrographs is meant to aid orientation and corresponds to the general area of the sheath from which each micrograph came. The cross sections in panels A and B were stained with a silver-based reticulin stain, the cross section in panel C was stained with standard hematoxylin and eosin, and the cross section in panel D was stained with periodic acid Schiff's hematoxylin and metanil yellow.

Carlson, J., M. P. Blanco-Parra, R. Bonfil-Sanders, R. Charles, P. Charvet, M. Chevis, N. K. Dulvy, M. Espinoza, V. Faria, F. Ferretti, et al.
2022. *Pristis pectinata*. The IUCN Red List of Threatened Species 2022:e.T18175A58298676. [Available from website.]

Castro, J. I.
2011. The sharks of North America, 613 p. Oxford Univ. Press, New York.

Dean, M. N., J. J. Bizzarro, and A. P. Summers.
2007. The evolution of cranial design, diet, and feeding mechanisms in batoid fishes. Integr. Comp. Biol. 47:70–81.

Federal Register.
2003. Endangered and threatened species; final endangered status for a distinct population segment of smalltooth sawfish (*Pristis pectinata*) in the United States. Fed. Regist. 68:15674–15680. [Available from website.]

Gudger, E. W.
1951. How difficult parturition in certain viviparous sharks and rays is overcome. J. Elisha Mitchell Sci. Soc. 67:56–86.

Hancock, T. L., G. R. Poulakis, R. M. Scharer, S. G. Tolley, and H. Urakawa.
2019. High-resolution molecular identification of smalltooth sawfish prey. Sci. Rep. 9:18307.

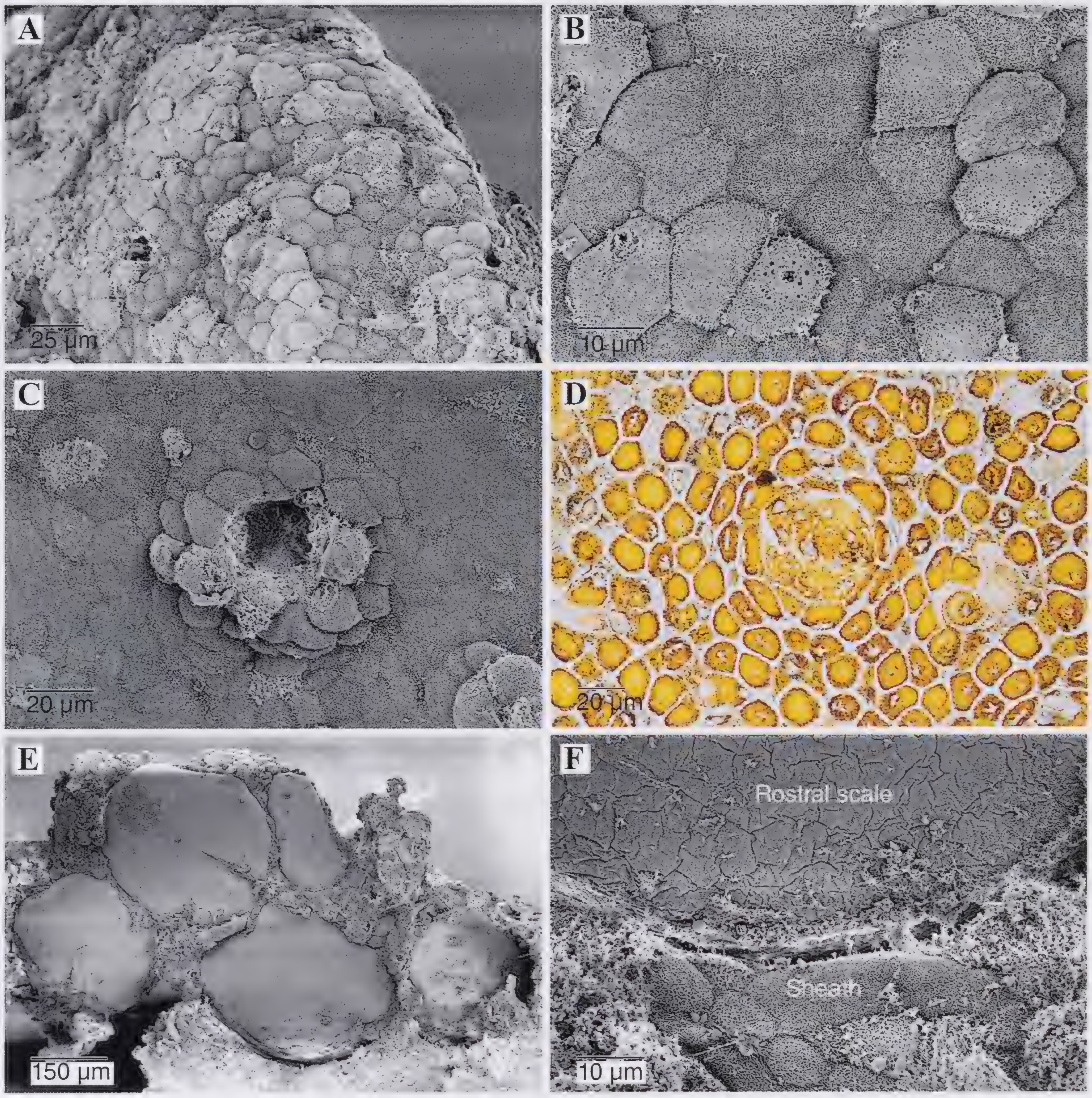

Figure 10

Scanning electron micrographs and a histological image of a cross section of the embryonic rostral sheaths of neonate smalltooth sawfish (*Pristis pectinata*). In (**A**) the first micrograph and (**B**) the close-up view, the outermost spherical epithelial cells have an uneven texture, a result of the cells starting to lose their integrity shortly after the birth of the fish. Evidence of degradation is also visible in (**C**) the scanning electron micrograph and (**D**) the histological image (of a cross section stained with a silver-based reticulin stain) that show surface pores and in (**E**) the micrograph that shows rostral scales. (**F**) This micrograph shows the junction between the sheath and a rostral scale as the sheath was degrading.

Hussakof, L.
1912. Note on an embryo of *Pristis cuspidatus*. Bull. Am. Mus. Nat. Hist. 31:327–330.

Kells, V., and K. Carpenter.
2011. A field guide to coastal fishes: from Maine to Texas, 446 p. Johns Hopkins Univ. Press, Baltimore, MD.

Kolmann, M. A., D. R. Huber, M. N. Dean, and R. D. Grubbs.
2014. Myological variability in a decoupled skeletal system: batoid cranial anatomy. J. Morphol. 275:862–881.

Last, P. R., and J. D. Stevens.
2009. Sharks and rays of Australia, 2nd ed., 644 p. Harvard Univ. Press, Cambridge, MA.

Lyons, K., A. S. Galloway, D. H. Adams, E. A. Reyier, A. M. Barker, D. S. Portnoy, and B. S. Frazier.
2020. Maternal provisioning gives young-of-the-year hammerheads a head start in early life. Mar. Biol. 167:157.

Miller, W. A.
1974. Observations on the developing rostrum and rostral teeth of sawfish: *Pristis perotteti* and *P. cuspidatus*. Copeia 1974:311–318.
1995. Rostral and dental development in sawfish (*Pristis perotteti*). J. Aquaric. Aquat. Sci. 7:98–107.

Poulakis, G. R., P. W. Stevens, A. A. Timmers, T. R. Wiley, and C. A. Simpfendorfer.
2011. Abiotic affinities and spatiotemporal distribution of the endangered smalltooth sawfish, *Pristis pectinata*, in a southwestern Florida nursery. Mar. Freshw. Res. 62:1165–1177.

Poulakis, G. R., H. Urakawa, P. W. Stevens, J. A. DeAngelo, A. A. Timmers, R. D. Grubbs, A. T. Fisk, and J. A. Olin.
2017. Sympatric elasmobranchs and fecal samples provide insight into the trophic ecology of the smalltooth sawfish. Endanger. Species Res. 32:491–506.

Quintero-Hunter, I., H. Grier, and M. Muscato.
    1991. Enhancement of histological detail using metanil yellow as a counterstain in periodic acid Schiff's hematoxylin staining of glycol methacrylate tissue sections. Biotech. Histochem. 66:169–172.

Scharer, R. M., P. W. Stevens, C. P. Shea, and G. R. Poulakis.
    2017. All nurseries are not created equal: large-scale habitat use patterns in two smalltooth sawfish nurseries. Endanger. Species Res. 34:473–492.

Setna, S. B., and P. N. Sarangdhar.
    1948. Observations on the development of *Chiloscyllium griseum* M. & H., *Pristis cuspidatus* Lath. and *Rhynchobatus djiddensis* (Forsk.). Rec. Indian Mus. 46:1–23.

Sheehan, D. C., and B. B. Hrapchak.
    1987. Theory and practice of histotechnology, 2nd ed., 481 p. Battelle Press, Columbus, OH.

Slaughter, B. H., and S. Springer.
    1968. Replacement of rostral teeth in sawfishes and sawsharks. Copeia 1968:499–506.

Southwell, T.
    1910. A descriptive note on the capture of a large saw-fish (*Pristis cuspidatus*) containing intra-uterine embryos. Spolia Zeylan 6:137–139.

Thorson, T. B.
    1976. The status of the Lake Nicaragua shark: an updated appraisal. *In* Investigations of the ichthyofauna of Nicaraguan lakes (T. B. Thorson, ed.), p. 561–574. Univ. Nebraska-Lincoln, Lincoln, NE.

Welten, M., M. M. Smith, C. Underwood, and Z. Johanson.
    2015. Evolutionary origins and development of saw-teeth on the sawfish and sawshark rostrum (Elasmobranchii; Chondrichthyes). R. Soc. Open Sci. 2:150189.

Whitley, G. P.
    1940. The fishes of Australia. Part 1. The sharks, rays, devilfish, and other primitive fishes of Australia and New Zealand, 280 p. R. Zool. Soc. N.S.W., Sydney, Australia.

Williams, A. B.
    1984. Shrimps, lobsters, and crabs of the Atlantic coast of the eastern United States, Maine to Florida, 550 p. Smithson. Inst. Press, Washington, D.C.

Wueringer, B. E., L. Squire, Jr., S. M. Kajiura, N. S. Hart, and S. P. Collin.
    2012. The function of the sawfish's saw. Curr. Biol. 22:R150–R151.

National Marine
Fisheries Service
NOAA

Fishery Bulletin
established in 1881

Spencer F. Baird
First U.S. Commissioner
of Fisheries and founder
of *Fishery Bulletin*

An identification guide to the larvae of lanternfishes (Teleostei: Myctophidae) from the Subtropical Convergence: subfamilies Lampanyctinae and Notolychninae

Yana Yu. Bolshakova (contact author)[1]
Artem M. Prokofiev[2]

Email address for contact author: yanusrunaa@mail.ru

[1] Shirshov Institute of Oceanology
Russian Academy of Sciences
36 Nakhimovskyi Prospekt
Moscow 117997, Russia

[2] Severtsov Institute of Ecology and Evolution
Russian Academy of Sciences
33 Leninsky Prospekt
Moscow 119071, Russia

Abstract—Descriptions of the lanternfish larvae of the subfamilies Lampanyctinae (12 species) and Notolychninae (1 species) that can be found in the Subtropical Convergence (STC) are presented: *Bolinichthys supralateralis*, *Ceratoscopelus* gr. *townsendi*, *Lampadena* sp., *Lampanyctus alatus*, *L. ater*, *L. australis*, *L.* gr. *achirus*, *L. intricarius*, *L. festivus*, *L. pusillus*, *Lampanyctus* sp. D, *Lepidophanes guentheri*, and *Notolychnus valdiviae*. Also provided is an identification key based on larval characters for all lanternfish subfamilies. We propose the use of a separate key for the postflexion larvae of all known genera of the round-eyed lanternfish subfamilies Diaphinae, Gymnoscopelinae, Lampanyctinae, and Notolychninae. For each genus, general characteristics of larval morphology are given. Species descriptions include the key characters for identification, variation in meristic characters, pigmentation, and other features important for diagnosis of Myctophidae at their larval stages. Photographs of the most important diagnostic features are provided for each species. The taxonomy of 4 problematic species in the area, *C.* gr. *townsendi*, *Lampanyctus* gr. *achirus*, *L. intricarius*, and *Lampanyctus* sp. D, is discussed. Preflexion, flexion, and postflexion stages of an unidentified *Lampadena* sp. from the northern limit of the STC are described for the first time; these larvae may belong to 1 of 3 species (*L. dea*, *L. notialis*, and *L. speculigera*) for which larvae have not yet been identified. The distribution of Lampanyctinae and Notolychninae in the STC is summarized.

The lanternfish family Myctophidae is one of the most speciose lineages of mesopelagic fish species. It is composed of 34 genera, currently comprising over 250 valid species (Fricke et al., 2023). Lanternfish species can be found circumglobally in waters of oceanic salinity from the surface down to depths of around 2000 m and, in abundance and biomass, make up at least 30–50% of all fishes caught in mid-water trawl nets (Bekker, 1983). Larvae of myctophids are also abundant in samplings of ichthyoplankton tows, as an obligatory component of the catches in small-mesh fishing gears (Moser and Ahlstrom, 1974). A wide set of morphological features for the identification of Myctophidae at the early stages of development has been described (Moser et al., 1984), and several guides have been prepared for select areas of the world's oceans, including the Northeast Atlantic Ocean (Russell, 1976), Northwest Atlantic Ocean (Fahay, 1983, 2007), western central Atlantic Ocean (Richards, 2005), eastern central Atlantic Ocean (Rodríguez, 2023) southwest Atlantic Ocean (Bonecker and Castro, 2006), southeast Atlantic Ocean (Benguela Current Region) (Olivar and Fortuño, 1991), central North Pacific Ocean (Miller et al., 1979), eastern North Pacific Ocean (Matarese et al., 1989; Moser and Ahlstrom, 1996), western North Pacific Ocean (Ozawa, 1986; Okiyama, 1988), and Southern Ocean (Efremenko, 1983). However, the larvae have not yet been described for a number of species, and there are no guides for some areas in the tropical, southern subtropical, and temperate Indo-Pacific.

The Subtropical Convergence (STC), a frontal zone between subantarctic and tropical water masses, is one such area. Both wide-tropical and subantarctic species of myctophids can be found in the transitional or mixed water zone within and off the STC. At least 80 species of myctophids from the STC are known, but early life stages have been described for only 60% of them. Only a few previously published papers contain descriptions of lanternfish larvae from the STC (Pertseva-Ostroumova, 1977; Belyanina and Kovalevskaya, 1979; Bolshakova and Evseenko, 2015, 2020; Bolshakova et al., 2021), and a

Manuscript submitted 21 October 2023.
Manuscript accepted 17 May 2024.
Fish. Bull. 122:89–118 (2024).
Online publication date: 4 June 2024.
doi: 10.7755/FB.122.3.3

The views and opinions expressed or implied in this article are those of the author (or authors) and do not necessarily reflect the position of the National Marine Fisheries Service, NOAA.

few guides cover the border areas to the north (Olivar and Fortuño, 1991) and south (Efremenko, 1983; Kellermann, 1990) of the STC.

Herein, we combine the existing data on myctophid larvae from the STC, provide photographic illustrations of known larvae, supplementing them with descriptions and identification keys. This material will make identification of the early stages of development of this key group of mesopelagic fishes easier for a wide community of marine biologists.

The larvae of lanternfishes can be divided into 2 major groups on the basis of the shape of the eye: narrow-eyed (dorsoventrally extended elliptical eyes) and round-eyed (more or less circular eyes) (Moser and Ahlstrom, 1970, 1974). A mass of choroid tissues may develop around the eye in a member of both groups; however, such a mass is usually noticeable in narrow-eyed larvae (especially in *Centrobranchus*, *Dasyscopelus*, and *Gonichthys*) but is mostly inconspicuous, in the form of a thin crescent on the ventral side of the eye, in round-eyed larvae (except for *Lobianchia* and *Triphoturus*, with their well-developed choroid tissues). With few exceptions (*Loweina* and *Notolychnus*), the narrow- and round-eyed larvae correspond to the subfamilies Myctophinae and Lampanyctinae, respectively.

The recognition of 2 subfamilies was originally based on a wide set of morphological characters (Paxton, 1972; Bekker, 1983; Paxton et al., 1984; Stiassny, 1996; Yamaguchi, 2000) and was later supported by molecular analyses (Poulsen et al., 2013; Denton, 2014). Three tribes (Electronini, Gonichthyini, and Myctophini) have been recognized within Myctophinae, and 4 tribes (Lampanyctini, Notolychnini, Diaphini, and Gymnoscopelini) have been recognized within Lampanyctinae (Paxton, 1972). Findings from 7-locus molecular phylogeny support the recognition of these tribes, except the paraphyletic Gonichthyini and Myctophini (Denton, 2014). Results of the most recent treatment (Martin et al., 2018) support the monophyly of Diaphini and Myctophinae and raise the rank of all lampanyctine tribes to subfamilies: Diaphinae, Gymnoscopelinae, Notolychninae, and Lampanyctinae *sensu novo*. This communication covers the species from the subfamilies Lampanyctinae and Notolychninae. We plan to treat the morphologically similar larvae of the round-eyed subfamilies Diaphinae and Gymnoscopelinae and the narrow-eyed taxa (subfamily Myctophinae) in forthcoming works.

Materials and methods

Geographic coverage

The STC is almost continuously traced throughout the globe at latitudes of about 35–45°S. In fact, this area is the one between the anticyclonic circulation of the southern parts of the Atlantic, Indian, and Pacific Oceans and the cyclonic circulation of the Antarctic Circumpolar Current, which separates the warm temperate subtropical region from the cool-temperate subantarctic region. It forms the geographic limit to the influence of subantarctic surface water and consists of a strong horizontal gradient in temperature, salinity, and nutrients. The limits of the STC were discussed by Backus (1986), Deacon (1966), and McGinnis (1982) and were further summarized by Longhurst (1998). He provided a detailed overview of the oceanography, geology, and biogeography of the STC. The geographic coverage of the atlas presented herein (Fig. 1) follows the limits of the STC provided by Longhurst (2007, 543) and Sutton et al. (2017, 89).

Specimens

The original data are based on the ichthyoplankton collection housed in the Shirshov Institute of Oceanology, Russian Academy of Sciences, Moscow. The previously published descriptions of the larvae of each species known from the STC were compiled in order to estimate the range of morphological variation. Information about the studied material, including the numbers of specimens, expeditions, localities, depth, and more, and the sources of the previously published descriptions of species from the STC are summarized in Table 1. The larval stage is divided into 3 substages over the development of the caudal fin (Kendall et al., 1984): preflexion (PrF) is the larval stage before the beginning of the bending of the terminal notochord, flexion (F) is the stage of bending of the notochord, and postflexion (PoF) is the stage after the end of the bend of the notochord. We developed a complete set of diagnostic traits for larvae at the postflexion stage, and for the purposes of the atlas, we present herein the illustrations and descriptions of larvae at this stage. If descriptions of the earlier stages existed in the literature, we provide the references for them in the species description, before the "Identification" section. Details about the collection of examined specimens, such as dates and general locations, are provided in Suppl. Table (online only).

Morphology

Counts and measurements follow the standard practice (Nafpaktitis, 1973; Fahay, 1983; Moser and Ahlstrom, 1996; Olivar and Beckley, 1997; Leis and Carson-Ewart, 2000). The scheme of measurements is shown in Figure 2. The body depth at pectoral fin base (BD) is indicated as follows: slender, BD <19% standard body length (SL); moderate, BD 19–24% SL; and deep, BD >24% SL. Eye shapes were determined according to Moser and Ahlstrom (1970). The terminology of photophores and luminous glands follows that of previous authors, notably Bolin (1939), Fraser-Brunner (1949), Nafpaktitis (1968), Paxton (1972), and Bekker (1983), and is presented in Figure 3. The pigment groups characteristic for myctophid larvae are depicted in Figure 4. Definitions of pigment groups follow Bolshakova and Prokofiev (2023).

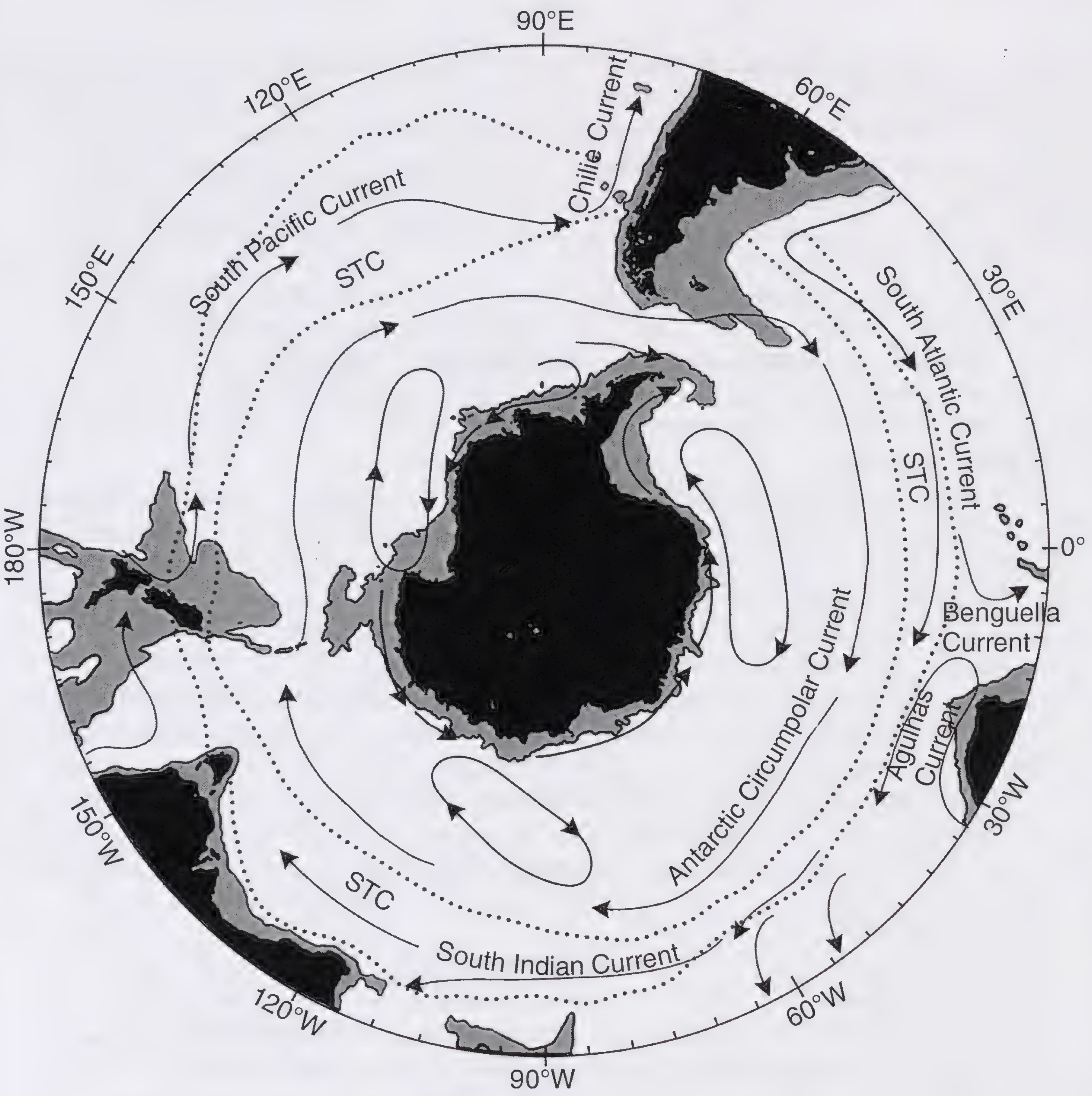

Figure 1

Schematic map of the study area showing the borders of the Subtropical Convergence (STC; dotted lines) (Deacon, 1966; Longhurst, 1998; Sutton et al., 2017), where larvae of the species of Lampanyctinae and Notolychninae examined in this study can be found. The arrows indicate the direction of the main currents (Steele et al., 2010).

Sequence of descriptions

Species descriptions In each description, the synonymic list provides all references containing morphological descriptions or figures of the larvae of a species under consideration, with indication of the substages described and the geographic area of sampling.

The "Identification" section emphasizes the key features for the identification of a species, meaning the most easily observable characters distinguishing a species from its congeners or other similar members of the family.

The "General characters" section contains meristic counts, size at which the photophores formed and sequence of their formation, size at which the fin rays developed, length at transformation, and some additional morphological characteristics of larvae useful for their identification. For genera, the most notable diagnostic features are highlighted in bold. Meristic data were taken from both the specimens studied and literature sources and include the data for the adults of the described larvae presented by Wisner (1976), Nafpaktitis et al. (1977), Hulley (1981), McGinnis (1982), Bekker (1983), and Zahuranec (2000).

The "Pigmentation" section provides a description of pigment pattern according to the nomenclature of Bolshakova and Prokofiev (2023). Before each pigment group, the number of pigment cells is indicated, if their number differs from one, and whether they are a paired or unpaired is noted. The order of each description is as follows: craniovisceral group with medullar, then medioventral group with abdominal, then mediodorsal group, lateral group, intervertebral group, and fin pigmentation.

The "General distribution" section provides information on the general distribution, with summary of the geographic range of a species under consideration, and on occurrence in the STC with clarification of the findings of a species directly in the STC.

Table 1

Number of specimens, standard body length (SL), geographic coordinates, depth layer, research vessel, expedition number, station (sta.), and date of collection for myctophid larvae in the subfamilies Lampanyctinae and Notolychninae from inside and outside the Subtropical Convergence (STC) and the sources of previously published descriptions. Original data from this study are based on the ichthyoplankton collection housed in the Shirshov Institute of Oceanology of the Russian Academy of Sciences. An asterisk (*) indicates that the specimen or specimens came directly from the STC.

		Literature sources	
Species in the STC	Studied specimens (number, SL, coordinates, layer, vessel, expedition no., sta., date)	Based on records for larvae from the STC	Based on records for larvae from outside the STC
Bolinichthys indicus	Larvae unknown		
B. supralateralis	2 (4.6, 10.5 mm SL), 4°45′N, 37°09′W, 0–200 m, *Akademic Vavilov*, 43, sta. 2664, 25 October 2016 3 (11.4–11.9 mm SL), 13°52′N, 45°00′W, 0–700 m, *Professor Logachev*, 39, sta. 189, 1 March 2018 1 (8.2 mm SL), 2°02′N, 36°32′W, 0–700 m, *Akademic Vavilov*, 43, sta. 2669, 26–27 October 2016	None	Pertseva-Ostroumova (1964); Olivar et al. (1999); Bolshakova and Evseenko (2020)
Ceratoscopelus gr. *townsendi*	2* (11.0, 11.7 mm SL), 38°48′S, 157°54′W, 0–200 m, *Dmitry Mendeleev*, 34, sta. 3049, 4 February 1985 57* (9.1–19.5 mm SL), 34°59′S, 158°06′W, 200-0, *Dmitry Mendeleev*, 34, sta. 3051, 6 February 1985 2 (12.5, 13.2 mm SL), 00°01′S, 36°01′W, 0–700 m, *Akademic Vavilov*, 43, sta. 2675, 26–27 November 2016	None	Shiganova (1977); Miller et al. (1979); Belyanina (1982); Ozawa (1986); Badcock and Araújo (1988); Moser and Watson (2001); Bonecker and Castro (2006)
Lampadena anomala	Larvae unknown		
L. dea	Larvae unknown		
L. notialis	Larvae unknown		
L. speculigera	Larvae unknown		
Lampadena sp.	1* (9.8 mm SL), 35°08′S, 128°35′E, 0–500 m, *Dmitry Mendeleev*, 16, sta. 1363, 26 February 1976 18* (5.4–10.0 mm SL), 35°19′S, 128°42′E, 0–200 m, *Dmitry Mendeleev*, 16, sta. 1359, 25 February 1976	First description in this study	None
Lampanyctus gr. *achirus*	2 (8.3, 8.5+ mm SL), 36°56′S, 07°19′E, 0–550 m, *Akademic Ioffe*, 29, sta. 2193, 26 November 2009 1* (12.8 mm SL), 43°06′S, 125°42′W, 0–50 m, *Dmitry Mendeleev*, 34, sta. 3056, 16 February 1985 3* (15.0–22.0 mm SL), 39°42′S, 126°01′W, 0–200 m, *Dmitry Mendeleev*, 34, sta. 3054, 14 February 1985	Bolshakova et al. (2021)	Moser and Ahlstrom (1974)
L. ater	1 (18.5 mm SL), 32°47′S, 01°49′E, 0–1150 m, *Akademic Ioffe*, 29, sta. 2187, 22 November 2009	None	Olivar (1985); Moser and Watson, (2001)
L. alatus	2 (5.8, 9.1 mm SL), 11°02′S, 50°37′E, 0–400 m, *Akademik Kurchatov*, 36, sta. 3740, 4 April 1983 2 (7.0, 8.2 mm SL), 16°18′N, 46°41′W, 0–75 m, *Akademic Ioffe*, 29, sta. 2163, 3 November 2009	None	Olivar and Beckley (1997); Moser and Watson (2001); Bolshakova and Evseenko (2016a)
L. australis	2* (10.0, 12.5 mm SL), 39°42′S, 126°01′W, 0–200 m, *Dmitry Mendeleev*, 34, sta. 3054, 14 February 1985 1 (9.2 mm SL), 49°41′S, 148°25′E, 0–200 m, *Dmitry Mendeleev*, 16, sta. 1335, 13 February 1976 1 (12.0 mm SL), 46°50′S, 158°01′W, 0–200 m, *Dmitry Mendeleev*, 34, sta. 3009, 16 January 1985 1 (11.5 mm SL), 44°20′S, 157°33′W, 0–200 m, *Dmitry Mendeleev*, 34, sta. 3010, 17 January 1985	Bolshakova et. al. (2021)	Olivar (1988); Olivar and Beckley (1997); Bolshakova and Evseenko (2016b)
L. festivus	1 (9.5 mm SL), 29°28′S, 00°11′E, 0–2000 m, *Akademic Ioffe*, 29, sta. 2184, 19 November 2009	None	Olivar and Beckley (1997); Bolshakova and Evseenko (2016b)

(*Continued on the next page*)

Table 1 (*continued*)

		Literature sources	
Species in the STC	Studied specimens (number, SL, coordinates, layer, vessel, expedition no., sta., date)	Based on records for larvae from the STC	Based on records for larvae from outside the STC
L. intricarius	18* (9.0–19.7 mm SL), 38°48′S, 157°54′W, 0–200 m, *Dmitry Mendeleev*, 34, sta. 3049, 4 February 1985 1 (12.7 mm SL), 36°56′S, 07°19′E, 0–550 m, *Akademic Ioffe*, 29, sta. 2193, 26 November 2009	Bolshakova and Evseenko (2015)	Regan (1916); Olivar (1988)
L. lepidolychnus	Absent	None	Olivar and Fortuño (1991); Olivar and Beckley (1997)
L. macdonaldi	Larvae unknown		
L. pusillus	1 (6.4 mm SL), 36°56′S, 07°19′E, 0–550 m, *Akademic Ioffe*, 29, sta. 2193, 26 November 2009 16* (6.2–11.5 mm SL), 38°48′S, 157°54′W, *Dmitry Mendeleev*, 34, 0–200 m, sta. 3049, 4 February 1985 1 (10.2 mm SL), 29°28′S, 00°11′E, 0–2000 m, *Akademic Ioffe*, 29, sta. 2184, 19 November 2009	None	Tåning (1918); Rodríguez et al. (2017)
L. wisneri	See remarks under *L.* gr. *achirus*		
Lampanyctus sp. D	2* (11.6, 11.7 mm SL), 45°31′S, 157°43′W, 0–200 m, *Dmitry Mendeleev*, 34, sta. 3042, 20–21 January 1985 9* (7.8–10.7 mm SL), 37°56′S, 125°55′W, 0–200 m, *Dmitry Mendeleev*, 34, sta. 3052, 12–13 February 1985 10* (8.4–13.8 mm SL), 38°48′S, 157°54′W, 0–200 m, *Dmitry Mendeleev*, 34, sta. 3049, 4 February 1985	Bolshakova et al. (2021)	None
Lepidophanes guentheri	2 (10.5, 11.0 mm SL), 14°44′N, 44°55′W, 0–700 m, *Professor Logachev*, 39, sta. 183, 27 February 2018 1 (14.3 mm SL), 15°45′S, 13°13′W, 0–225 m, *Akademic Ioffe*, 29, sta. 2175, 11 November 2009	None	Moser and Ahlstrom (1972); Shiganova (1977); Moser and Watson (2001); Bonecker and Castro (2006)
Taaningichthys bathyphilus	Larvae unknown		
Notolychnus valdiviae	2 (7.8; 9.8 mm SL), 29°57′S, 168°41′E, 0–200 m, *Dmitry Mendeleev*, 16, sta. 1259, 4 January 1976 5 (7.5–10.0 mm SL), 6°12′S, 54°21′E, 0–500 m, *Academic Kurchatov*, 36, sta. 3716, 25 March 1983 10 (4.8–10.5 mm SL), 10°35′S, 50°51′E, 0–500 m, *Academic Kurchatov*, 36, sta. 3737, 2–3 April 1983	None	Tåning (1918); Pertseva-Ostroumova (1964); Moser and Ahlstrom (1974); Shiganova (1975); Moser et al. (1984); Moser and Ahlstrom (1996)

Abbreviations Abbreviations used in the text and figures for meristic characters and other features are shown in Table 2. We use the abbreviation *gr.* (for *grex*, a Latin word meaning *group*) before the species name to indicate a putative species complex or mix of different species (i.e., *Ceratoscopelus* gr. *townsendi* and *Lampanyctus* gr. *achirus*).

Results

Two identification keys are presented. The first is a key based on larval characters for all lanternfish subfamilies: Myctophinae, Notolychninae, Lampanyctinae, Gymnoscopelinae, and Diaphinae. The second key is for the postflexion larvae of all known genera of round-eyed lanternfish.

Key to subfamilies of Myctophidae based on larval characters

1a Narrow eyes; noticeable choroid tissue on ventral surface of eye usually present (except for *Loweina*, with slightly oval eyes lacking choroid tissue; *Diogenichthys* lacking choroid tissue; and some species of *Protomyctophum* and of *Hygophum* lacking choroid tissue); some have stalked eyes; number of rays in dorsal fin (D) fewer than number of rays in anal fin (A) (D<A)......................................**Myctophinae** (not treated here)

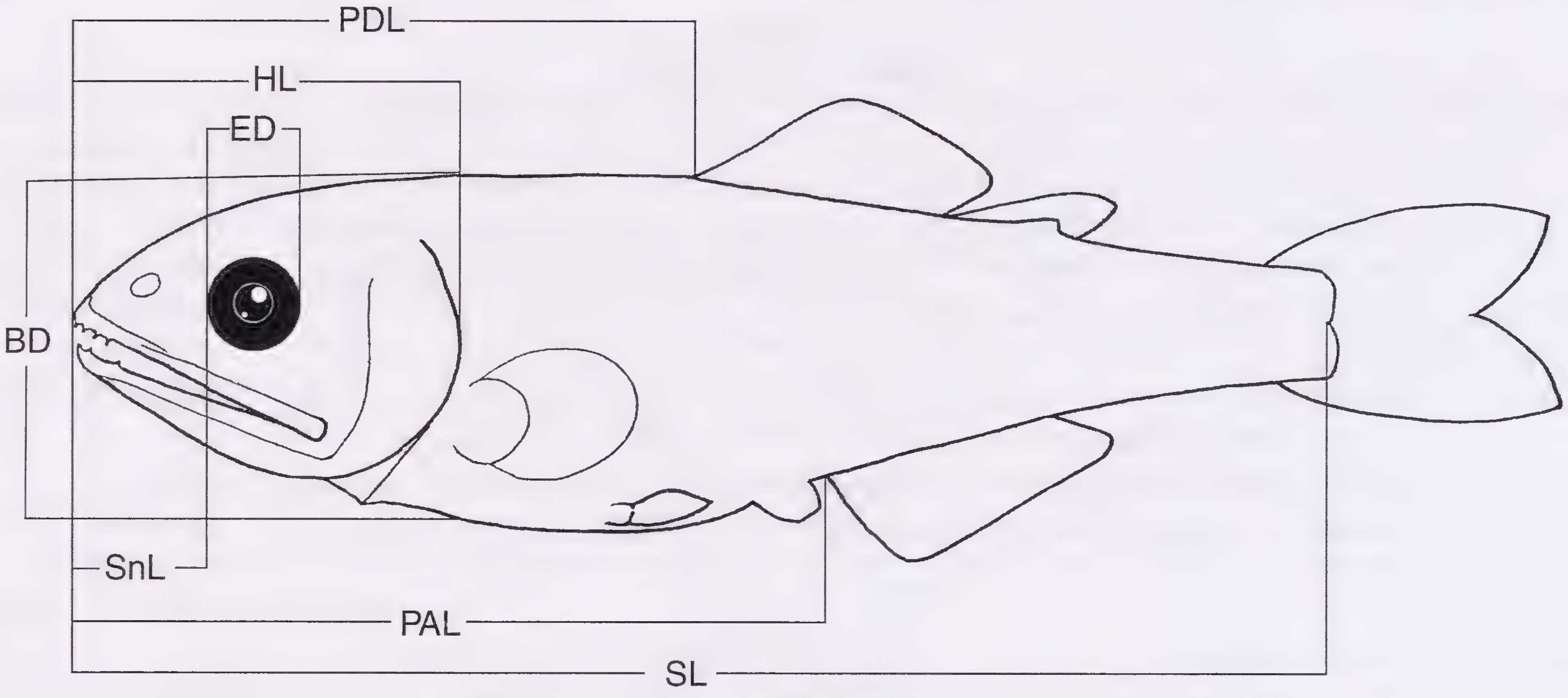

Figure 2

Scheme of measurements used for larvae in this study. The measurements include standard body length (SL), head length (HL), body depth at pectoral fin base (BD), preanal length (PAL), predorsal length (PDL), snout length (SnL), and horizontal eye diameter (ED).

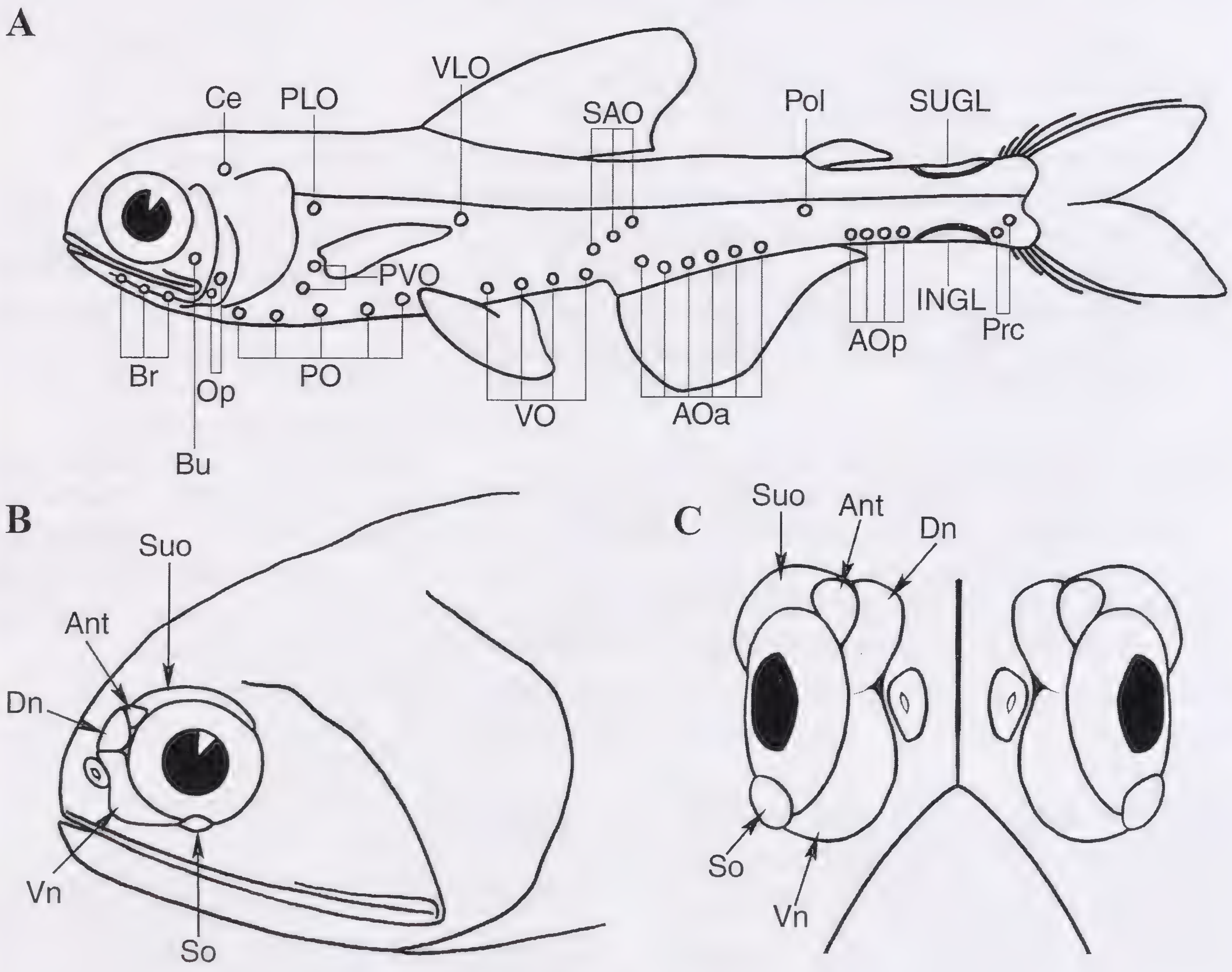

Figure 3

Illustrations showing the locations of photophores and orbital glands of larvae of the family Myctophidae: (**A**) total scheme without luminous orbital glands, (**B**) lateral view of the luminous orbital glands, and (**C**) frontal view of the luminous orbital glands. The photophores include the pectolateral (PLO), pectoventral (PVO), pectoral (PO), ventrolateral (VLO), ventral (VO), supraanal (SAO), anterior anal (AOa), posterior anal (AOp), posterolateral (Pol), precaudal (Prc), branchiostegal (Br), opercular (Op), cervical (Ce), and buccal (Bu) photophores. The luminous glands include the dorsonasal gland (Dn), anteorbital gland (Ant), suborbital gland (So), ventronasal gland (Vn), supraorbital gland (Suo), supracaudal luminous gland (SUGL), and infracaudal luminous gland (INGL).

1b Rounded or slightly oval eyes, usually without conspicuous choroid tissue (except for *Lobianchia* having ventral choroid tissue; *Notolychnus*, with eyes irregular in shape and with ventral and dorsal choroid tissue; *Triphoturus*, with oval eyes having ventral choroid tissue); always sessile; dorsal fin-ray count usually a few more than or nearly equal to anal fin-ray count (D≥A) (except for *Lampichthys* and *Lampanyctus*, with D<A) 2

2a Short gut; preanal length (PAL) 44–53% SL; 6–7 rays in pelvic fin; larval photophores absent .... **Notolychninae**

2b Moderate or slender gut; PAL 56–75% SL (50–54% in *Scopelopsis*; 52–58% in *Parvilux*); 8–9 (7–8 in *Scopelopsis*); pelvic-fin rays; at least 2nd branchiostegal photophore (Br$_2$) present, except for *Taaningichthys minimus* and *L. intricarius* 3

3a Only Br$_2$ or additionally ventronasal gland or pectolateral photophore formed second in order .... **Lampanyctinae**

3b Fifth pectoral photophores second to form 4

4a Mediodorsal (MD) or mediolateral (ML) pigment always present .... **Gymnoscopelinae** (not treated here)

4b Mediodorsal and ML pigment always absent .... **Diaphinae** (except for *Diaphus ostenfeldi*, with MD pigment present) (not treated here)

Key to genera of round-eyed lanternfish based on postflexion larvae (standard length >7–12 mm)

Each genus that is not represented in the STC is marked by an asterisk (*).

1a No photophores or only 2nd branchiostegal photophore (Br$_2$) during the larval stage .... **2** [*Bolinichthys*, *Lampanyctus* (except for *L. alatus*), *Notolychnus*, *Parvilux**, *Stenobrachius**, *Taaningichthys*, *Triphoturus**]

1b Additional photophores (ventronasal gland [Vn], pectolateral photophore [PLO], ventrolateral photophore [VLO], and fifth and first pectoral photophores [PO$_5$ and PO$_1$]) are formed .... **3** [*Ceratoscopelus*, *Diaphus*, *Gymnoscopelus*, *Idiolychnus**, *Lampadena*, *Lampanyctodes*, *Lampichthys*, *Lepidophanes*, *Lobianchia*, *Notoscopelus*, *Scopelopsis*]

2a Body depth at pectoral fin base (BD) ≥24% standard body length (SL); upper jaw length >60% head length (HL); head large (HL 27–50% SL) .... ***Lampanyctus***

2b Body depth at pectoral fin base ≤24% SL (up to 27% in *Bolinichthys*); jaws short, <50% HL; head small, HL 23–30% SL .... **13** [*Bolinichthys*, *Notolychnus*, *Parvilux**, *Stenobrachius**, *Taaningichthys*, *Triphoturus*]

3a Sequence of photophore development: Br$_2$, PO$_5$, PO$_1$ .... **4** [*Diaphus*, *Gymnoscopelus*, *Idiolychnus**, *Lobianchia*]

3b Sequence of photophore development different, with Vn and PLO always formed earlier than PO$_1$ (Br$_2$, PO$_5$, Vn, PLO/VLO or Br$_2$, Vn, PO$_5$, PLO, PO$_1$, or Br$_2$, Vn, PLO, PO$_5$, or Br$_2$, PLO, PO$_5$, Vn, PO$_1$) .... **7** [*Ceratoscopelus*, *Lampadena*, *Lampanyctodes*, *Lampichthys*, *Lepidophanes*, *Notoscopelus*, *Scopelopsis*]

4a Body slender (BD 13–22% SL); 41–45 myomeres; mediodorsal (MD) pigment usually present; transformation at SL >20 mm SL .... ***Gymnoscopelus***

4b Body moderate to deep (BD 19–38% SL); 31–38 myomers; MD pigment absent; transformation at SL <15 mm SL .... **5** [*Diaphus*, except for *D. ostenfeldi*, *Idiolychnus**, *Lobianchia*]

4c Body moderate in depth (BD 24–28% SL); 37–38 myomers; MD pigment present at 9.5 mm SL; transformation at SL ~20 mm SL .... ***Diaphus ostenfeldi***

5a Pectoral fin large, reaching to or behind anus, wing-shaped and bilobed (upper rays elongated); BD >30% SL .... **6** [*Idiolychnus**, *Lobianchia*]

5b Pectoral fin normal, not reaching anus; BD <30% SL .... ***Diaphus***

6a Numerous abdominal myoseptal melanophores (MSa); slightly oval eyes with ventral choroid tissue .... ***Lobianchia***

6b Abdominal myoseptal melanophores absent; round eyes without choroid tissue .... ***Idiolychnus****

7a Sequence of photophore development: Br$_2$, PO$_5$, Vn, PLO/VLO; number of rays in dorsal fin (D) 16–27; number of rays in anal fin (A) 18–27 .... **8** [*Lampichthys*, *Notoscopelus*, *Scopelopsis*]

7b Another sequence of photophore development (Br$_2$, Vn, PO$_5$, PLO, PO$_1$; Br$_2$, Vn, PLO, PO$_5$; or Br$_2$, PLO, PO$_5$, Vn, PO$_1$); D 11–13; A 11–17 .... **10** [*Ceratoscopelus*, *Lampadena*, *Lampanyctodes*, *Lepidophanes*]

8a Body depth at pectoral fin base 24–35% SL; subdorsal mediolateral melanophores (MLD) present; anteroventral foregut melanophores (FGv) absent .... ***Notoscopelus***

8b Body depth at pectoral fin base 19–24% SL; MLD absent; FGv present .... **9** [*Lampichthys*, *Scopelopsis*]

9a Lower-jaw symphyseal melanophores (LJS) present; posterior lower-jaw melanophores (LJP) present; D 16–18; A 21–23 .... ***Lampichthys***

9b Lower-jaw symphyseal melanophores absent; LJP absent; D 20–24; A 23–27 .... ***Scopelopsis***

10a Sequence of photophore development: Br$_2$, Vn, PLO, PO$_5$; subdorsal (SMD) and preadipose (PMDa) pigment always absent; basicaudal (BC) pigment always absent .... **11** [*Ceratoscopelus*, *Lepidophanes*]

10b Another sequence of photophore development (Br_2, Vn, PO_5, PLO, PO_1 or Br_2, PLO, PO_5, Vn, PO_1); SMD or PMDa pigment always present; BC present or absent .... **12** [*Lampadena*, *Lampanyctodes*]
11a Anteroventral foregut and otical melanophores (Ot) absent .... ***Ceratoscopelus***
11b Anteroventral foregut melanophores and Ot present .... ***Lepidophanes***
12a Sequence of photophore development: Br_2, PLO, PO_5, Vn, PO_1; number of gill rakers in the outer row of first gill arch (GR) <30 .... ***Lampadena***
12b Sequence of photophore development: Br_2, Vn, PO_5, PLO, PO_1; GR ≥30 .... ***Lampanyctodes***
13a Eyes round or slightly oval without choroid tissue .... **14** [*Bolinichthys*, *Parvilux**, *Stenobrachius**, *Taaningichthys*]

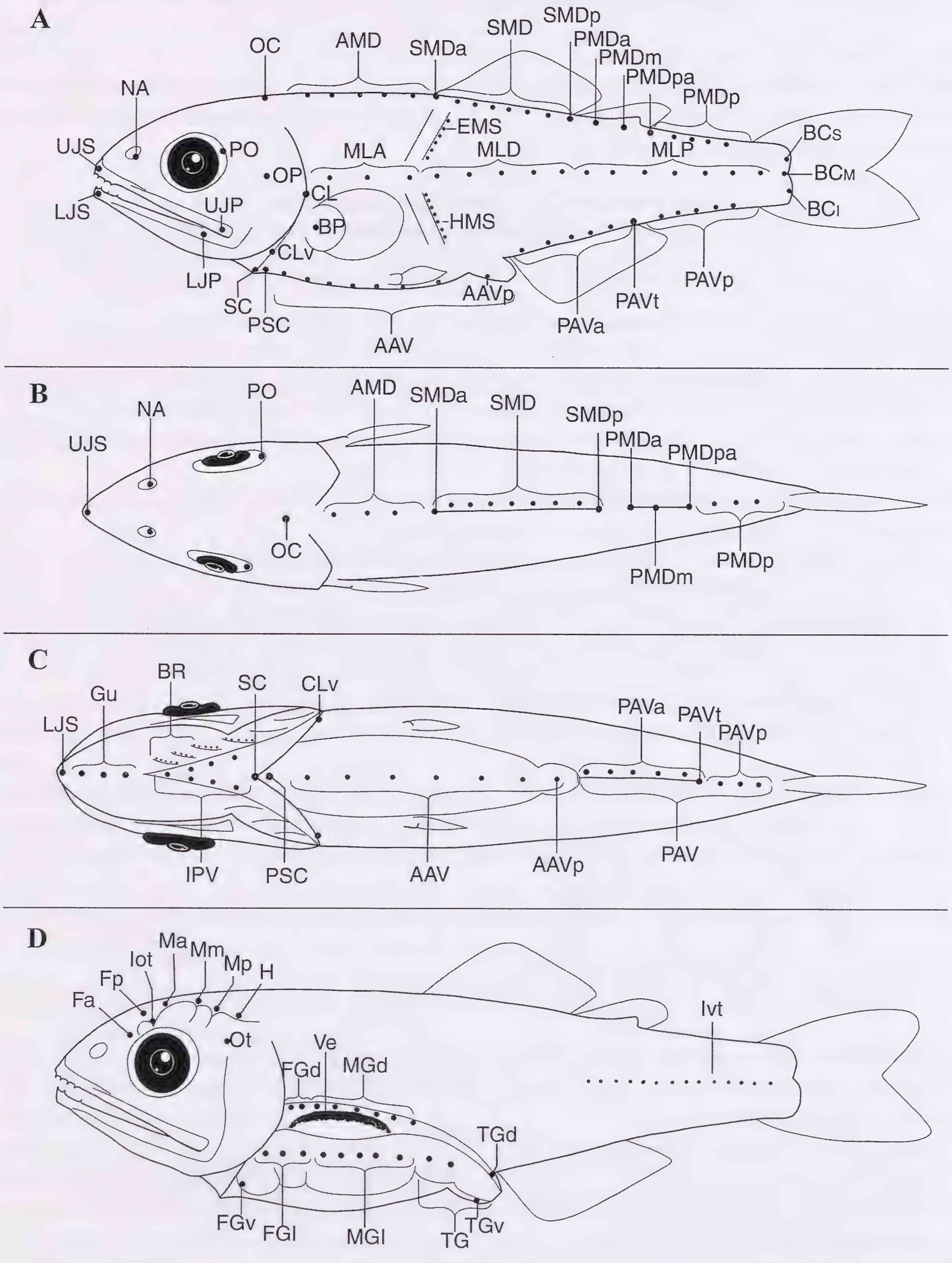

Figure 4

Scheme of the external pigmentation of larvae of the family Myctophidae: (**A**) lateral view, (**B**), dorsal view, and (**C**) ventral view. (**D**) Scheme of the internal pigmentation of larvae of this family. Abbreviations are defined in Table 2.

Table 2

Abbreviations used in the text and figures for photophores, orbital glands, meristic characters, measurements, and pigmentation. These features are part of the descriptions for species of myctophid larvae (subfamilies Lampanyctinae and Notolychninae) from the Subtropical Convergence and can be used to identify them.

Abbreviation	Name	Abbreviation	Name
	Photophores and orbital glands		
PLO	Pectolateral photophore	Br	Branchiostegal photophores
PVO	Pectoventral photophores	Op	Opercular photophore(s)
PO	Pectoral photophores	Ce	Cervical photophore
VLO	Ventrolateral photophore	Bu	Buccal photophore(s)
VO	Ventral photophores	Dn	Dorsonasal gland
SAO	Supraanal photophores	Ant	Anteorbital gland
AOa	Anterior anal photophores	So	Suborbital gland
AOp	Posterior anal photophores	Vn	Ventronasal gland
Pol	Posterolateral photophore(s)	Suo	Supraorbital gland
Prc	Precaudal photophores	SUGL	Supracaudal luminous gland
		INGL	Infracaudal luminous gland
	Meristic characters		
D	Number of rays in dorsal fin	C	Number of rays in caudal fin
A	Number of rays in anal fin	GR	Number of gill rakers in the outer row of first gill arch
P_1	Number of rays in pectoral fin	V	Number of vertebrae
P_2	Number of rays in pelvic fin		
	Measurements		
SL	Standard body length	PDL	Predorsal length
HL	Head length	SnL	Snout length
BD	Body depth at pectoral fin base	ED	Horizontal eye diameter
PAL	Preanal length		
	Pigmentation		
Mediodorsal group		Craniovisceral group	
MD	Mediodorsal	LJS	Lower-jaw symphyseal
AMD	Antedorsal	UJS	Upper-jaw symphyseal
SMD	Subdorsal	LJP	Posterior lower-jaw
SMDa	Anterior subdorsal	UJP	Posterior upper-jaw
SMDp	Posterior subdorsal	BR	Branchiostegal
PMD	Postdorsal	NA	Nasal
PMDa	Preadipose	OP	Opercular
PMDm	Subadipose	OC	Occipital
PMDp	Supracaudal	PO	Postorbital
PMDpa	Postadipose	Gu	Gular
Mediolateral group		Fin pigmentation	
ML	Mediolateral	Pp	Pectoral-fin pigmentation
MLA	Anterior mediolateral	Vp	Ventral-fin pigmentation
MLD	Subdorsal mediolateral	Cp	Caudal-fin pigmentation
MLP	Posterior mediolateral	Adp	Adipose-fin pigmentation
MS	Myoseptal	Dp	Dorsal-fin pigmentation
MSa	Abdominal myoseptal	Ap	Anal-fin pigmentation
MSc	Caudal myoseptal	DFp	Dorsal fin-fold pigmentation
EMS	Epaxial myoseptal	VFp	Ventral fin-fold pigmentation
EMSa	Epaxial abdominal myoseptal	Medullar group	
EMSc	Epaxial caudal myoseptal	Fa	Anterior forebrain
HMS	Hypaxial myoseptal	Fp	Posterior forebrain
HMSa	Hypaxial abdominal myoseptal	Ma	Anterior midbrain
HMSc	Hypaxial caudal myoseptal	Mm	Medial midbrain
CL	Lateral cleithral	Mp	Posterior midbrain
CLv	Ventral cleithral	H	Hindbrain
BP	Basipectoral	Ot	Otical
BC	Basicaudal	Iot	Transverse interorbital

(Continued on the next page)

Table 2 (*continued*)

Abbreviation	Name	Abbreviation	Name
Pigmentation			
BC_{S}	Basicaudal superior	Abdominal group	
BC_{M}	Basicaudal medium	FG	Foregut
BC_{I}	Basicaudal inferior	FGl	Lateral foregut
Medioventral group		FGv	Anteroventral foregut
IPV	Prepectoral (isthmic)	FGd	Dorsal foregut
AAV	Preanal	MG	Midgut
AAVp	Periproctal	MGd	Dorsal midgut
PAV	Postanal	MGl	Lateral midgut
PAVa	Subanal	TG	Terminal gut section
PAVt	Terminal subanal	TGd	Dorsal terminal gut
PAVp	Infracaudal	TGv	Ventral terminal gut
SC	Symphyseal-cleithral	Ve	Vesicular
PSC	Postsymphyseal-cleithral	Intervertebral pigmentation	
		Ivt	Sagittal intervertebral

13b Eyes elliptical or irregular in shape with choroid tissue .... **17** [*Notolychnus*, *Triphoturus*]
14a Horizontal eye diameter 36–46% SL .... **15** [*Bolinichthys*, *Parvilux*]
14b Horizontal eye diameter 17–33% SL .... **16** [*Stenobrachius*, *Taaningichthys*]
15a Preanal length >59% SL; supracaudal melanophores (PMDp) absent .... ***Bolinichthys***
15b Preanal length <58% SL; PMDp present .... ***Parvilux****
16a Body depth at pectoral fin base 13–18% SL; full row of sagittal intervertebral melanophores (Ivt) present; BC present; Br_2 absent .... ***Taaningichthys***
16b Body depth at pectoral fin base 17–24% SL; Ivt absent; BC absent; Br_2 form at 7 mm SL .... ***Stenobrachius****
17a Basicaudal melanophores present; preanal (AAV) and postadipose melanophores (PMDpa) absent; eyes irregular in shape with dorsal and ventral crescent choroid mass .... ***Notolychnus***
17b Basicaudal melanophores absent; AAV and PMDpa present; eyes elliptical with ventral lunate choroid mass .... ***Triphoturus***

Subfamily Lampanyctinae Paxton, 1972

Identification Larvae of the lampanyctine genera, except for *Ceratoscopelus*, *Lepidophanes*, and *Lampadena*, can be distinguished from those of Gymnoscopelinae and Diaphinae by the absence of the photophores or the presence of only a 2nd branchiostegal photophore (Br_2) at their larval stages. Lampanyctinae can be separated from the Notolychninae by a greater preanal length (PAL) and more pelvic-fin rays. *Ceratoscopelus*, *Lepidophanes*, and *Lampadena* larvae can be separated from the Diaphinae and Gymnoscopelinae larvae by another sequence of photophore development (ventronasal gland [Vn] or pectolateral photophore [PLO], second to form versus fifth pectoral photophores [PO_5], respectively). Larvae of the Lampanyctinae can be distinguished from those of Myctophinae by the combination of rounded eyes without choroid tissue (except for *Triphoturus* spp. that have choroid tissue), with the number of rays in the dorsal fin a few more than or nearly equal to the number of rays in the anal fin (except for *Lampichthys* and *Lampanyctus*, with the number of rays in dorsal fin [D] fewer than the number of rays in anal fin [A]).

Genera *Bolinichthys* Paxton, 1972, *Ceratoscopelus* Günther, 1864, *Lampadena* Goode and Bean in Gill, 1893, *Lampanyctus* Bonaparte, 1840 (including *Nannobrachium* Günther, 1887), *Lepidophanes* Fraser-Brunner, 1949, *Parvilux* Hubbs and Wisner, 1964, *Stenobrachius* Eigenmann and Eigenmann, 1890, *Taaningichthys* Bolin, 1959, and *Triphoturus* Fraser-Brunner, 1949.

Bolinichthys Paxton, 1972

General characters Body moderately deep (**BD 19–27% SL**); head relatively small (head length [HL] 25–30% SL); snout short (snout length [SnL] 21–26% HL); eye large (**horizontal eye diameter [ED] >36–43% HL**); anus opens slightly behind the midbody (PAL 59–67% SL). **Only Br_2** during the larval stage or additional Vn, PLO, or PO_5 appear during transformation; Br_2 appear at 5 mm SL; transformation usually occurs at **12–13 mm SL**.

Pigmentation Pigment is sparse: posterior midbrain (Mp); otical (Ot); vesicular (Ve); postanal (PAV), only in *B. longipes*; and mediolateral (ML), only in *B. distofax*.

Similar genera *Bolinichthys* larvae similar to some *Lampanyctus* larvae lacking rostrum (i.e., *Lampanyctus* sp. D) but have a shorter snout (SnL <10% SL versus >10% SL in *Lampanyctus* larvae) and a lower anal-fin ray count (11–15 versus 14–21 in *Lampanyctus* larvae). Larvae of *Bolinichthys* are also similar to those of *Ceratoscopelus* but have larger eyes (ED 36–43% HL versus 24–32% HL in *Ceratoscopelus*), deeper body (BD 19–27% SL versus 14–19% SL), and Vn absent until transformation and to those of *Parvilux* but have a greater PAL (>59 % SL versus <58% SL in *Parvilux*) (Moser and Ahlstrom, 1974, 1996) and no supracaudal melanophores.

Remarks Adults of *B. indicus* (Hulley, 1981; Bekker, 1983) and *B. supralateralis* (Hulley, 1981; McGinnis, 1982; Bekker, 1983; Hulley and Duhamel, 2009; Roberts et al., 2015) were recorded in the STC. The larvae of the first species are unknown.

Bolinichthys supralateralis (Parr, 1928)
Stubby lanternfish
Figure 5

Lepidophanes pyrsobolus: Pertseva-Ostroumova, 1964, 88, fig. 8d (PoF); Pacific Ocean.

Bolinichthys spp.: Olivar et al., 1999, 110, fig. 9, (PoF); Agulhas Current.

Bolinichthys supralateralis: Bolshakova and Evseenko, 2020, 137, fig. 3 (F, PoF); North Atlantic Ocean.

Negative reference: *Bolinichthys distofax* as *B. supralateralis* in Moser and Ahlstrom, 1974, 408, fig. 11D (PoF) (corrected to *B. distofax* in Moser et al., 1984).

Identification

- –Large round eyes (ED 39–41% HL) versus all Myctophidae species (≤18–36% HL), except for *Notoscopelus resplendens*, *N. caudispinosus*, *Lampanyctus pusillus*, and *L. festivus* (extralimital species: large eyes also in *P. ingens* from the California Current and in *L. tenuiformis* and *L. steinbecki* from tropical and subtropical waters); and
- –Lack of external pigment on the body versus pigment present in all Myctophidae larvae with round eyes, except for *Lampanyctus* sp. D.

General characters D: 12–14, A: 13–15, number of rays in the pectoral fin (P_1): 12–14, number of rays in pelvic fin (P_2): 8, number of gill rakers in the outer row of first gill arch (GR): 5–7+1+12–15, total 18–22, number of vertebrae (V): 33–34. Length at transformation >12 mm SL. At ~8 mm SL, Br_2 appear. All the rays in the fins are distinguishable in the 8.2-mm-SL larva, and the definitive number of gill rakers is noticeable to a size of 11.5 mm SL.

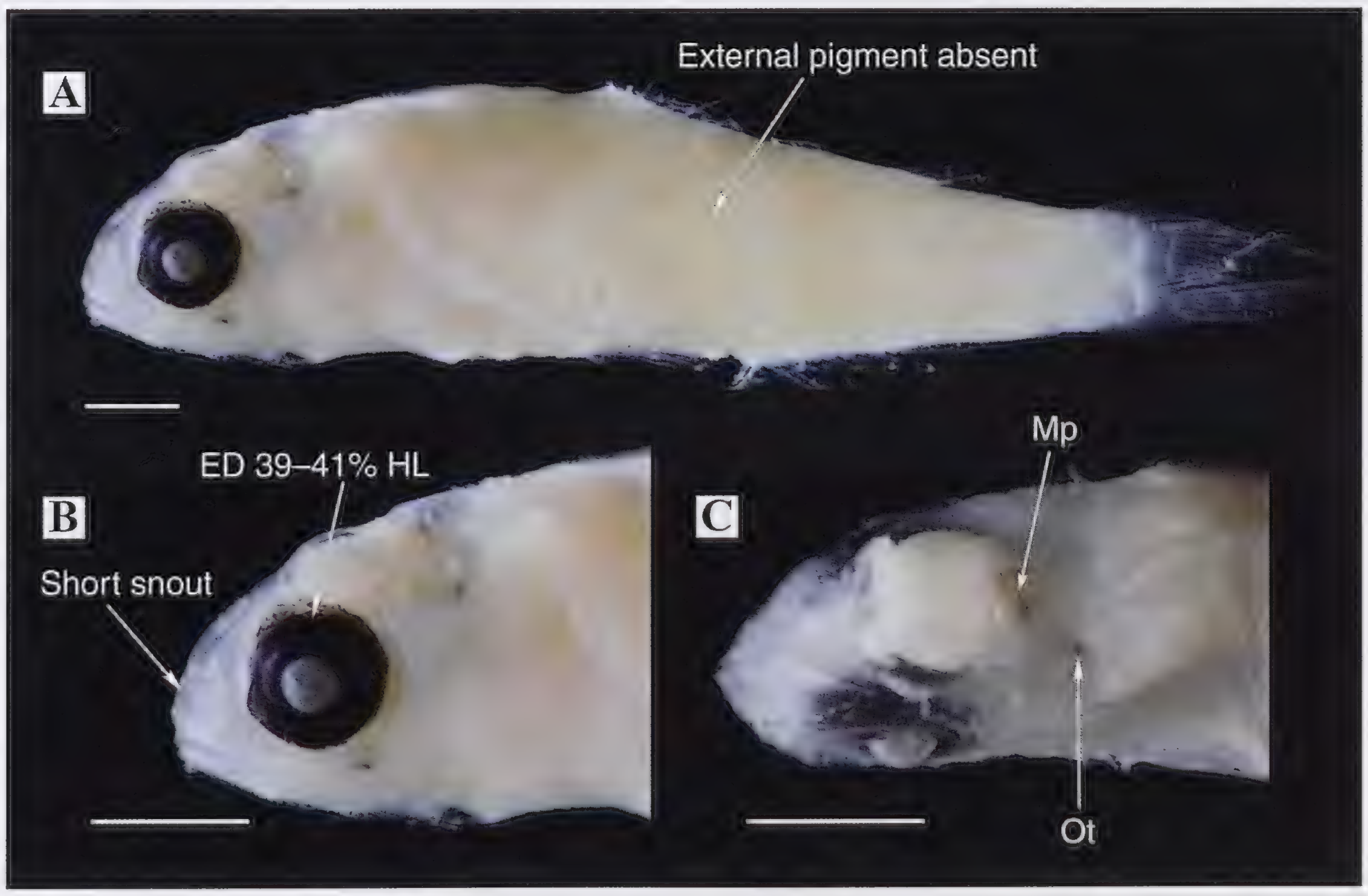

Figure 5

A larva of *Bolinichthys supralateralis* (stubby lanternfish) (11.4 mm standard body length, ID code: IORAS 04473): (**A**) lateral view, (**B**) lateral view of the head, and (**C**) dorsolateral view of the head. The ratio of horizontal eye diameter (ED) to head length (HL) is large compared to those for larvae of other myctophid species. The locations of the posterior midbrain (Mp) and otical (Ot) melanophores are shown in panel C. The scale bar in each panel indicates a length of 1 mm.

Pigmentation Paired Mp, paired Ot, dorsal terminal gut (TGd), Ve.

General distribution Tropical, subtropical, and north temperate waters in the Atlantic Ocean, the western Indian Ocean, and tropical and subtropical waters in the western Pacific Ocean. Occurrence in the STC: in the region of the northern limit of the STC in the South Atlantic and western Indian Oceans (Hulley, 1981; McGinnis, 1982; Bekker, 1983; Hulley and Duhamel, 2009; Roberts et al., 2015).

Ceratoscopelus Günther, 1864

General characters Body slender (**BD <19% SL**); head relatively small (HL 24–27% SL); snout short (SnL 19–27% HL); eye small, slightly oval (**ED >24–32% HL**); anus opens slightly behind the midbody (PAL 58–62% SL). During the larval stage, Br_2, Vn, PLO, and PO_5; Br_2 appear at 7 mm SL; **Vn appear at 7.8 mm SL**; transformation usually occurs at **17–20 mm SL**.

Pigmentation Pigment is sparse: hindbrain (H), Ve, infracaudal (PAVp) and/or supracaudal (PMDp), and terminal subanal (PAVt).

Similar genera Similar to *Lepidophanes*, but have no otical melanophores, and to *Taaningichthys* but photophores appear during larval stages at 5–7 mm SL (appear at >18 mm SL in *Taaningichthys*) and sagittal intervertebral melanophores (Ivt) are absent.

Remarks The species composition of the genus *Ceratoscopelus* is uncertain. Two or 3 valid species are recognized in that genus (Bekker and Borodulina, 1968; Bekker, 1983; Badcock and Araújo, 1988; Fricke et al., 2023). *Ceratoscopelus maderensis* (Lowe, 1839) in the North Atlantic can be easily separated by a number of characters (Nafpaktitis et al., 1977; Hulley, 1981; Bekker, 1983), but the status of the other 2 species, *C. townsendi* (Eigenmann and Eigenmann, 1889) and *C. warmingii* (Lütken, 1892), is controversial. *Ceratoscopelus townsendi* can be separated from *C. warmingii* primarily upon a single feature, the presence of a supraorbital luminous patch (Nafpaktitis and Nafpaktitis, 1969; Wisner, 1976; Bekker, 1983; Badcock and Araújo, 1988). Badcock and Araújo (1988) defined 6 morphotypes on the basis of the arrangement of luminous patches on the body but united all of them under the name *C. townsendi*. This complex is currently under study by A. Prokofiev and probably represents a complex of sibling species different in the arrangement of luminous patches and relative disposition of some photophores on the body, modal gill-raker count, details of dentition, and proportions.

The name *C. townsendi* should be restricted for the populations of the California Current. For the *Ceratoscopelus* larvae from that area, the timing of the formation of fins and photophores is somewhat different from those in other regions, but they are otherwise the same in morphology and pigmentation (Ahlstrom, 1971; Badcock and Araújo, 1988). Two other published names, *Scopelus warmingii* (Lütken, 1892) and *Lampanyctus polyphotis* (Beebe, 1932), are applicable to the populations from the North Atlantic Ocean. Populations from the STC may belong to some undescribed species (different in the Atlantic Ocean and Indo-Pacific), which cannot be evaluated by the larval characters at present.

Ceratoscopelus gr. *townsendi*
Figure 6

Myctophum (*Lampanyctus*) *elongatum*: Roule and Angle, 1930, 44, plate 2, fig. 448, 49 (PoF); Canary Islands (Northeast Atlantic Ocean).

Ceratoscopelus townsendi: Moser and Ahlstrom, 1996, 396, figure on p. 397 (PrF, F, PoF, juvenile [Juv]); California Current.

Diaphus metopoclampus: Rodríguez, 2023, 104 (PoF); central Northeast Atlantic Ocean.

Ceratoscopelus warmingii: Shiganova, 1977, 94, fig. 16G (PoF) (in part.: fig. 16, A and G); Atlantic Ocean. Miller et al., 1979, 31, fig. 37 (PrF); central North Pacific Ocean (Hawaiian Islands). Belyanina, 1982, 22, fig. 19 (PoF); tropical western Pacific Ocean. Ozawa, 1986, 155, plate 19, D and E (PrF, F), plate 20, A–D (PoF, Juv); Northwest Pacific Ocean. Badcock and Araújo, 1988, 20, fig. 4 (F, PoF); Azores front (Northeast Atlantic Ocean). Olivar et al., 1999, 111, fig. 10 (PoF); Agulhas Current. Moser and Watson, 2001, 64, figure on p. 65 (PrF, F, PoF, Juv); western central Atlantic Ocean. Bonecker and Castro, 2006, 137, figure on p. 137 (PoF); tropical southwest Atlantic Ocean. Suntsov et al., 2008, 67, fig. 6d (PoF); area unknown.

Negative reference: *Lampadena luminosa* as *C. townsendi* in Pertseva-Ostroumova, 1964, 89, fig. 9A (Northeast Pacific Ocean).

Notes: Shiganova (1977) apparently described a mix of 2 or more species: *C. warmingii* (fig. 16, A and G), *C. maderensis* (fig. 16, B–D, F), and uncertain species (fig. 16, E and H). Rodríguez (2023) erroneously identified the 8.1-mm-SL larva of *C.* gr. *townsendi* as *D. metopoclampus*. The larva has Vn, which appear in *Diaphus* larvae only during metamorphosis, and there were also no basicaudal melanophores characteristic of *Diaphus* larvae.

Identification

- –Supracaudal and PAVp melanophores absent versus present in *Lepidophanes guentheri* (extralimital species: also present in *C. maderensis* from the North Atlantic Ocean);
- –Mediodorsal melanophores absent versus present in *Lampadena* spp. and *Lepidophanes guentheri*;
- –Anteroventral foregut and basicaudal melanophores absent versus present in *Diaphus* spp.; and

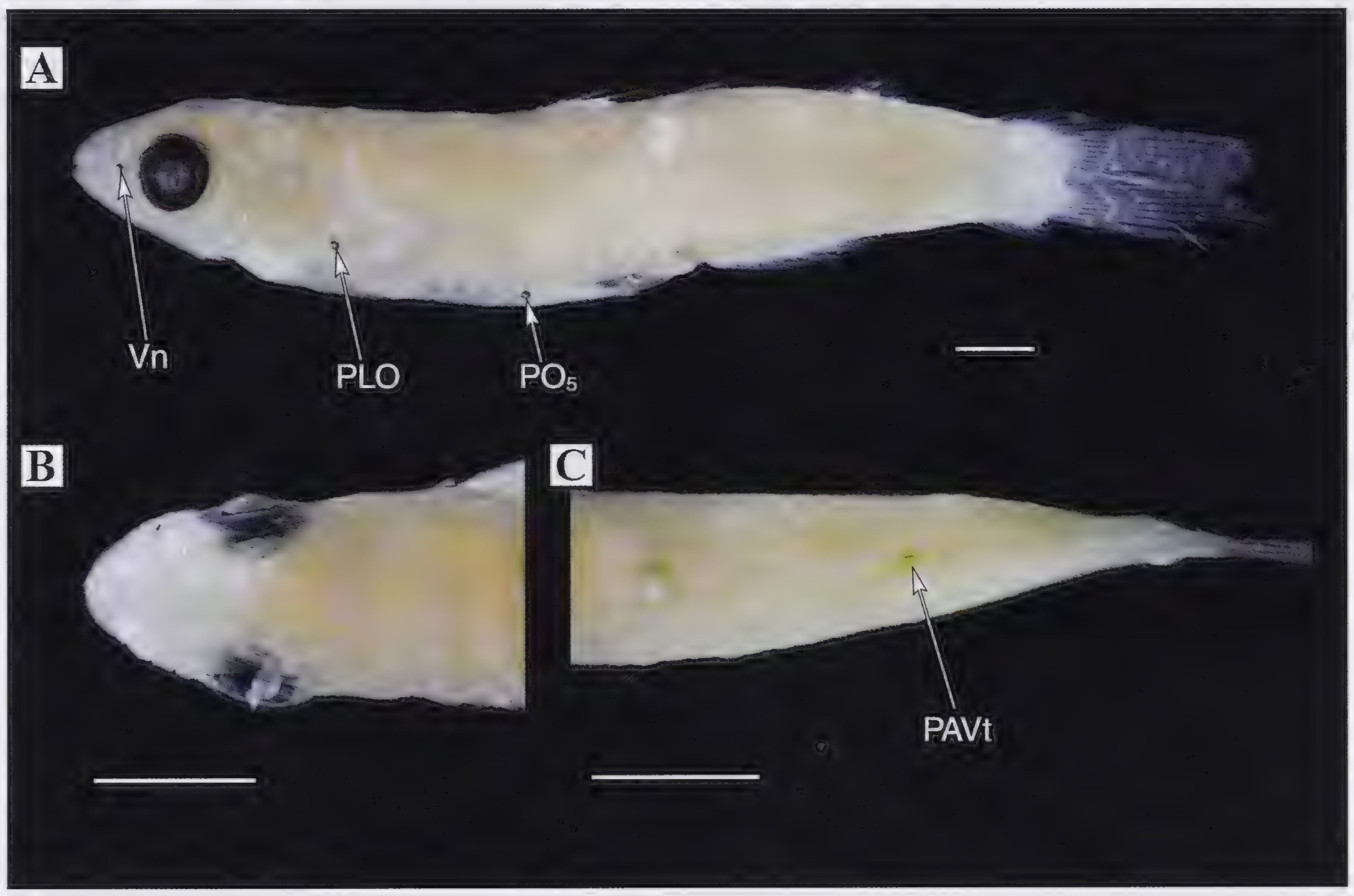

Figure 6

A larva of *Ceratoscopelus* gr. *townsendi* (13.2 mm standard body length, ID code: IORAS 04474): (**A**) lateral view, showing the location of the ventronasal gland (Vn), pectolateral photophore (PLO), and fifth pectoral photophore (PO_5); (**B**) dorsal view of the head; and (**C**) ventral view of the tail, showing the location of the terminal subanal melanophore (PAVt). The scale bar in each panel indicates a length of 1 mm.

–Ventronasal gland forming at 8 mm SL versus Vn absent in *B. supralateralis*, *Diaphus* spp., and *Taaningichnys* spp. to the transformation stage.

General characters D: 13–15, A: 13–15, P_1: 12–15, P_2: 8; GR: 3–5+1+8–10(11), total 13–15(16), V: 35–36. Length at transformation >15 mm SL. The Br_2 appear at ~5–7 mm SL, Vn and PLO appear at ~8 mm SL, and PO_5 appear at 9 mm SL. All the rays in the fins are distinguishable in the 9–10-mm-SL larva, and the definitive number of gill rakers is noticeable to a size of 13 mm SL.

Pigmentation Paired Mp, 2–3 H, TGd, PAVt, Ve, 1–4 Ivt.

General distribution Circumglobal in tropical and warm temperate waters. Occurrence in the STC: in the region of the northern limit of the STC (Parin et al., 1973; Hulley, 1981; McGinnis, 1982; Bekker, 1983; Bekker and Evseenko, 1986; Young et al., 1996; Figueroa et al., 1998; Roberts et al., 2015).

Lampadena Goode and Bean in Gill, 1893

General characters Body moderate (**BD 19–24% SL**) to moderately deep (**BD 27–28% SL**); head moderate (HL 27–31% SL); snout short (SnL 19–29% HL); eye moderately large (**ED >26–37% HL**); anus opens slightly behind the midbody (PAL 62–67% SL). During the larval stage, Br_2, PLO, PO_5, first pectoral photophores (PO_1), and Vn; Br_2 appear at 6–7 mm SL; PLO appear at 8 mm SL; transformation usually occurs at **20 mm SL**.

Pigmentation Rows of mediodorsal (MD) and PAV most prominent, occipital (OC), Ve, anteroventral foregut (FGv), dorsal foregut (FGd), dorsal midgut (MGd); some species have posterior mediolateral (MLP).

Similar genera Similar to *Taaningichthys* larvae, but photophores appear during larval stages at 6–7 mm SL (versus at >18 mm SL in *Taaningichthys*) and body is deeper (BD >19% SL versus <19% SL in *Taaningichthys*); similar to *Ceratoscopelus*, but with FGv and MD melanophores (absent in *C. warmingii*) and with PLO formed earlier than Vn; similar to *Lepidophanes*, but with deeper body (BD >19% SL versus <19% SL in *Lepidophanes*); and similar to *Diaphus* spp., but with another sequence of photophore formation (Br_2, PLO, PO_5 versus Br_2, PO_5, PO_1).

Remarks Ten valid species are recognized in the genus *Lampadena* (Fricke et al., 2023), but the early stages of development are known only for 3 of them: *L. chavesi* (Bolshakova and Evseenko, 2016a), *L. luminosa* (Pertseva-Ostroumova, 1964; Moser and Ahlstrom, 1974; Ozawa, 1986; Olivar et al., 1999), and *L. urophaos* (Moser and Ahlstrom, 1972, 1996). Fahay (1983) tentatively assigned the larvae of *Lampadena* sp. 1 (Ozawa, 1986) and *Lampadena* sp. (Moser and Watson, 2001) to

L. anomala, but this definition is not warranted because the meristic characters overlap within *Lampadena* species, and there are no photophores in the described larvae. Several types of *Lampadena* larvae were described but not identified to the species level (Moser and Ahlstrom, 1972; Miller et al., 1979; Ozawa, 1986; Bonecker and Castro, 2006).

All described *Lampadena* larvae share a combination of characters given previously herein, and we expect a similar situation for the species known in the STC. Adults of 4 species were found in the area of the STC: *L. anomala* (single record at 38°38′S in the western Atlantic Ocean: Hulley, 1981), *L. dea* (Hulley, 1981; McGinnis, 1982; Bekker, 1983; Bekker and Evseenko, 1986), *L. notialis* (Hulley, 1981; McGinnis, 1982; Bekker, 1983), and *L. speculigera* (Hulley, 1981; McGinnis, 1982; Bekker, 1983). However, none of these 4 species are identified at larval stages. The unidentified *Lampadena* larvae described herein may belong to 1 of the last 3 aforementioned species.

Lampadena sp.
Figure 7

Identification

- –Anterior mediodorsal melanophore (AMD) present versus absent in *Ceratoscopelus*, *Lepidophanes*, and other *Lampadena* species (extralimital species: AMD also present in *L. urophaos* from the subtropical North Atlantic and Pacific Oceans);
- –Basicaudal melanophores absent versus present in *Diaphus* spp.; and
- –Ventronasal gland absent in 9.8-mm-SL larva versus Vn forming at ~8 mm SL in *Ceratoscopelus* spp. and *Lepidophanes guentheri*.

General characters D: 12–13, A: 12–14, P_1: ~11 (have not yet fully formed), GR: 6+1+15+ (have not yet fully formed), total 22+, V: 39–40. Flexion at 6.0–6.2 mm SL; length at transformation >10 mm SL. The Br_2 appear at ~6–7 mm SL, PLO appear at 8–9 mm SL; PO_5 appear after PLO at ~8–9 mm SL. All the rays in the fins are distinguishable in the 9–10-mm-SL larvae, and the number of gill rakers is not definitive at a size of 9.8 mm SL.

Pigmentation Preflexion: single AMD; paired posterior subdorsal (SMDp); 3–4 unpaired PMDp (in the form of stripes); paired TGd; 6–7 PAV, Ve; F: the same; PoF: single Mp, single H, single AMD, paired SMDp, 3–4 unpaired PMDp, paired TGd, 1–2 PAVp (often immersed), Ve.

General distribution Larvae were found in samples off the southern coast of Australia, where the northern border of the STC lies.

Remarks The larvae have a set of features (proportions, sequence of photophore formation, pigmentation) characteristic for moderate-bodied *Lampadena* larvae. These larvae differ from those already described in the literature by the presence of an AMD melanophore located on 3rd to 4th trunk myomere. This melanophore appears in the PrF stage and remains in 10-mm-SL larvae. The formation of gill rakers is not yet completed, but about 22 rakers are already present on the first arch in the 3 largest larvae (8.6–10.0 mm SL), greatly exceeding the range known for *L. anomala* (GR: 16–18). The remaining 3 species (*L. dea*, *L. notialis*, and *L. speculigera*) reported off the southern coast of Australia have similar meristic characters; therefore, further identification is difficult.

Lampanyctus Bonaparte, 1840

General characters Body deep (**BD >24% SL**); head large (**HL >27% SL**) (50% SL in *L. achirus*); snout moderate (SnL 26–38% HL) or large (38–56% HL) (65% SL in *L. achirus*); **jaws long with prominent teeth**, ≥60% HL at PoF stage; eye moderately large (ED >24–39% HL); anus opens slightly behind the midbody (PAL 58–65% SL) or shifted posteriorly (65–78% SL). **Only Br_2** during the larval stage, except for *L. alatus* (Vn or PO_5 present) and *L. intricarius* (Br_2 absent during the larval stage); Br_2 appear at 5–11 mm SL; transformation usually occurs at **20 mm SL** (*L. alatus* and *L. pusillus* to 11 mm SL). In addition, see main characters of the larval types.

Pigmentation Medullar pigment in most species; most diverse pigment pattern among all genera.

Similar genera Some *Lampanyctus* larvae similar to *Bolinichthys* but have a longer snout (SnL >10% SL versus <10% SL in *Bolinichthys* larvae) and more numerous anal-fin rays (14–21 versus 11–15 in *Bolinichthys* larvae).

Note that larvae of *Lampanyctus* can be grouped into 2 types:

Larvae with long rostrum: main characters

- –Snout produced into rostrum with large jaws: SnL ≥15% SL;
- –Dorsal fin displaced posteriorly: predorsal length (PDL) ≥55% SL;
- –Teeth at tip of upper jaw pointing slightly upward; and
- –Relatively large gut in PoF stage: PAL ≥65% SL.

Larvae without rostrum: main characters

- –Relativity short snout: SnL <15% SL;
- –dorsal fin located anterior to or near mid-body: PDL <55% SL (except for *L. pusillus*, *L. steinbecki*, and *L. tenuiformis*);
- –No teeth at tip of upper jaw pointing upward (except for *L. festivus*); and
- –Moderate or short gut in PoF stage: PAL <65% SL (except for *L. pusillus*, *L. steinbecki*, and *L. tenuiformis*).

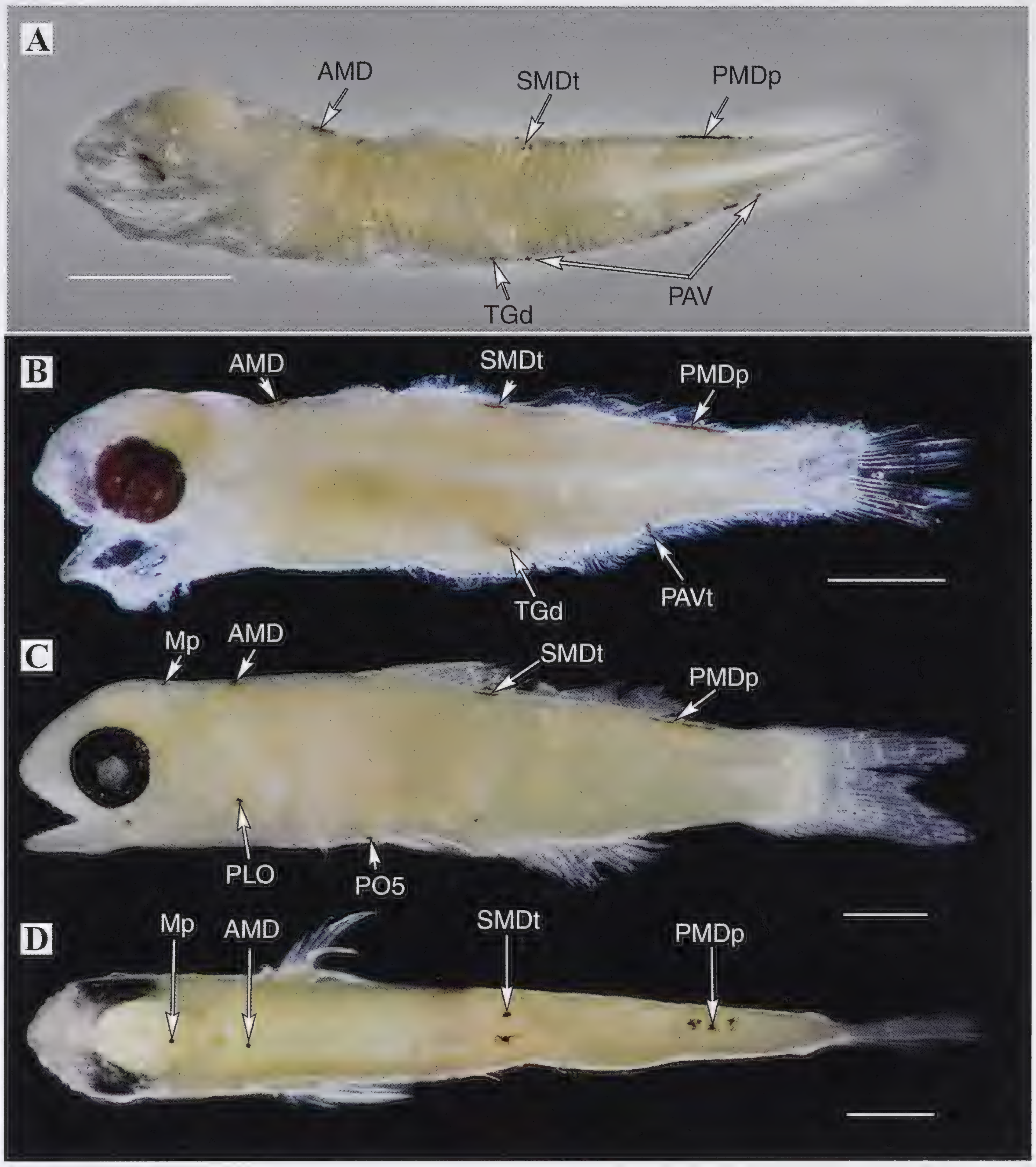

Figure 7

Larvae of *Lampadena* sp.: (**A**) 6.2 mm standard body length (SL), ID code: IORAS 04491; (**B**) 7.5 mm SL, IORAS 04490; (**C**) 9.8 mm SL, IORAS 04489 (lateral view); and (**D**) 9.8 mm SL, IORAS 04489 (dorsal view). The following melanophore pigment groups and photophores are shown: antedorsal (AMD), posterior subdorsal (SMDp), supracaudal (PMDp), dorsal terminal gut (TGd), postanal (PAV), posterior midbrain (Mp), pectolateral photophore (PLO), and fifth pectoral photophore (PO_5). The scale bar in each panel indicates a length of 1 mm.

Remarks Adults of 10 described and 3 undescribed species were recorded from the STC: *Lampanyctus achirus* (Hulley, 1981; McGinnis, 1982; Bekker, 1983; Bekker and Evseenko, 1986; Zahuranec, 2000; Roberts et al., 2015), *L. ater* (Hulley, 1981; McGinnis, 1982; Bekker, 1983; Zahuranec, 2000; Roberts et al., 2015), *L. alatus*, *L. australis*, *L. festivus*, *L. lepidolychnus* (Hulley, 1981; McGinnis, 1982; Bekker, 1983; Roberts et al., 2015), *L. intricarius*, *L. macdonaldi*, *L. pusillus* (Hulley, 1981; McGinnis, 1982; Bekker, 1983; Bekker and Evseenko, 1986; Roberts et al., 2015), *L. wisneri* (Hulley, 1981; McGinnis, 1982; Zahuranec, 2000), and *Lampanyctus* sp. B, C, and D (McGinnis, 1982).

The systematic position of the larvae identified as *L. lepidolychnus* (Olivar and Beckley, 1997) requires further study (see the “Remarks” section for *L. intricarius*). The early stages of development of *L. macdonaldi* and *Lampanyctus* sp. B are unknown, adults of the latter species are most similar in meristic features to *L. festivus*. *Lampanyctus* sp. C can be identical with *L. australis* because the meristic characters of these species match, and a characteristic vertical band of pigment was noted for juvenile *Lampanyctus* sp. C at <30 mm SL (McGinnis, 1982; Bolshakova et al., 2021). *Lampanyctus* sp. D is an undescribed species abundant in the western and central South Pacific Ocean (McGinnis, 1982).

Larvae with long rostrum

Lampanyctus gr. *achirus*
Figure 8

Lampanyctus sp. (possibly *L. achirus*): Moser and Ahlstrom, 1974, 406, fig. 10D (PoF).

Lampanyctus achirus: Olivar and Beckley, 1997, 49 (description without illustration); Agulhas Current (southwestern Indian Ocean). Bolshakova et al., 2021, 113, fig. 3 (F, PoF); southwest Pacific Ocean.

Identification

- –Longest toothy rostrum (SnL 50–65% HL) versus ≤50% HL among all Myctophidae species;
- –Preopercular spines present versus absent in most *Lampanyctus* larvae except for *L. ater* (extralimital species: also present in *L. niger* from the central and western Pacific Ocean); and
- –Lack of medullar pigment versus present in all *Lampanyctus* larvae (extralimital species: medullar pigment also absent in *L. idostigma* from the eastern Pacific Ocean).

General characters D: 15–17, A: 18–20, P_1: 14–16, P_2: 8; GR: 5–6+1+11–13, total 17–19, V: 35–36. Length at transformation >22 mm SL. The Br_2 appear at 9 mm SL. All the rays in the fins are distinguishable in the 14.5-mm-SL larva, and the definitive number of gill rakers is noticeable to a size of 16.0 mm SL.

Pigmentation Upper-jaw symphyseal (UJS) in a row, lower-jaw symphyseal (LJS), 1–3 nasal, 1 postorbital (PO), 1–4 opercular (OP), TGd, numerous basipectoral (BP), hypaxial abdominal myoseptal (HMSa), pectoral-fin pigmentation (Pp).

General distribution Circumglobal in subantarctic zone. Occurrence in the STC: throughout the area (Hulley, 1981; McGinnis, 1982; Bekker, 1983; Bekker and Evseenko, 1986; Zahuranec, 2000; Roberts et al., 2015).

Remarks Two very similar species, *L. achirus* and *L. wisneri* (as *Lampanyctus* sp. A: McGinnis, 1982; as *Nannobrachium wisneri*: Zahuranec, 2000), are known in the STC. *Lampanyctus wisneri* differs from *L. achirus* in the lower gill raker count (4+11–12, total 15–16, versus 5–6+13, total 18–19), greater PDL, absence of pectoral fins in the specimens larger than 35 mm SL, and smaller maximum size (~80 mm SL in *L. wisneri* versus ~160 mm SL in *L. achirus*) (Zahuranec, 2000).

Of all aforementioned features, only the number of gill rakers can be estimated on larvae. By this character, the described larvae (Bolshakova et al., 2021; this study) agree with *L. achirus* (5+12 (4), 5+13 (2), 5+14 (3), and 6+13 (3)). However, *L. achirus* is a subantarctic species that is distributed between the STC in the north and the Antarctic Polar Front to the south (McGinnis, 1982), whereas all the described larvae were obtained from an area north of 46°S and have never been caught south of this latitude. This boundary corresponds to the southernmost limit of the distribution of *L. wisneri*.

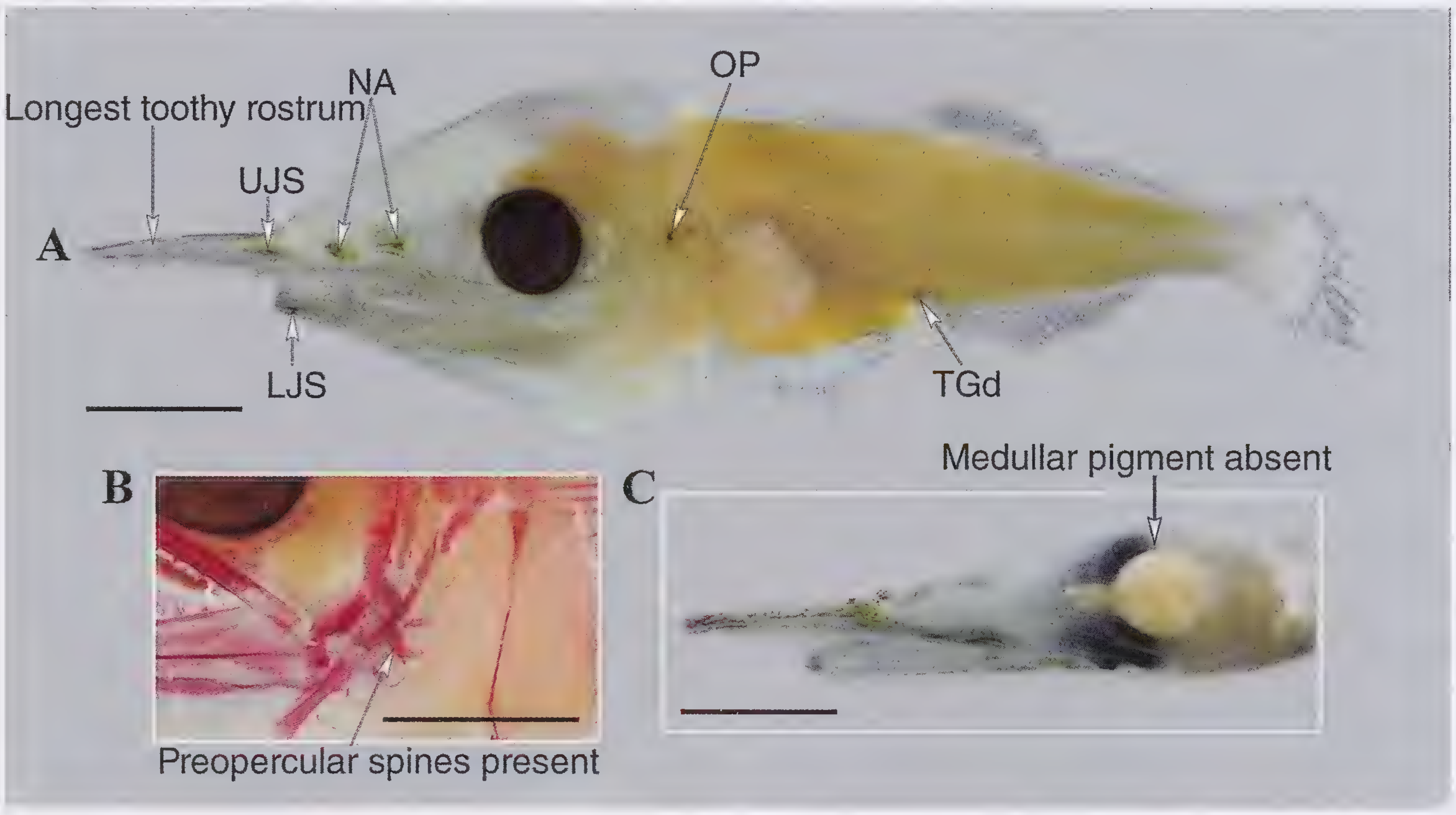

Figure 8

Larvae of *Lampanyctus* gr. *achirus*: (**A**) 8.3 mm standard body length (SL), ID code: IORAS 04475; (**B**) 12.8 mm SL, IORAS 04476 (preopercular spines), and (**C**) 8.3 mm SL, IORAS 04475 (dorsal view of the head). The upper-jaw symphyseal (UJS), lower-jaw symphyseal (LJS), nasal (NA), opercular (OP), and dorsal terminal gut (TGd) melanophore pigment groups are shown in panel A. The scale bar in each panel indicates a length of 1 mm.

Therefore, identification of the described larvae becomes controversial.

The presence of the larvae morphologically congruent with the subantarctic species (*L. achirus*) in the area of distribution of its closest relative (*L. wisneri*) and the absence of the larvae referable to *L. wisneri* in the same area raise a question on the validity of the latter species. On the other hand, all larvae attributed to *L. achirus* were collected from the area of distribution of *L. wisneri* (Olivar and Beckley, 1997; Bolshakova et al., 2021), except for a larva that Moser and Ahlstrom (1974, fig. 10D) figured without indicating an origin. Therefore, all descriptions of *L. achirus* may belong to *L. wisneri*, the larvae of true *L. achirus* may not be known, and the variation in gill-raker count in both species may be greater than indicated by Zahuranec (2000) and may not warrant the separation of these species. This problem requires further study, and for the purposes of our work, we treat these larvae as *L.* gr. *achirus*.

Lampanyctus ater Tåning, 1928
Dusky lanternfish
Figure 9

Nannobrachium atrum: Moser and Watson, 2001, 102, (PrF, F, PoF); western central Atlantic Ocean.
Lampanyctus ater: Olivar, 1985, 285, fig. 5.46 (PrF, PoF); Benguela Current (southeast Atlantic Ocean). Olivar, 1988, 406 (single larval stage without illustration); Benguela Current. Rodríguez, 2023, 122 (PrF, PoF), 123 (PrF, F, PoF); central Northeast Atlantic Ocean.

Identification

- –Preopercular spines present versus absent in most *Lampanyctus* larvae except for *L. achirus* (extralimital species: also present in *L. niger* from the central and western Pacific Ocean);
- –Poorly pigmented larvae: only preadipose (PMDa) and terminal gut melanophores present on body versus different pigmentation in all other *Lampanyctus* larvae (extralimital species: pigment also is sparse in *L. nobilis* from the tropical zone of 3 oceans and in *L. acanthurus* from the North Pacific).

General characters D: 14–16, A: 16–20, P_1: 11–12, P_2: 8; GR: 4–5+1+11 (10–12), total 15–18, V: 35–36. Length at transformation >15 mm SL. The Br_2 appear at 6 mm SL. All the rays in the fins are distinguishable in the 14.5-mm-SL larva.

Pigmentation Lower-jaw symphyseal, UJS, paired Mp, FGv, paired TGd, PMDa.

General distribution Tropical and subtropical Atlantic, South Pacific, and Indian Oceans. Occurrence in the STC: throughout the area except in the Pacific Ocean east of 165°W (Hulley, 1981; McGinnis, 1982; Bekker, 1983; Young et al., 1996; Zahuranec, 2000; Roberts et al., 2015).

Larvae without rostrum

Lampanyctus alatus Goode and Bean, 1896
Winged lanternfish
Figure 10

Lampanyctus alatus: Olivar and Beckley, 1997, 49, fig. 1 (PrF, PoF); Agulhas Current. Moser and Watson, 2001, 82 (PrF, PoF, Juv); western central Atlantic Ocean. Bolshakova and Evseenko, 2016b, 526, fig. 4 (PoF); tropical South Atlantic Ocean.

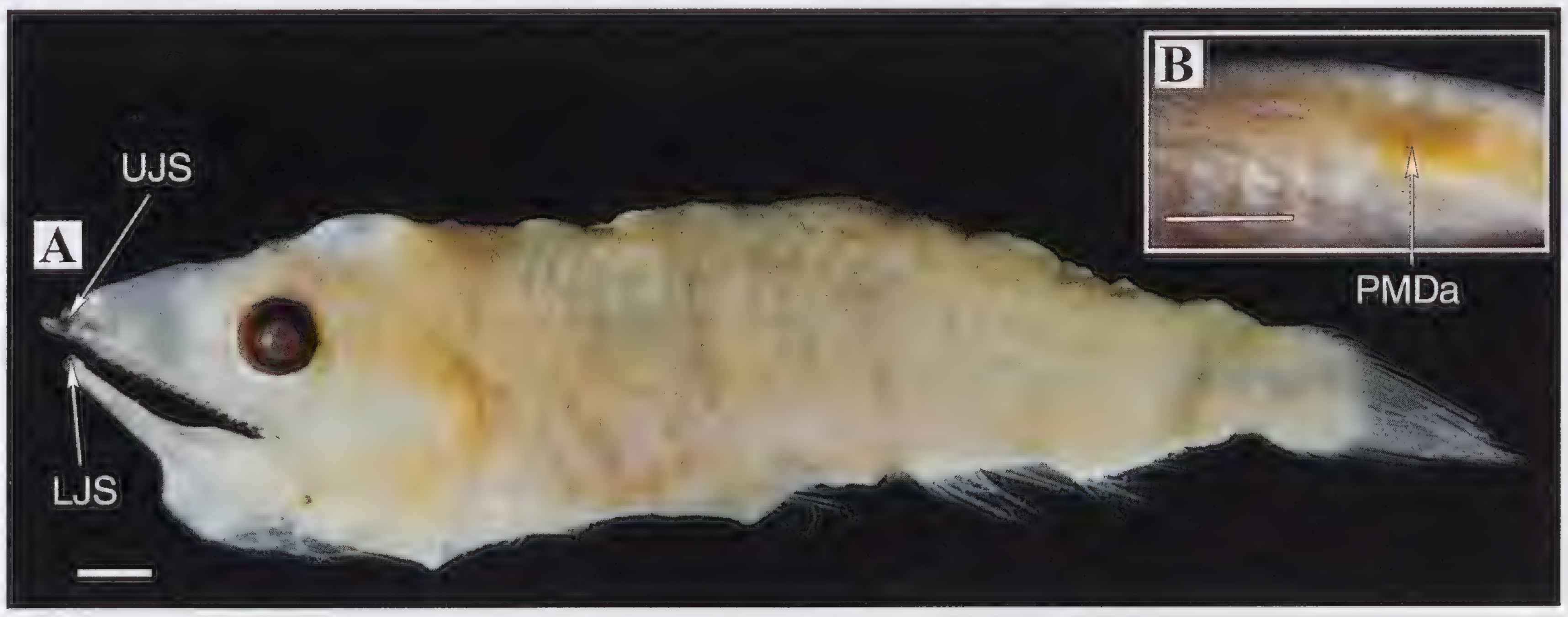

Figure 9

A larva of *Lampanyctus ater* (dusky lanternfish) (18.5 mm standard body length, ID code: IORAS 04477): (**A**) lateral view, showing the locations of the lower-jaw symphyseal (LJS) and upper-jaw symphyseal (UJS) melanophores, and (**B**) dorsal view of the tail, showing the location of the preadipose (PMDa) melanophore. The scale bar in each panel indicates a length of 1 mm.

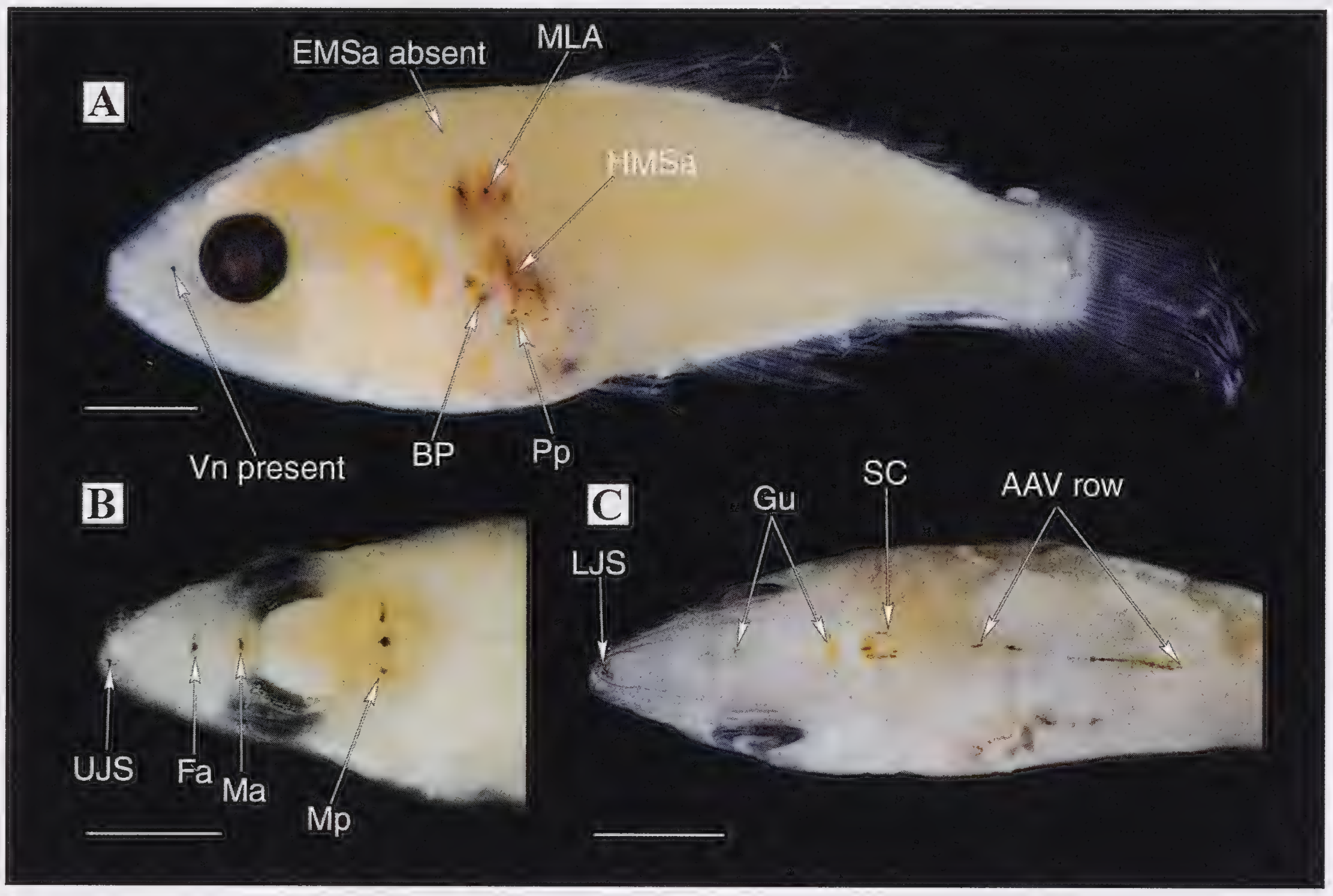

Figure 10

A larva of *Lampanyctus alatus* (winged lanternfish) (9.1 mm standard body length, ID code: IORAS 04478): (**A**) lateral view, (**B**) dorsal view of the head, and (**C**) ventral view of the body. The following melanophore pigment groups and photophore are shown: anterior mediolateral (MLA), hypaxial abdominal myoseptal (HMSa), basipectoral (BP), pectoral-fin pigmentation (Pp), upper-jaw symphyseal (UJS), anterior forebrain (Fa), anterior midbrain (Ma), posterior midbrain (Mp), lower-jaw symphyseal (LJS), gular (Gu), symphyseal-cleithral (SC), preanal (AAV), and ventronasal gland (Vn). Epaxial abdominal myoseptal (EMSa) pigmentation is absent. The scale bar in each panel indicates a length of 1 mm.

Identification

–A series of 4–6 preanal (AAV) melanophores present versus absent in all *Lampanyctus* larvae except for *L. pusillus* and *L. intricarius*; and

–The PO_5 or Vn form at 8–10 mm SL versus no PO_5 and Vn in all other *Lampanyctus* species during the larval stage.

General characters D: 11–12, A: 16–18, P_1: 11–13, P_2: 8; GR: 3–4+1+8–9, total 12–14, V: 33–35. Length at transformation ~12 mm SL. The Br_2 appear at 4.5–5.0 mm SL. All the rays in the fins are distinguishable in the 7-mm-SL larva.

Pigmentation Lower-jaw symphyseal, UJS, 1–2 gular (Gu), anterior forebrain (Fa), anterior midbrain (Ma), paired and unpaired Mp, H, symphyseal-cleithral (SC), 4–6 AAV, TGd, MGd, paired lateral cleithral (CL), 1–2 inner BP, 2–5 anterior mediolateral (MLA), HMSa, Pp.

Similar species in the STC Similar to larvae of *L. australis* but lack PMDa melanophore and broad vertical band of pigment. Similar to *L. pusillus* but moderately slender body (BD 28–33% SL) versus deep body in *L. pusillus* (BD 35–43% SL).

General distribution The tropical and subtropical Atlantic Ocean and Indo-Pacific. Occurrence in the STC: from north of the STC to 38°S in the western South Atlantic, in the region of the northern limit of the STC in the eastern South Atlantic and Indian Oceans, and in the western Pacific Ocean (to 180°E) in the region of the northern limit of the STC (Hulley, 1981; McGinnis, 1982; Bekker, 1983; Young et al., 1996; Roberts et al., 2015).

Lampanyctus australis Tåning, 1932
Southern lanternfish
Figure 11

Lampanyctus sp. 1: Olivar, 1988, 410, fig. 11 (PrF, F, PoF); Benguela Current.

Lampanyctus australis: Olivar and Beckley, 1997, 52, fig. 3 (F, PoF); Agulhas Current. Bolshakova and Evseenko, 2016a, 852, fig. 4 (PoF); Walvis Ridge (southeast Atlantic Ocean). Bolshakova et al., 2021, 115, fig. 4 (PoF); southwest Pacific Ocean.

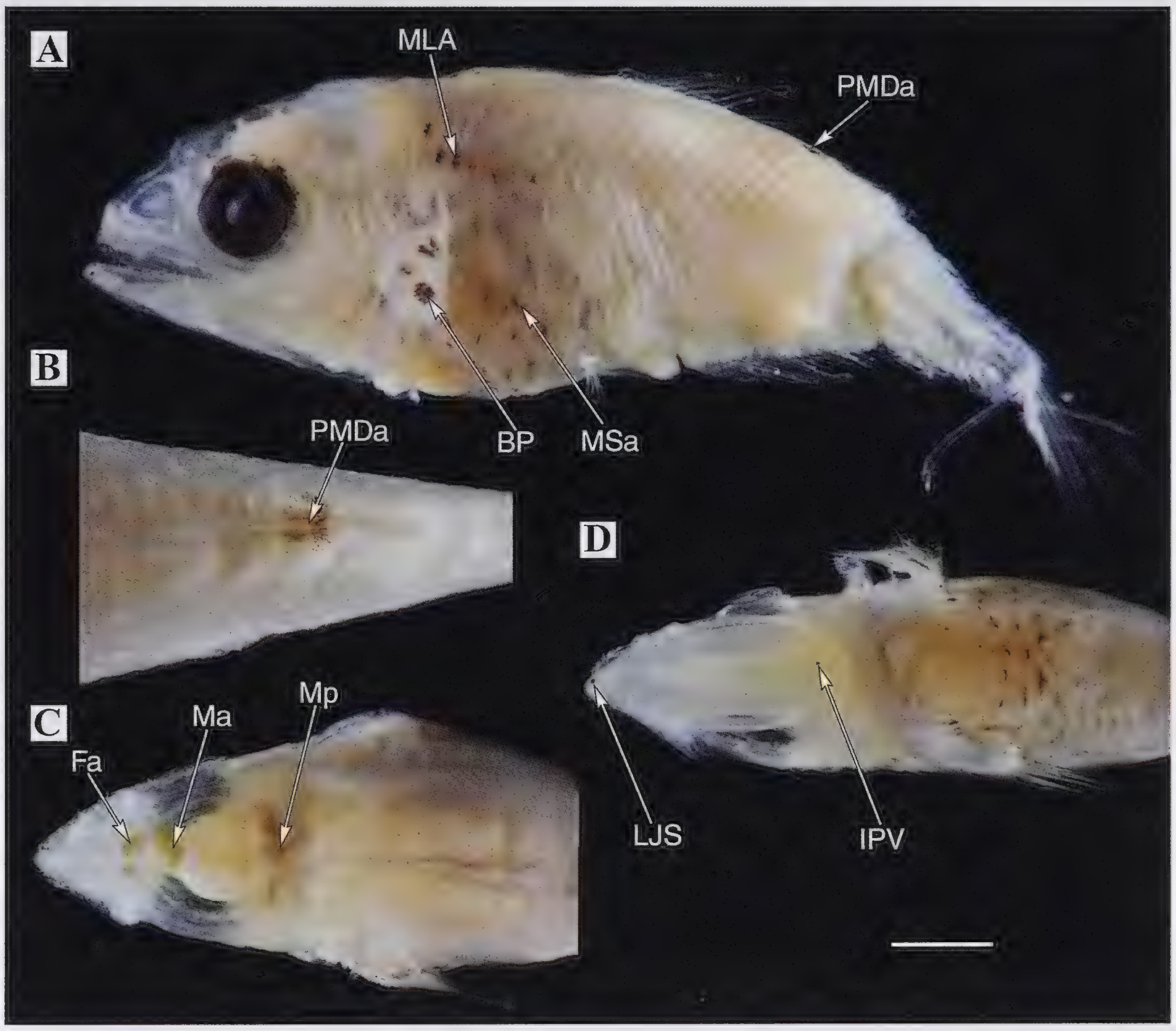

Figure 11

A larva of *Lampanyctus australis* (southern lanternfish) (10.0 mm standard body length, ID code: IORAS 04479): (**A**) lateral view, (**B**) dorsal view of the tail, (**C**) dorsal view of the body, and (**D**) ventral view of the body. The following melanophore pigment groups are shown: anterior mediolateral (MLA), preadipose (PMDa), basipectoral (BP), abdominal myoseptal (MSa), anterior forebrain (Fa), anterior midbrain (Ma), posterior midbrain (Mp), lower-jaw symphyseal (LJS), and prepectoral (isthmic) (IPV). The scale bar indicates a length of 1 mm.

Identification A broad vertical band of pigment posterior to the pectoral fin present versus absent in other *Lampanyctus* larvae (extralimital species: also present in *L. crocodilus* from the North Atlantic Ocean and *L. nobilis* from the tropical zone of 3 oceans).

General characters D: 12–14, A: 16–19, P_1: 13–15, P_2: 8; GR: 6(7)+1+14(13), total 19–21, V: 35–37. Length at transformation >15 mm SL. The Br_2 appear at 5.5 mm SL. All the rays in the fins are distinguishable in the 10.0-mm-SL larva.

Pigmentation Lower-jaw symphyseal; sometimes UJS; paired Ma; unpaired: Fa, Mp, H; sometimes single prepectoral (isthmic) (IPV); periproctal (AAVp); TGd; often PMDa; inner CL; 2–3 inner BP; abdominal myoseptal (broad vertical band); 4–6 MLA; Pp.

Similar species in the STC Similar to *L. alatus* but have no preanal series of melanophores and have more GR: 19–21 versus 12–14 in *L. alatus*.

General distribution Circumglobal in Southern Hemisphere south to 30°S. Occurrence in the STC: throughout the area except the central Pacific sector (Parin et al., 1973; Hulley, 1981; McGinnis, 1982; Bekker, 1983; Young et al., 1996; Roberts et al., 2015).

Lampanyctus festivus Tåning, 1928
Festive lanternfish
Figure 12

Lampanyctus sp. B: Olivar and Beckley, 1997, 57, fig. 8 (PrF, F, PoF); Agulhas Current.
Lampanyctus festivus: Bolshakova and Evseenko, 2016a, 854, fig. 5 (PoF); Walvis Ridge.

Identification

–Postorbital and opercular melanophores present versus absent in other *Lampanyctus* larvae, except for *L. achirus* and *L. pusillus* (extralimital species: also present in *L. regalis* from the North Pacific Ocean);

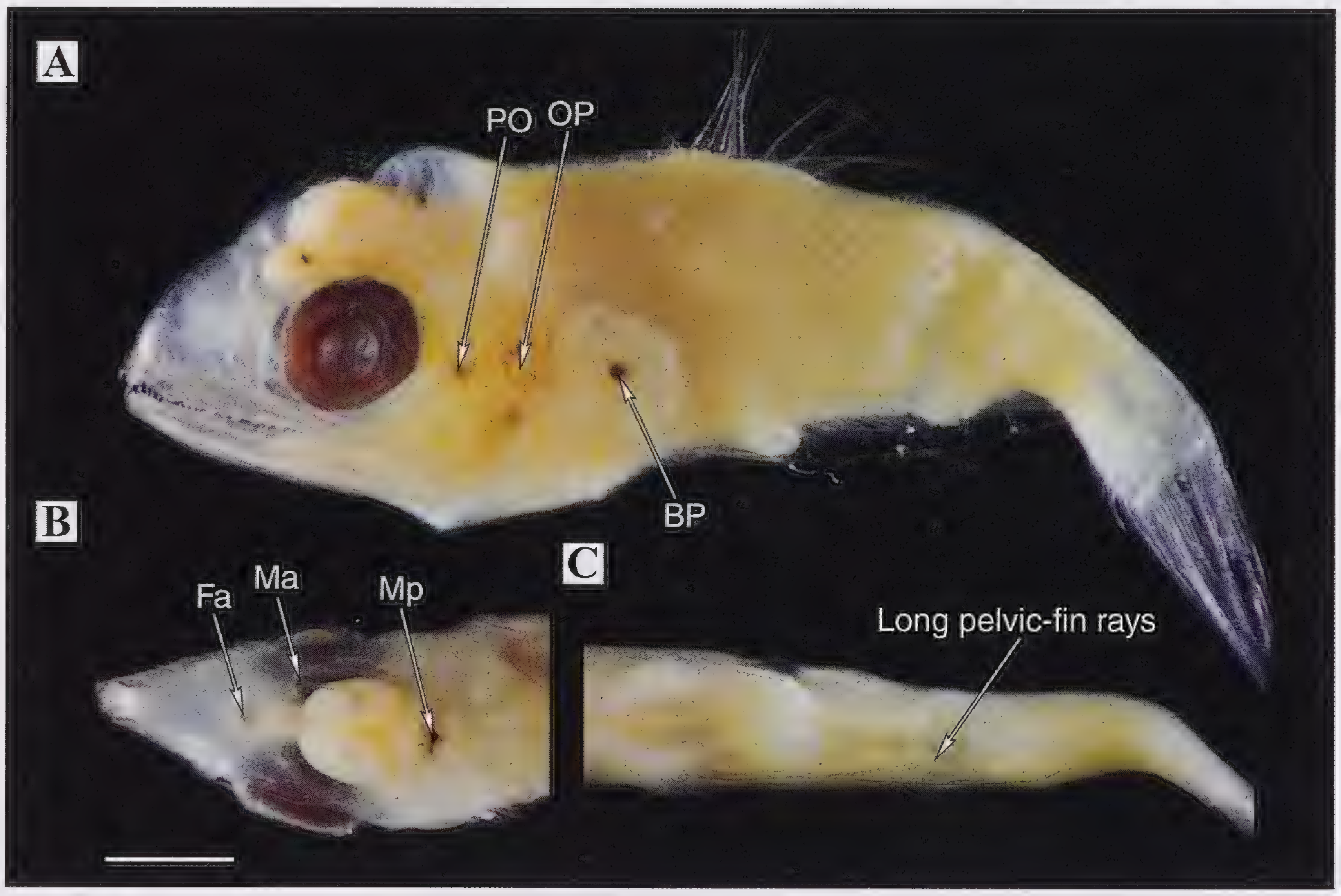

Figure 12

A larva of *Lampanyctus festivus* (festive lanternfish) (9.5 mm standard body length, ID code: IORAS 04481): (**A**) lateral view, (**B**) dorsal view of the head, and (**C**) ventral view of the body and tail, showing a long ray on the pelvic fin. The following melanophore pigment groups are shown: postorbital (PO), opercular (OP), basipectoral (BP), anterior forebrain (Fa), anterior midbrain (Ma), and posterior midbrain (Mp). The scale bar indicates a length of 1 mm.

- –Single large BP melanophore versus several or lacking in other *Lampanyctus* larvae (extralimital species: single melanophore also in *L. niger* from the tropical and subtropical North Pacific Ocean);
- –No TGd pigmentation and PMDa melanophore versus at least one of those present in other *Lampanyctus* larvae except for *L. achirus*; and
- –Long pelvic-fin rays: rays reach from middle to end of anal fin base at ≥4.7 mm SL versus rays do not reach the middle of the anal fin in other *Lampanyctus* larvae.

General characters D: 13–16, A: 18–22, P_1: 15–17, P_2: 8; GR: 4+1+8–10, total 13–15, V: 36–37. Length at transformation >10 mm SL. The Br_2 appear at 4.7 mm SL. All the rays in the fins are distinguishable in the 8.9-mm-SL larva.

Pigmentation Postorbital, 1–3 OP, Fa, paired Ma, single Mp, FGv, MGd, BP, Pp.

General distribution Bipolar subtropical distribution in the Atlantic and Pacific Oceans and equatorial waters of the Indian Ocean. Occurrence in the STC: eastern and western sectors of the South Atlantic and Pacific Oceans (Hulley, 1981; McGinnis, 1982; Bekker, 1983; Young et al., 1996; Roberts et al., 2015).

Lampanyctus intricarius Tåning, 1928
Diamondcheek lanternfish
Figure 13

Myctophum benoiti: Regan, 1916, 139, plate 6, figs. 1 and 2 (PrF, PoF); southwest Atlantic Ocean.
Lampanyctus? isaacsi: Olivar, 1988, 407, fig. 9 (PrF, F, PoF); Benguela Current.
? *Lampanyctus lepydolichnus*: Olivar and Beckley, 1997, 53, fig. 4 (PrF, F, PoF); Agulhas Current.
Lampanyctus intricarius: Bolshakova and Evseenko, 2015, 596, figs. 2–4 (PoF); southwest and southeast Pacific and southeast Atlantic Oceans. Bolshakova et al., 2021, 117 (description without illustration); southwest Pacific Ocean.

Identification

- –Both PDL and AAV unpaired series of melanophores present versus absent or paired in other *Lampanyctus* larvae;
- –Caudal myoseptal melanophores present versus absent in other *Lampanyctus* larvae, except for *Lampanyctus* sp. D (extralimital species: also present in *L. lineatus* from the tropical and subtropical Atlantic, South Pacific, and Indian Oceans); and

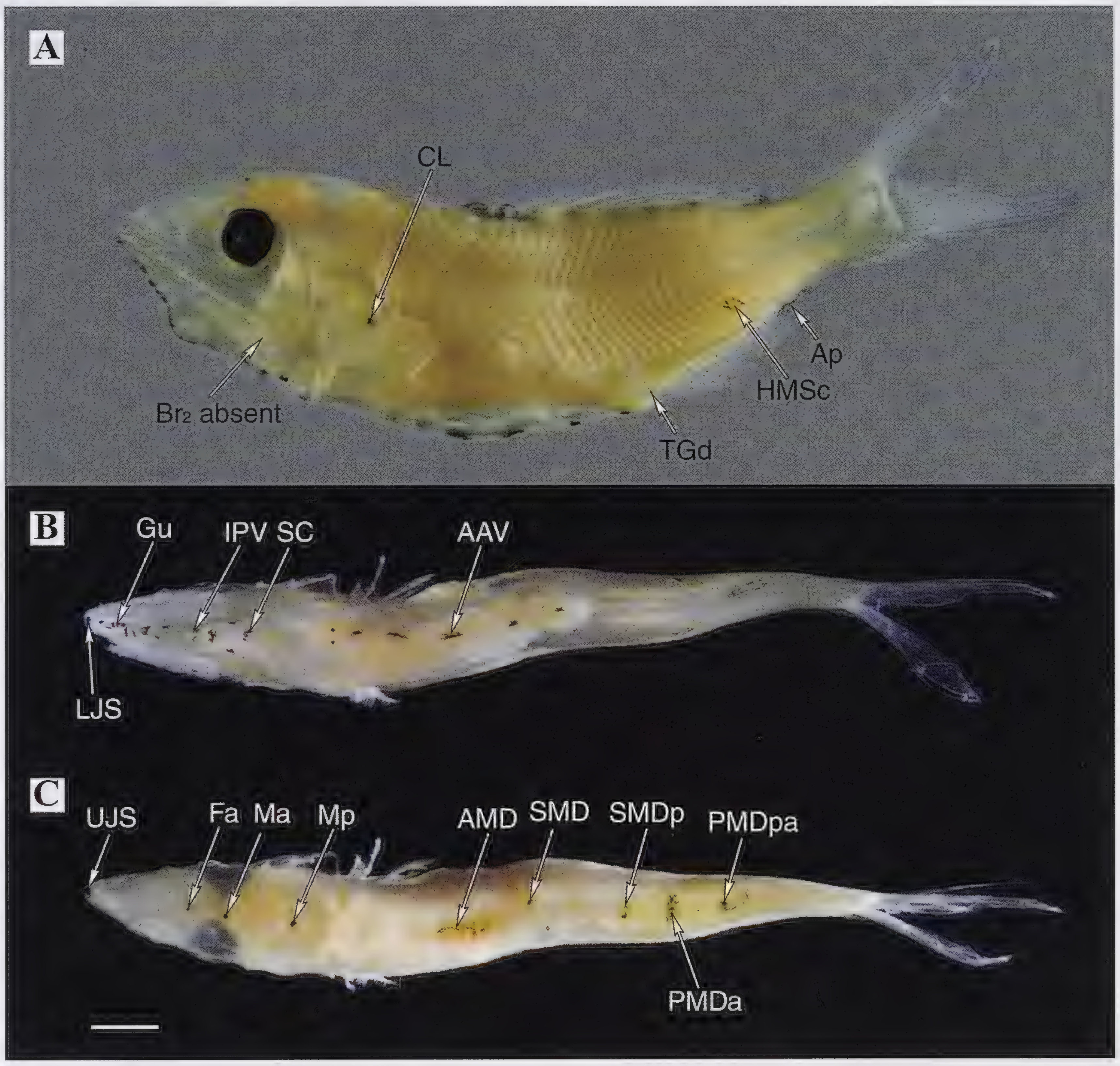

Figure 13

A larva of *Lampanyctus intricarius* (diamondcheek lanternfish) (12.7 mm standard body length, ID code: IORAS 04480): (**A**) lateral view, (**B**) ventral view, and (**C**) dorsal view. The following melanophore pigment groups are shown: lateral cleithral (CL), dorsal terminal gut (TGd), hypaxial caudal myoseptal (HMSc), anal-fin pigmentation (Ap), lower-jaw symphyseal (LJS), gular (Gu), prepectoral (isthmic) (IPV), symphyseal-cleithral (SC), preanal (AAV), upper-jaw symphyseal (UJS), anterior forebrain (Fa), anterior midbrain (Ma), posterior midbrain (Mp), antedorsal (AMD), subdorsal (SMD), posterior subdorsal (SMDp), preadipose (PMDa), and postadipose (PMDpa). The 2nd branchiostegal photophores (Br_2) are absent. The scale bar indicates a length of 1 mm.

–No photophores developed during the larval stage versus at least Br_2 are present in other *Lampanyctus* larvae.

General characters D: 14–16, A: (17)18–20, P_1: 13–15, P_2: 8; GR: 4+1+9–11, total 14–16, V: 37–38. Length at transformation >25 mm SL. No photophores developed during the larval stage. All the rays in the fins are distinguishable in the 7-mm-SL larva. Larvae have dorsal and ventral fin folds. The body of larvae is laterally compressed.

Pigmentation Lower-jaw symphyseal, few UJS, row of Gu, Fa, Ma, Mp, paired irregular row of IPV, SC, single row of AAV, 1–2 paired subanal (PAVa), PAVt, TGd, single row of AMD, 1–2 paired SMD, posterior subdorsal, PMDa, paired or unpaired postadipose, 1–2 CL, 1–2 hypaxial caudal myoseptal, dorsal-fin pigmentation, anal-fin pigmentation, Pp, ventral-fin pigmentation, adipose-fin pigmentation.

General distribution Circumglobal in the Southern Hemisphere south of 20° S to the STC; North Atlantic Ocean in temperate region. Occurrence in the STC: throughout the area (Parin et al., 1973; Hulley, 1981; McGinnis, 1982; Bekker, 1983; Bekker and Evseenko, 1986; Young et al., 1996; Roberts et al., 2015).

Remarks Larvae of *L. intricarius* described from the southwest and southeast Pacific Ocean and the southeast Atlantic Ocean (Bolshakova and Evseenko, 2015) and larvae from the Agulhas (Olivar and Beckley, 1997) and Benguela Current regions (Olivar and Fortuño, 1991) in the southeast Atlantic Ocean identified as *L. lepidolychnus* show no differences in meristic characters, pigmentation pattern, and body proportions. Olivar and Beckley (1997) referred the larvae from the Agulhas Current region to *L. lepidolychnus* the basis of meristic characters and simultaneous catches of the adults of that species. Although initially identified as *L. isaacsi* (Olivar and Fortuño, 1991), the larvae from the Benguela Current region were later considered indistinguishable from those in the Agulhas Current and possibly belonging to 1 of 2 closely related species: *L. lepidolychnus* or *L. intricarius* (Olivar and Beckley, 1997). *Lampanyctus lepidolychnus* prefers the coastal waters and has not been recorded in the southwest Pacific Ocean east of 165°W (Hulley, 1981; McGinnis, 1982; Bekker, 1983; Bekker and Evseenko, 1986), where some of the larvae described as *L. intricarius* (Bolshakova and Evseenko, 2015; Bolshakova et al., 2021) were caught. Adults of these 2 species differ mainly in their body proportions and position of photophores but do not differ in meristic characters (Hulley, 1981). It is not clear if all these larvae belong to the same species, or differences between *L. lepidolychnus* or *L. intricarius* at larval stages have not yet established.

Lampanyctus pusillus (Johnson, 1890)
Pigmy lanternfish
Figure 14

Lampanyctus alatus: Tåning, 1918, 108, fig. 42 (F, PoF, Juv); Mediterranean Sea.

Lampanyctus pusillus: Olivar, 1985, 292 (description without illustration); Benguela Current. Olivar, 1988, 410 (short description without illustration); Benguela Current. Rodríguez et al., 2017, 68, 69 (PrF, F, PoF); Mediterranean Sea. Bolshakova et al., 2021, 121 (description without illustration); southwest Pacific Ocean.

Identification

- –Paired MD and ML and numerous myoseptal (MS) melanophores present versus absent in other *Lampanyctus* larvae;
- –Both TGd and AAVp melanophores present versus absent in other *Lampanyctus* larvae, except for *L. australis* and *L. intricarius* (extralimital species: also present in *L. tenuiformis* from the tropical zone of 3 oceans); and
- –Number of vertebrae 30–32 versus ≥33 in other *Lampanyctus* larvae (extralimital species: also 32–34 in *L. cuprarius* from the tropical and subtropical Atlantic Ocean and *L. idostigma* from the eastern Pacific Ocean).

General characters D: 11–13, A: (13)14–15, P_1: 13–14, P_2: 8; GR: 3+1+8(9), total 12(13), V: 30–32. Length at transformation ~12 mm SL. The Br_2 appear to 5 mm SL. All the rays in the fins are distinguishable in the 8.5-mm-SL larva. Larvae have moderately deep body (BD 35–43% SL) and blunt snout. Most heavily pigmented larvae within genus.

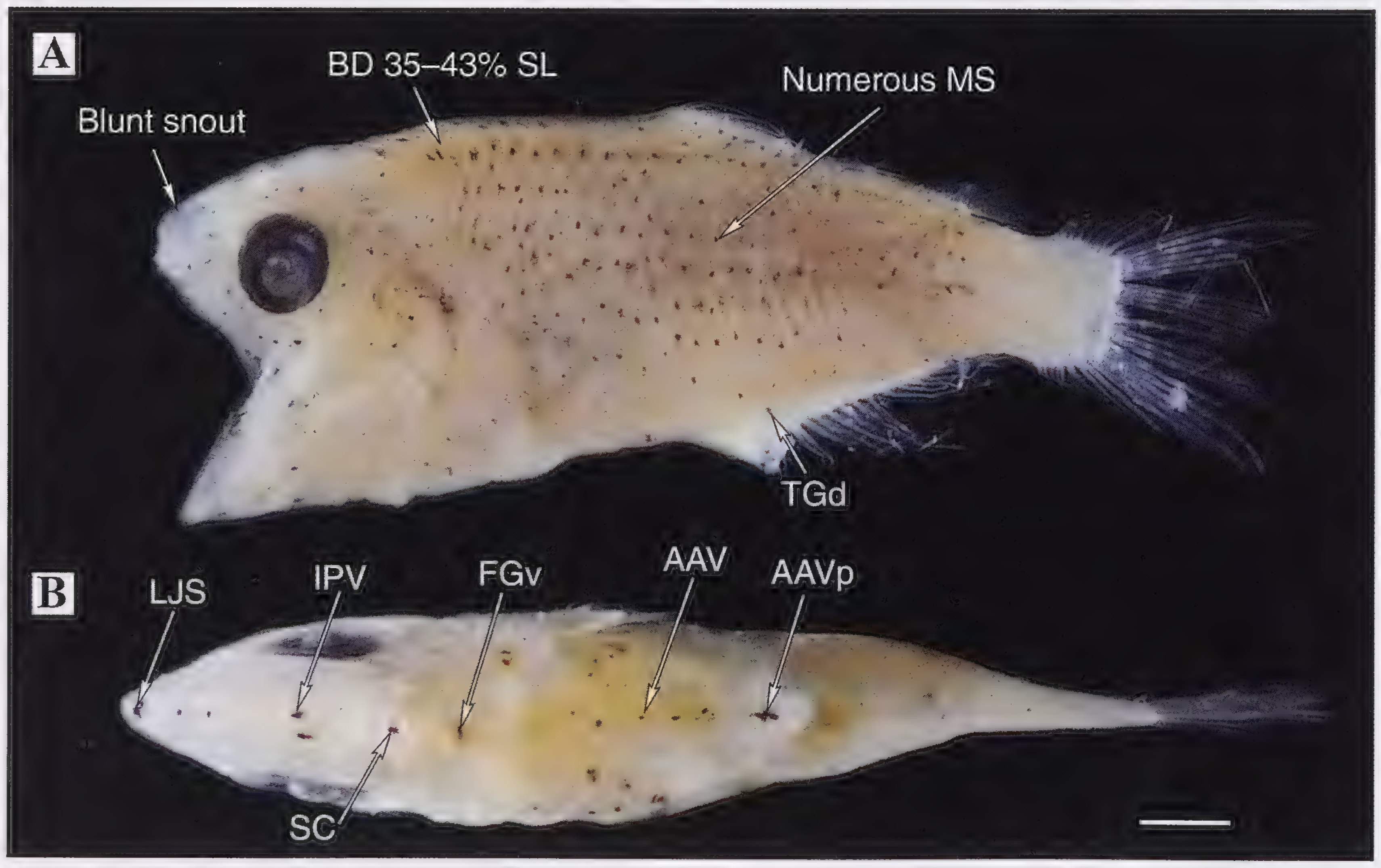

Figure 14

A larva of *Lampanyctus pusillus* (pigmy lanternfish) (11.5 mm standard body length [SL], IORAS 04482): (**A**) lateral view and (**B**) ventral view. The following melanophore pigment groups are shown: myoseptal (MS), dorsal terminal gut (TGd), lower-jaw symphyseal (LJS), prepectoral (isthmic) (IPV), symphyseal-cleithral (SC), anteroventral foregut (FGv), preanal (AAV), and periproctal (AAVp). The scale bar indicates a length of 1 mm. BD=body depth at pectoral fin base.

Pigmentation Several UJS, LJS, posterior lower-jaw (LJP), 1–3 Gu, Fa, Ma, paired and unpaired Mp, H, 1–2 paired Ot, a few PO, a few OP, paired row of IPV, SC, unpaired row of AAV, AAVp, several paired PAVa, 1–2 paired FGv, 2–3 clusters MGd, TGd, CL, 2 or more BP, row of ML, paired row of MD, numerous MS.

General distribution Circumglobal in the Southern Hemisphere north of 46°S; North Atlantic Ocean in temperate and subtropical regions. Occurrence in the STC: northern limits of the area (Parin et al., 1973; Hulley, 1981; McGinnis, 1982; Bekker, 1983; Bekker and Evseenko, 1986; Young et al., 1996; Roberts et al., 2015).

Lampanyctus sp. D
Figure 15

Lampanyctus nobilis: Olivar and Beckley, 1997, 56, fig. 6 (PoF); Agulhas Current.

Lampanyctus sp. D: Bolshakova et al., 2021, 119, figs. 6 and 7 (F, PoF); southwest Pacific Ocean.

Identification Only medullar and TGd pigmentation versus more pigment present in other *Lampanyctus* larvae (extralimital species: also poorly pigmented in *L. nobilis* from tropical region of all oceans).

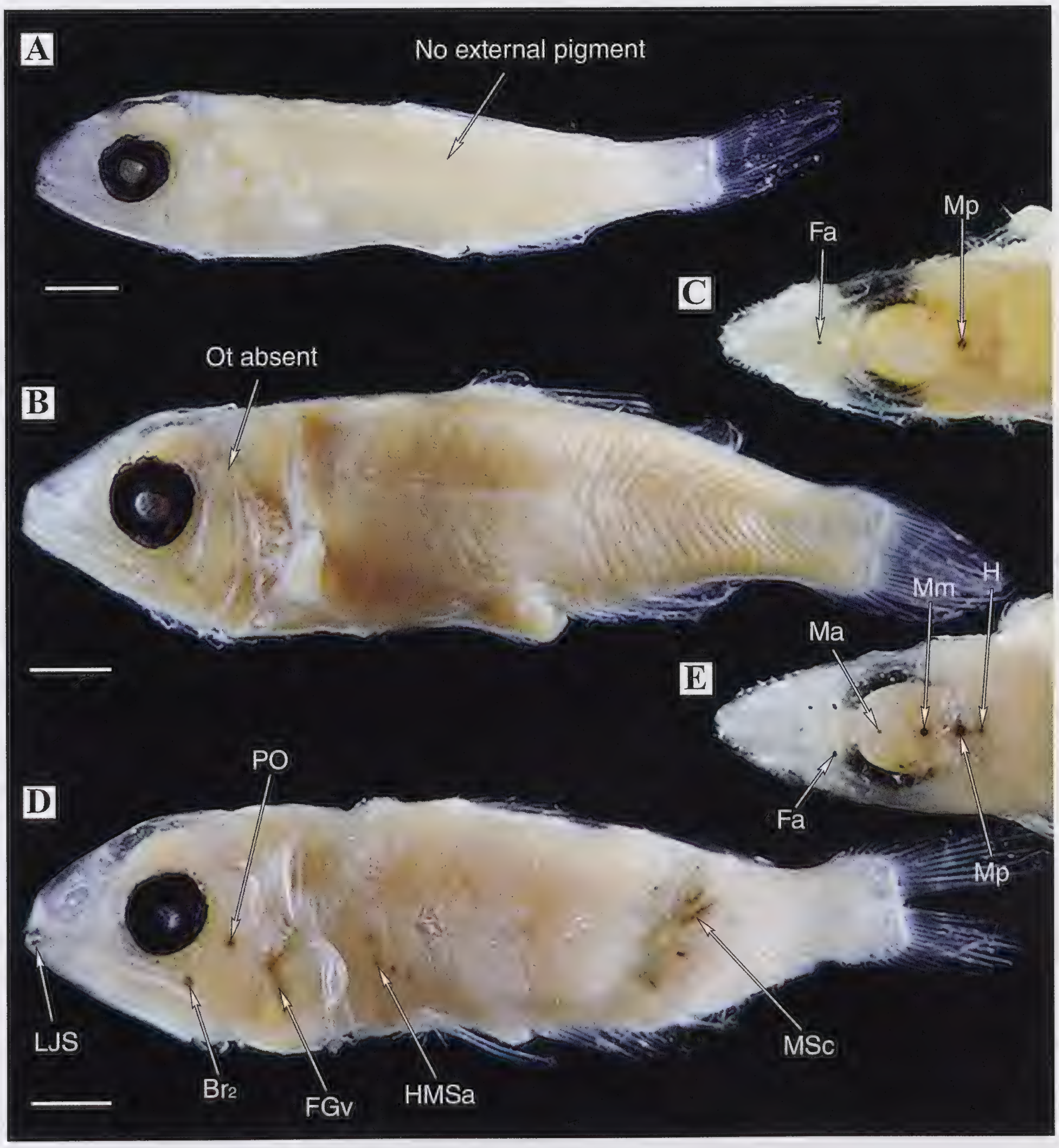

Figure 15

Larvae of *Lampanyctus* sp. D: (**A**) 10.0 mm standard body length (SL), ID code: IORAS 04485 (lateral view); (**B**) 11.6 mm SL, IORAS 04483 (lateral view); (**C**) 11.6 mm SL, IORAS 04483 (dorsal view of the head); (**D**) 11.7 mm SL, IORAS 04484 (lateral view); and (**E**) 11.7 mm SL, IORAS 04484 (dorsal view of the head). The following melanophore pigment groups and photophore are shown: anterior forebrain (Fa), posterior midbrain (Mp), lower-jaw symphyseal (LJS), anteroventral foregut (FGv), hypaxial abdominal myoseptal (HMSa), caudal myoseptal (MSc), anterior midbrain (Ma), medial midbrain (Mm), hindbrain (H), postorbital (PO), and 2nd branchiostegal photophores (Br_2). Otical (Ot) pigmentation is absent. The scale bars in panels indicate a length of 1 mm.

General characters D: 13–15, A: 16–17, P_1: 13–14, P_2: 8; GR: 4(5)+1+10, total 15(16), V: 35–36. Length at transformation >17.0 mm SL. The Br_2 appear to 9.5 mm SL. All the rays in the fins are distinguishable in the 10.3-mm-SL larva, and the number of gill rakers is definitive in the 13.0-mm-SL larva.

Pigmentation Anterior forebrain; paired Ma; Mp; TGd; FGv; FGd; often: inner PO, 1 or 2 CL; sometimes: caudal myoseptal; rarely: LJS, 1 or 2 unpaired medial midbrain, H, HMSa.

General distribution The central and western South Pacific Ocean. Occurrence in the STC: between 38°S and 42°S in the Pacific Ocean (McGinnis, 1982; Bolshakova et al., 2021).

Remarks The larva of *Lampanyctus* sp. D described from the Agulhas Current region by Olivar and Beckley (1997) belongs to *L. indicus* (Bolshakova et al., 2021). *Lampanyctus* sp. D in the sense described herein is identical to the undescribed *Lampanyctus* sp. D established by McGinnis (1982) on adults from the Southern Ocean.

The larvae described as *L. nobilis* (Olivar and Beckley, 1997) are similar in pigmentation, proportions, and meristic characters to our specimens of *Lampanyctus* sp. D. They differ from the typical larvae of *L. nobilis* (Moser et al., 1984; Moser and Ahlstrom, 1996) in the absence of a row of the isthmic and Gu melanophores (not specified in the description and not marked on the figure) and in the lower counts of D, A, and V.

Lepidophanes Fraser-Brunner, 1949

General characters The larvae have a slender body (**BD <19% SL**); head moderate (HL 25–27% SL); snout short (SnL 23–25% HL); eye moderately small (**ED 21–29% HL**); anus opens slightly behind midbody (PAL 63–67% SL). During the larval stage, Br_2, Vn, PO_5, and PLO; Br_2 appear at 5.6 mm SL (in *L. guentheri*) or at 12.3 mm SL in *L. gaussi*; transformation usually occurs at **13 mm SL**.

Pigmentation Occipital, Ot, usually 2 pairs PMDp, 1–2 PAVp, Ivt series.

Similar genera Similar to *Ceratoscopelus* and *Taaningichthys*, see descriptions of these genera for details.

Remarks Adults of *L. guentheri* have been recorded in the STC (Hulley, 1981; McGinnis, 1982; Bekker, 1983).

Lepidophanes guentheri (Goode and Bean, 1896)
Largemouth lampfish
Figure 16

Lepidophanes guentheri: Moser and Ahlstrom, 1972, 551, fig. 8 (PoF, Juv); Northeast Atlantic Ocean. Shiganova, 1977, 88, fig. 14 (F, PoF, Juv); Atlantic Ocean. Moser and Watson, 2001, 94, figure on p. 95 (PrF, F, PoF, Juv); western central Atlantic Ocean. Bonecker and Castro, 2006, figure on p. 148 (PoF, Juv); tropical southwest Atlantic Ocean.

Identification

- –Supracaudal and infracaudal melanophores present versus absent in all Myctophidae larvae except for *Lampadena* spp. (extralimital species: also present in *C. maderensis* from the North Atlantic Ocean, *T. minimus* from subtropical waters, and *Lepidophanes gaussi* from the subtropical Atlantic Ocean); and
- –Ventronasal gland present at 8 mm SL versus Vn absent in *Lampadena* spp. larvae <13.5 mm SL.

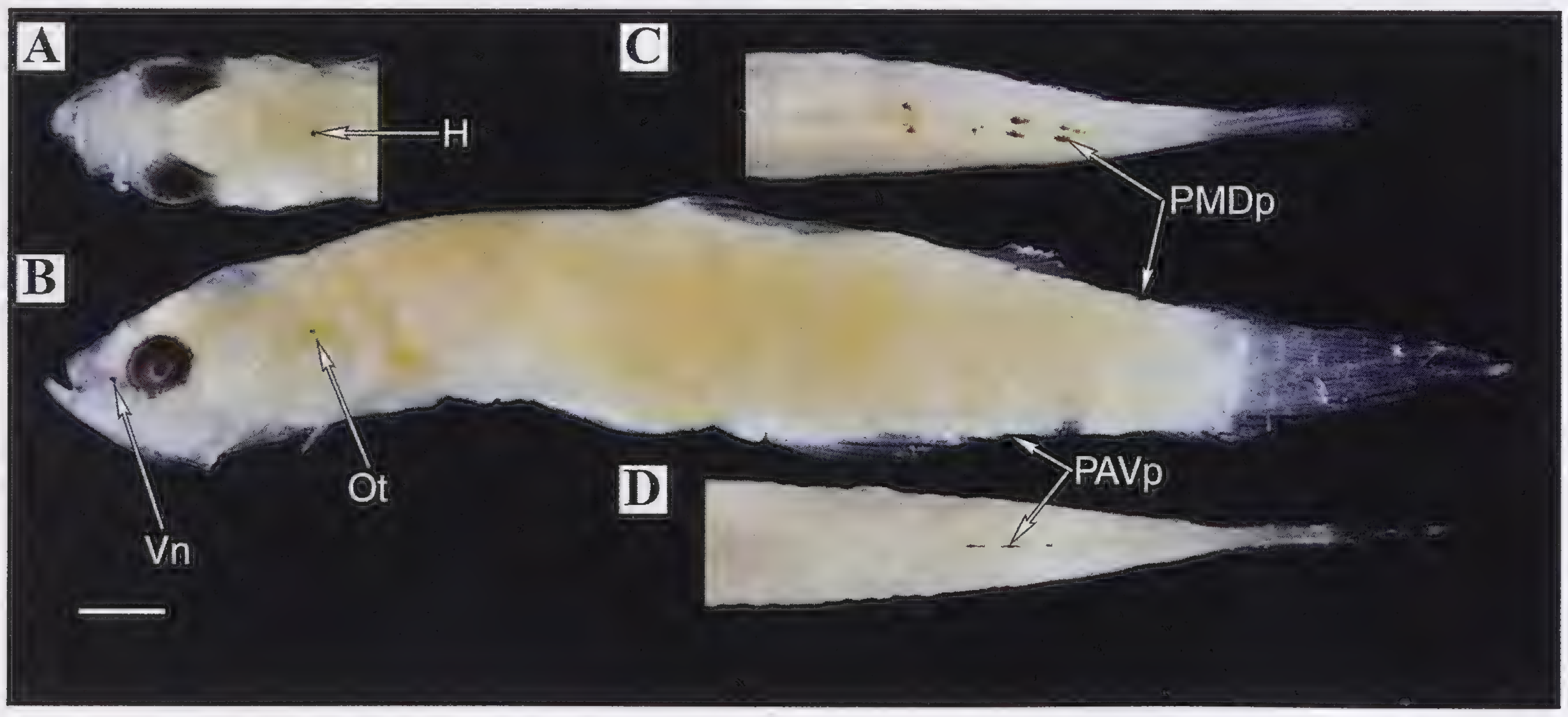

Figure 16

A larva of *Lepidophanes guentheri* (largemouth lampfish) (14.3 mm standard body length, ID code: IORAS 04486): (**A**) dorsal view of the head, (**B**) lateral view, (**C**) dorsal view of the tail, and (**D**) ventral view of the tail. The following melanophore pigment groups and photophore are shown: hindbrain (H), otical (Ot), supracaudal (PMDp), infracaudal (PAVp), and ventronasal gland (Vn). The scale bar indicates a length of 1 mm.

General characters D: 13–15, A: 13–15(16), P_1: (11)12–14, P_2: 8; GR: 4+1+8–10, total 13–15, V: 36. Length at transformation ~14 mm SL. The Br_2 appear at ~5.6 mm SL, Vn and PO_5 appear at ~7.5 mm SL, and PLO appear at ~9.0 mm SL. All the rays in the fins are distinguishable in the 10-mm-SL larva, and the definitive number of gill rakers is noticeable to a size of 11–12 mm SL.

Pigmentation Hindbrain, Ot, 3–4 PAVp, TGd, 3–4 Ve, 2–4 PMDp.

General distribution The tropical and subtropical Atlantic Ocean. Occurrence in the STC: in the region of the northern limit of the STC in the eastern Atlantic Ocean and throughout the STC in the sector of the western Atlantic Ocean (Hulley, 1981; McGinnis, 1982; Bekker, 1983; Figueroa et al., 1998).

Taaningichthys Bolin, 1959

General characters Body slender (**BD <19% SL**); head moderate (HL 21–26% SL); snout short (SnL 21–26% HL); eye moderately small (ED >26–29% HL); anus opens slightly behind midbody (PAL 60–65% SL). **No photophores** during the larval stage (Br_2 form at transformation stage); transformation usually occurs at **21 mm SL.**

Pigmentation Medullar melanophores, SMD, postdorsal and PAV series, Ivt series.

Similar genera Similar to *Lampadena*, *Lepidophanes*, and *Ceratoscopelus*, but photophores appear only toward the end of the larval stage (during the transformation) at >18 mm SL (versus early in the larval stage at 5–7 mm SL); more slender than *Lampadena* (BD <19% SL versus >19% SL); saggital intervertebral melanophores present (versus absent in *Lampadena* and *Lepidophanes*); subdorsal pigment present (versus absent in *Lepidophanes* and *Ceratoscopelus*).

Remarks This genus contains 3 species (Fricke et al., 2023): *T. bathyphilus*, *T. minimus*, and *T. paurolychnus*. The early stages of development are known only for *T. minimus* (Pertseva-Ostroumova, 1964, 86, fig. 7, as *Lampadena* sp.; Moser and Ahlstrom, 1972, 1996; Ozawa, 1986). The slender body, present MD and PAV pigment, and the absence of photophores, even Br_2, until transformation, characterize the described larvae. Adults of *T. bathyphilus* alone have been recorded in the STC (Hulley, 1981; McGinnis, 1982; Bekker, 1983). The early stages of development of *T. bathyphilus* are unknown, but we expect that the larvae of *Taaningichthys* species have similar diagnostic characters, especially the late appearing photophores.

Subfamily Notolychninae Paxton, 1972

Diagnosis Larvae of Notolychninae can be distinguished from the larvae of the subfamilies Diaphinae, Gymnoscopelinae (except for *Scopelopsis*), and Lampanyctinae by their short gut, absence of larval photophores, and lower number of pelvic-fin rays. Notolychninae can be further separated from all diaphine, gymnoscopeline, and lampanyctine larvae except for *Triphoturus* spp. by the eye shape (elliptical or trapezoidal versus round). Notolychninae larvae can be separated from Myctophinae larvae by the absence of larval photophores (versus at least Br_2 in Myctophinae larvae).

Genera Monotypic.

Notolychnus Fraser-Brunner, 1949

General characters Diagnostic characters are described later in the description of the only species in this genus.

Notolychnus valdiviae (Brauer, 1904)
Topside lanternfish
Figure 17

Myctophum valdiviae: Tåning, 1918, 151, fig. 47 (PoF, Juv); Mediterranean Sea.

Notolychnus valdiviae: Pertseva-Ostroumova, 1964, 85, fig. 6 (PoF); Pacific Ocean. Moser and Ahlstrom, 1974, 409, fig. 12e (PoF); area unknown. Shiganova, 1975, 78, fig. 4 (PrF, F, PoF, Juv); Northwest Atlantic Ocean. Moser et al., 1984, 234, fig. 120a (PoF); California Current?. Moser and Ahlstrom, 1996, 426, figure on p. 427; Northeast Pacific Ocean. Olivar et al., 1999, 109 (description without illustration); Agulhas Current.

Identification

- –No photophores during the larval stage versus at least Br_2 present in Myctophidae larvae, except for *Taaningichthys minimus*; and
- –Preanal length 44–53% SL versus 56–75% SL in other Lampanictinae larvae except for *Scopelopsis* (extralimital species: 52–58% SL in *P. ingens* from the California Current).

General characters D: 10–12, A: 12–15, P_1: 12–15, P_2: 6–7, GR: 2+8–9, total 10–11, V: 27–31. Body slender (BD 16–23% SL); head relatively small (HL 25–31% SL); snout moderate (SnL 32–39% HL); **eye small, elliptical or trapezoidal** with dorsal (in PrF larvae) and ventral choroid tissue (**ED 18–25% HL, in width, and 27–38% HL, in height**); anus opens near the middle of the body (**PAL 44–53% SL**). Length at transformation ~10 mm SL. No photophores during the larval stage, even Br_2. All photophores appear almost simultaneously at a 9–10 mm SL. All the rays in the fins are distinguishable in the ~7–8-mm-SL larva, and the definitive number of gill rakers is noticeable to a size of 7–8 mm SL.

Pigmentation Three to 4 PAVa, 1 PAVt, 1–2 PAVp, 1–2 basicaudal medium, paired TGd, 3–4 paired lateral midgut, Ve, Cp.

General distribution Circumglobal in tropical and subtropical waters. Occurrence in the STC: in the region of the

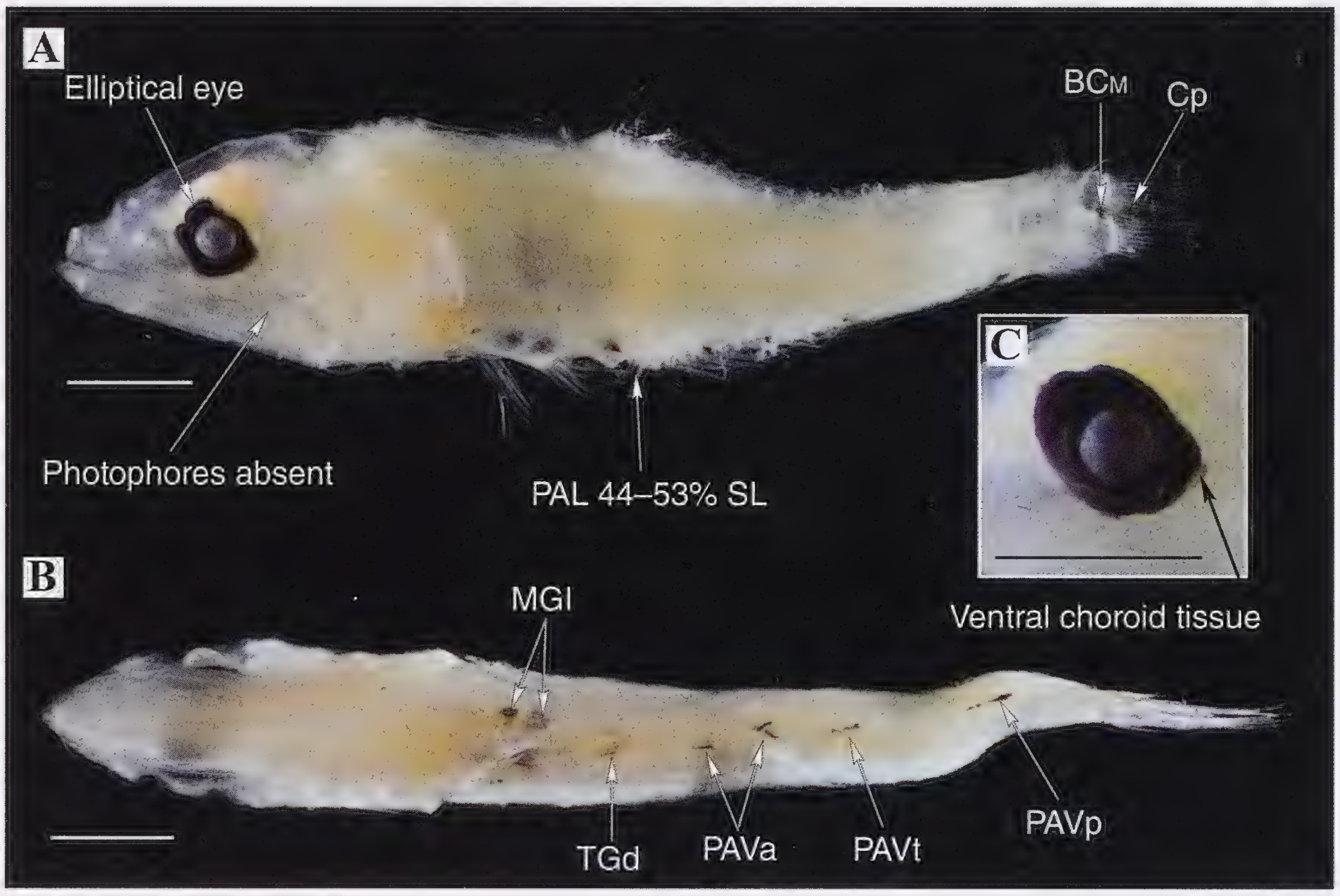

Figure 17

Larvae of *Notolychnus valdiviae* (topside lanternfish): (**A**) lateral view and (**B**) ventral view of a larvae with an 8.5 mm standard body length (SL) (ID code: IORAS 04487). (**C**) Close up of the eye of a 6.2-mm-SL specimen (IORAS 04488). The following melanophore pigment groups are shown: basicaudal medium (BC_M), caudal-fin pigmentation (Cp), lateral midgut (MGl), dorsal terminal gut (TGd), subanal (PAVa), terminal subanal (PAVt), and infracaudal (PAVp). The scale bar in each panel indicates a length of 1 mm. PAL=preanal length.

northern limit of the STC (Nafpaktitis et al., 1977; Hulley, 1981; McGinnis, 1982; Bekker, 1983).

Discussion

Notolychninae is monotypic and includes a single species, *N. valdiviae*, with a broad tropical, circumglobal distribution between 40°N and 40°S (Paxton, 1972; Nafpaktitis et al., 1977; Bekker, 1983). In the STC, it is known by a single record east of New Zealand at 44°S, 173°E (McGinnis, 1982). The subfamily Lampanyctinae consists of 9 genera (*Bolinichthys*, *Ceratoscopelus*, *Lampadena*, *Lampanyctus*, *Lepidophanes*, *Taaningichthys*, *Parvilux*, *Stenobrachius*, and *Triphoturus*), and all but the last 3 genera occur in the STC (Paxton, 1972; Hulley, 1981; McGinnis, 1982; Paxton et al., 1984; Denton, 2014; Martin et al., 2018). Some species of these genera are distributed in tropical and subtropical waters: *B. indicus*, *B. supralateralis*, *C. warmingii*, *Lampanyctus alatus*, *L. ater*, *L. festivus*, *L. pusillus*, and *Lepidophanes guentheri*. Larvae of these species are found only sporadically along the northern border of the STC. *Lampanyctus achirus* is a subantarctic species; although its larvae are often recorded in the STC (Bolshakova et al., 2021), those larvae may represent misidentified larvae of *L. wisneri* (see the "Remarks" section in the species description for *L.* gr. *achirus*).

McGinnis (1982) listed 21 transitional species, 8 of which belong to Lampanyctinae: *Lampadena notialis*, *Lampanyctus australis*, *L. intricarius*, *L. iselinoides*, *L. lepidolychnus*, *L. macdonaldi*, *Lampanyctus* sp. A (=*L. wisneri*), and *Lampanyctus* sp. D. Hulley (1981) indicated 15 myctophid species from the Atlantic Ocean belonging to a convergence subpattern (4 of them are Lampanyctinae: *Lampadena dea*, *L. notialis*, *Lampanyctus australis*, and *L. lepidolychnus*), and Zahuranec (2000) noted 2 *Nannobrachium* (=*Lampanyctus*) species (*L. achirus* and *L. wisneri*) that are distributed in and near the STC. We do not include *L. iselinoides* (larvae unknown) in the species of the STC because this species is restricted to the coastal waters of Chile between 30°S and 50°S, an area located in the Chilean Current, but does not belong to the STC. *Lampadena dea*, *L. notialis*, *Lampanyctus australis*, *L. intricarius*, *L. lepidolychnus*, *L. wisneri*, and *Lampanyctus* sp. D are apparently true convergence species (i.e., species that appear to be distributed only in oceanic waters in the region of and slightly north of the STC). Larvae of *L. australis*, *L. intricarius*, and *Lampanyctus* sp. D are found in a narrow range between 38°S and 42°S in the South Pacific Ocean, where they are very numerous in sample collections (Bolshakova et al., 2021). In general, the distribution of the larvae of the lampanyctine species known from the STC coincides with the distribution of adults, but larvae of this group have been found in a narrower range of latitudes (Bekker and Evseenko, 1986; Bolshakova et al., 2021).

Resumen

Se presentan descripciones de las larvas de peces linterna de las subfamilias Lampanyctinae (12 especies) y Notolychninae (1 especie) que pueden encontrarse en la Convergencia Subtropical (CST): *Bolinichthys supralateralis*, *Ceratoscopelus* gr. *townsendi*, *Lampadena* sp., *Lampanyctus alatus*, *L. ater*, *L. australis*, *L.* gr. *achirus*, *L. intricarius*, *L. festivus*, *L. pusillus*, *Lampanyctus* sp. D, *Lepidophanes guentheri* y *Notolychnus valdiviae*. También se proporciona una clave de identificación basada en caracteres larvarios para todas las subfamilias de peces linterna. Proponemos el uso de una clave separada para las larvas postflexión de todos los géneros conocidos de las subfamilias de peces linterna de ojos redondos Diaphinae, Gymnoscopelinae, Lampanyctinae y Notolychninae. Para cada género se indican las características generales de la morfología larvaria. Las descripciones de las especies incluyen los caracteres clave para la identificación, la variación en los caracteres merísticos, la pigmentación y otras características importantes para el diagnóstico de Myctophidae en sus fases larvarias. Se proporcionan fotografías de las características diagnósticas más importantes de cada especie. Se discute la taxonomía de 4 especies problemáticas de la zona, *C.* gr. *townsendi*, *Lampanyctus* gr. *achirus*, *L. intricarius* y *Lampanyctus* sp. D. Se describen por primera vez los estadios de preflexión, flexión y postflexión de una *Lampadena* sp. no identificada del límite norte del CST; estas larvas pueden pertenecer a 1 de las 3 especies (*L. dea*, *L. notialis* y *L. speculigera*) cuyas larvas aún no han sido identificadas. Se resume la distribución de Lampanyctinae y Notolychninae en el CST.

Acknowledgments

This study was supported by the Russian Science Foundation, project no. 19-14-00026.

Literature cited

Ahlstrom, E. H.
1971. Kinds and abundance of fish larvae in the eastern tropical Pacific, based on collections made on EASTROPAC I. Fish. Bull. 69:3–77.
Backus, R. H.
1986. Biogeographic boundaries in the open ocean. *In* Pelagic biogeography: proceedings of an international conference; Netherlands, 29 May–5 June 1985 (A. C. Pierrot-Bults, S. van der Spoel, B. J. Zahuranec, and R. K. Johnson, eds.), p. 9–13. UNESCO Tech. Pap. Mar. Sci. 49.
Badcock, J., and T. M. H. Araújo.
1988. On the significance of variation in a warm water cosmopolitan species, nominally *Ceratoscopelus warmingii* (Pisces, Myctophidae). Bull. Mar. Sci. 42:16–43.
Beebe, W.
1932. Nineteen new species and four post-larval deep-sea fish. Zoologica 13:47–107.
Bekker, V. E.
1983. Myctophid fishes of the world ocean, 248 p. Nauka, Moscow, Russia. [In Russian.]
Bekker, V. E., and O. D. Borodulina.
1968. Lanternfishes of the genus *Ceratoscopelus* Günther. Systematics and distribution. Vopr. Ikhtiol. 8:779–798. [In Russian.]
Bekker, V. E., and S. A. Evseenko.
1986. Distribution of mesopelagic fishes and biogeographic boundaries in the southern part of the Pacific Ocean in January–February 1985. Vopr. Ikhtiol. 26:890–901. [In Russian.]
Belyanina, T. N.
1982. Larvae of the midwater fishes in the western tropical Pacific Ocean and the seas of the Indo-Australian Archipelago. Tr. Inst. Okeanol. Akad. Nauk SSSR 118:5–42. [In Russian.]
Belyanina, T. N., and N. V. Kovalevskaya.
1979. Materials on the development and distribution of larvae of luminous anchovies (family Myctophidae) in the notal waters of the Australian–New Zealand region. Tr. Inst. Okeanol. Akad. Nauk SSSR 106:69–96. [In Russian.]
Bolin, R. L.
1939. A review of the myctophid fishes of the Pacific coast of the United States and of Lower California. Stan. Ichthyol. Bull. 1:89–156.
1959. Iniomi. Myctophidae from the “Michael Sars” North Atlantic deep-sea expedition 1910. Report on the scientific results of the “Michael Sars” North Atlantic deep-sea expedition 1910, vol. 4, part 2, no. 7, 45 p. Trustees Bergen Mus., Bergen, Norway.
Bolshakova, Ya. Yu., and S. A. Evseenko.
2015. Larvae of the lanternfish *Lampanyctus intricarius* (Myctophidae) from the southwestern Pacific Ocean. J. Ichthyol. 55:596–600.
2016a. On the species composition of ichthyoplankton of the Walvis Ridge (South Atlantic). J. Ichthyol. 56:848–860.
2016b. On species composition of ichthyoplankton of the Mid-Atlantic Ridge (South Atlantic). J. Ichthyol. 56:522–533.
2020. Ichthyoplankton of the central North Atlantic Ocean: larval development of lanternfish species (Pisces: Myctophidae). Fish. Bull. 118:135–144.
Bolshakova, Ya. Yu., and A. M. Prokofiev.
2023. Nomenclature of pigmentation of the larvae of lanternfish (Myctophidae). J. Ichthyol. 63:878–890.
Bolshakova, Ya. Yu., S. A. Evseenko, and D. V. Bolshakov.
2021. Morphology of larvae of 6 *Lampanyctus* species in the central South Pacific Ocean with notes on their occurrence. Fish. Bull. 119:112–122.
Bonaparte, C. L.
1840. Iconografia della fauna italica per le quattro classi degli animali vertebrati. Tomo 3. Pesci. Fasc. 27–29, puntata 136–154, 10 plates. Tip. Salviucci, Rome.
Bonecker, A. C. T., and M. S. de Castro.
2006. Atlas de larvas de peixes da região central da zona economica exclusiva brasileira. Ser. Livros 19, 214 p. Mus. Nac., Rio de Janeiro, Brazil.
Brauer, A.
1904. Die Gattung Myctophum. Zool. Anz. 28:377–404.
Deacon, G. E. R.
1966. Subtropical convergence. *In* The encyclopedia of oceanography. Encyclopedia of earth sciences series, vol. 1 (R. W. Fairbridge, ed.), p. 884–885. Reinhold Publ. Corp., New York.

Denton, J. S. S.
2014. Seven-locus molecular phylogeny of Myctophiformes (Teleostei; Scopelomorpha) highlights the utility of the order for studies of deep-sea evolution. Mol. Phylogenet. Evol. 76:270–292.

Efremenko, V. N.
1983. Atlas of fish larvae of the Southern Ocean. Cybium 7(2):3–74.

Eigenmann, C. H., and R. S. Eigenmann.
1889. Notes from the San Diego Biological Laboratory. The fishes of Cortez Banks. West Am. Sci. 6:123–132.
1890. Additions to the fauna of San Diego. Proc. Calif. Acad. Sci., Ser. 2. 3:1–24.

Fahay, M. P.
1983. Guide to the early stages of marine fishes occurring in the western North Atlantic Ocean, Cape Hatteras to the southern Scotian Shelf. J. Northwest Atl. Fish. Soc. 4:1–423.
2007. Early stages of fishes in the western North Atlantic Ocean (Davis Strait, southern Greenland and Flemish Cap to Cape Hatteras), vol. 1, 931 p. Northwest Atl. Fish. Organ., Dartmouth, Canada.

Figueroa, D. E., J. M. Díaz de Astarloa, and P. Martos.
1998. Mesopelagic fish distribution in the southwest Atlantic in relation to water masses. Deep Sea Res. I 45:317–332.

Fraser-Brunner, A.
1949. A classification of the fishes of the family Myctophidae. Proc. Zool. Soc. London 118:1019–1106.

Fricke, R., W. N. Eschmeyer, and R. Van Der Laan (eds.).
2023. Eschmeyer's catalog of fishes: genera, species, references. [Available from website, accessed September 2023.]

Gill, T. N.
1893. A comparison of antipodal faunas. Mem. Natl. Acad. Sci. 6(mem. 5):91–124.

Goode, G. B., and T. H. Bean.
1896. Oceanic ichthyology, a treatise on the deep-sea and pelagic fishes of the world, based chiefly upon the collections made by the steamers *Blake*, *Albatross*, and *Fish Hawk* in the northwestern Atlantic, with an atlas containing 417 figures. Spec. Bull. U.S. Natl. Mus. 2, 553 p.

Günther, A.
1864. Catalogue of the fishes in the British Museum. Catalogue of the Physostomi, containing the families Siluridae, Characinidae, Haplochitonidae, Sternoptychidae, Scopelidae, Stomiatidae in the collection of the British Museum, vol. 5, 455 p. Order Trustees Br. Mus., London.
1887. Report on the deep-sea fishes collected by H.M.S. *Challenger* during the years 1873–76. *In* Report on the scientific results of the voyage of H.M.S. *Challenger*. Zoology, vol. 22, part 57, p. 1–268. Neill and Co., Edinburgh, Scotland.

Hubbs, C. L., and R. L. Wisner.
1964. *Parvilux*, a new genus of myctophid fishes from the northeastern Pacific, with two new species. Zool. Meded. 39:445–463.

Hulley, P. A.
1981. Results of the research cruises of FRV "Walther Herwig" to South America: 58. Family Myctophidae (Osteichthyes, Myctophiformes). Archiv. Fischereiwiss. 31(1):1–303.

Hulley, P. A., and G. Duhamel.
2009. A review of the lanternfish genus *Bolinichthys* Paxton, 1972 (Myctophidae). Cybium 33:259–304.

Johnson, J. Y.
1890. On some new species of fishes from Madeira. Proc. Zool. Soc. London 1890:452–459.

Kellermann, A. (ed.).
1990. Identification key and catalogue of larval Antarctic fishes. Ber. Polarforsch. [Rep. Polar Res.] 67, 136 p.

Kendall, A. W., Jr., E. H., Ahlstrom, and H. G. Moser.
1984. Early life history stages of fishes and their characters. *In* Ontogeny and systematics of fishes. Based on an international symposium dedicated to the memory of Elbert Halvor Ahlstrom; La Jolla, 15–18 August 1983 (H. G. Moser, W. J. Richards, D. M. Cohen, M. P. Fahay, A. W. Kendall, Jr., and S. L. Richardson, eds.), p. 11–22. Am. Soc. Ichthyol. Herpetol., Spec. Publ. 1.

Leis, J. M., and B. M. Carson-Ewart (eds.).
2000. The larvae of Indo-Pacific coastal fishes: an identification guide to marine fish larvae. Fauna Malesiana Handbook 2, 850 p. Brill, Leiden, Netherlands.

Longhurst, A. R.
1998. Ecological geography of the sea, 391 p. Acad. Press, San Diego, CA.
2007. Ecological geography of the sea, 2nd ed., 557 p. Acad. Press, San Diego, CA.

Lowe, R. T.
1839. A supplement to a synopsis of the fishes of Madeira. Proc. Zool. Soc. London 1839(part 7):76–92.

Lütken, C. F.
1892. Spolia Atlantica. Scopelini Musei zoologici Universitatis Hauniensis. Bidrag til Kundskab om det aabne Havs Laxesild eller Scopeliner. Med et tillaeg om en anden pelagisk fiskeslaegt. K. Danske Vidensk. selskabs skr., ser. 6, 7:221–297.

Martin, R. P., E. E. Olson, M. G. Girard, Wm. L. Smith, and M. P. Davis.
2018. Light in the darkness: new perspective on lanternfish relationships and classification using genomic and morphological data. Mol. Phylogenet. Evol. 121:71–85.

Matarese, A. C., A. W. Kendall, Jr., D. M. Blood., and B. M. Vinter.
1989. Laboratory guide to early life history stages of northeast Pacific fishes. NOAA Tech. Rep. NMFS 80, 652 p.

McGinnis, R. F. (ed.).
1982. Biogeography of lanternfishes (Myctophidae) south of 30°S. Antarctic Res. Ser. 35, 110 p. Am. Geophys. Union, Washington, D.C.

Miller, J. M., W. Watson, and J. M. Leis.
1979. An atlas of common nearshore marine fish larvae of the Hawaiian Islands. Sea Grant Misc. Rep. UNIHI-Seagrant-MR-80-02, 179 p. Univ. Hawaii Sea Grant Coll. Progr., Honolulu, HI.

Moser, H. G., and E. H. Ahlstrom.
1970. Development of lanternfishes (family Myctophidae) in the California Current. Part 1. Species with narrow-eyed larvae. Bull. Los Angel. Cty. Mus. Nat. Hist. Sci. 7, 145 p.
1972. Development of the lanternfish, *Scopelopsis multipunctatus* Brauer 1906, with a discussion of its phylogenetic position in the family Myctophidae and its role in a proposed mechanism for the evolution of photophore patterns in lanternfishes. Fish. Bull. 70:541–564.
1974. Role of larval stages in systematic investigations of marine teleosts: the Myctophidae, a case study. Fish. Bull. 72:391–413.
1996. Myctophidae: lanternfishes. *In* The early stages of fishes in the California Current region (H. G. Moser, ed.), p. 387–475. CalCOFI Atlas 33.

Moser, H. G., and W. Watson.
2001. Preliminary guide to the identification of the early life history stages of myctophiform fishes of the western central Atlantic. NOAA Tech. Memo. NMFS-SEFSC-453, 118 p.

Moser, H. G., E. H. Ahlstrom, and J. R. Paxton.
1984. Myctophidae: development. *In* Ontogeny and systematics of fishes. Based on an international symposium

dedicated to the memory of Elbert Halvor Ahlstrom; La Jolla, 15–18 August 1983 (H. G. Moser, W. J. Richards, D. M. Cohen, M. P. Fahay, A. W. Kendall Jr., and S. L. Richardson, eds.), p. 218–239. Am. Soc. Ichthyol. Herpetol., Spec. Publ. 1.

Nafpaktitis, B. G.

1968. Taxonomy and distribution of lanternfishes, genera *Lobianchia* and *Diaphus*, in the North Atlantic. Dana Rep. 73, 131 p.

1973. A review of the lanternfishes (family Myctophidae) described by Å. Vedel Tåning. Dana Rep. 83, 46 p.

Nafpaktitis, B. G., and M. Nafpaktitis.

1969. Lanternfishes (family Myctophidae) collected during cruises 3 and 6 of the R/V *Anton Bruun* in the Indian Ocean. Bull. Los Angel. Cty. Mus. Nat. Hist. 5, 79 p.

Nafpaktitis, B. G., R. H. Backus, J. E. Craddock, R. L. Haedrich, B. H. Robison, and C. Karnella.

1977. Family Myctophidae. *In* Fishes of the western North Atlantic. Part 7. Order Iniomi (Myctophiformes): neoscopelids, lanternfishes, Atlantic mesopelagic zoogeography (R. H. Gibbs Jr., ed.), p. 3–265. Sears Found. Mar. Res., Yale Univ., New Haven, CT.

Okiyama, M. (ed.)

1988. An atlas of the early stage fishes in Japan, 1154 p. Tokai Univ. Press, Tokyo, Japan. [In Japanese.]

Olivar, M. P.

1985. Ictioplancton del Atlantico sudoriental. Ph.D. diss., 710 p. Univ. Barcelona, Barcelona, Spain. [Available from website.]

1988. Planktonic stages of lanternfishes (Osteichthyes, Myctophidae) in the Benguela upwelling region. Investig. Pesq. 52:387–420.

Olivar, M. P., and J. M. Fortuño.

1991. Guide to the ichthyoplankton of the Southeast Atlantic (Benguela Current region). Sci. Mar. 55:1–383.

Olivar, M. P., and L. E. Beckley.

1997. Larval development of *Lampanyctus* species (Pisces: Myctophidae) from the southwestern Indian Ocean, and species groups based on larval characters. Bull. Mar. Sci. 60:47–65.

Olivar, M. P., H. G. Moser, and L. E. Beckley.

1999. Lanternfish larvae from the Agulhas current (SW Indian Ocean). Sci. Mar. 63:101–120.

Ozawa, T.

1986. Studies on the oceanic ichthyoplankton in the western North Pacific, 430 p. Kyushu Univ. Press, Fukuoka-shi, Japan.

Parin, N. V., V. E. Bekker, O. D. Borodulina, and V. M. Chuvasov.

1973. Deep-sea pelagic fishes of the southeastern Pacific Ocean and adjacent waters. Tr. Inst. Okeanol. Akad. Nauk SSSR 94:71–172. [In Russian.]

Parr, A. E.

1928. Deepsea fishes of the order Iniomi from the waters around the Bahama and Bermuda islands. With annotated keys to the Sudididae, Myctophidae, Scopelarchidae, Evermannellidae, Omosudidae, Cetomimidae and Rondeletidae of the world. Scientific results of the third oceanographic expedition of the *Pawnee* 1927. Bull. Bingham Oceanogr. Collect., vol. 3, article 3, 193 p.

Paxton, J. R.

1972. Osteology and relationships of the lanternfishes (family Myctophidae). Bull. Nat. Hist. Mus. Los Angel. Cty. Sci. 13, 81 p.

Paxton, J. R., E. H. Ahlstrom, and H. G. Moser.

1984. Myctophidae: relationships. *In* Ontogeny and systematics of fishes. Based on an international symposium dedicated to the memory of Elbert Halvor Ahlstrom; La Jolla, 15–18 August 1983 (H. G. Moser, W. J. Richards, D. M. Cohen, M. P. Fahay, A. W. Kendall, Jr., and S. L. Richardson, eds.), p. 239–244. Am. Soc. Ichthyol. Herpetol., Spec. Publ. 1.

Pertseva-Ostroumova, T. A.

1964. Some morphological characteristics of myctophid larvae (Myctophidae, Pisces). Tr. Inst. Okeanol. Akad. Nauk SSSR 73:76–92. [In Russian.]

1977. On the development of some species of the genus *Gymnoscopelus* (Myctophidae). J. Ichthyol. 17:58–65. [In Russian.]

Poulsen, J. Y., I. Byrkjedal, E. Willassen, D. Rees, H. Takeshima, T. P. Satoh, G. Shinohara, M. Nishida, and M. Miya.

2013. Mitogenomic sequences and evidence from unique gene rearrangements corroborate evolutionary relationships of myctophiformes (Neoteleostei). BMC Evol. Biol. 13:111.

Regan, C. T.

1916. Larval and post-larval fishes. Br. Antarct. ("Terra Nova") Exped. 1910, Nat. Hist. Rep., Zool. 1(4):125–156.

Richards, W. J. (ed.).

2005. Early stages of Atlantic fishes: an identification guide for the western central North Atlantic, vol. 1, 1335 p. CRC Press, Boca Raton, FL.

Roberts, C. D., A. L. Stewart, and C. D. Struthers (eds.).

2015. The fishes of New Zealand, vol. 1, 255 p. Te Papa Press, Wellington, New Zealand.

Rodríguez, J. M.

2023. Eggs and larvae of common marine fish species of northwest Africa, 357 p. FAO, Rome.

Rodríguez, J. M., F. Alemany, and A. Garcia.

2017. A guide to the eggs and larvae of 100 common western Mediterranean Sea bony fish species, 2542 p. FAO, Rome.

Roule, L., and F. Angel.

1930. Larves et alevins de poissons provenant des croisières du Prince Albert I de Monaco. Résultats des campagnes scientifiques accomplies sur son yacht par Prince Albert I, vol. 79, 148 p. Imprimerie de Monaco.

Russell, F. S.

1976. The eggs and planktonic stages of British marine fishes, 524 p. Acad. Press, London.

Shiganova, T. A.

1975. Postembryonic development of *Notolychnus valdiviae* (Brauer, 1904) Myctophidae, Osteichthyes. Tr. Inst. Okeanol. Akad. Nauk SSSR 101:75–87. [In Russian.]

1977. Larvae and juveniles of the lanternfishes (Myctophidae, Pisces) of the Atlantic Ocean. Tr. Inst. Okeanol. Akad. Nauk SSSR 109:42–112. [In Russian.]

Steele, J. H., S. A. Thorpe, and K. K. Turekian (eds.).

2010. Ocean currents, 656 p. Acad. Press, London.

Stiassny, M. L. J.

1996. Basal ctenosquamate relationships and the interrelationships of the myctophiform (scopelomorph) fishes. *In* Interrelationships of fishes (M. L. J. Stiassny, L. R. Parenti, and G. D. Johnson, eds.), p. 405–426. Acad. Press, San Diego, CA.

Suntsov, A. V., E. A Widder, and T. T. Sutton.

2008. Bioluminescence. *In* Fish larval physiology (R. N. Finn and B. G. Kapoor, eds.), p. 51–88. CRC Press, Boca Raton, FL. [E-book in PDF available from website.]

Sutton, T. T., M. R. Clark, D. C. Dunn, P. N. Halpin, A. D. Rogers, J. Guinotte, S. J. Bograd, M. V. Angel, J. A. A. Perez, K. Wishner, et al.

2017. A global biogeographic classification of the mesopelagic zone. Deep Sea Res. I 126:85–102.

Tåning, A. V.

1918. Mediterranean Scopelidae (*Saurus, Aulopus, Chlorophthalmus* and *Myctophum*). *In* Report of the Danish oceanographic expeditions 1908–1910 to the Mediterranean and adjacent seas. Volume 2. Biology (A, 7), 154 p. Høst and Son, Copenhagen, Denmark.

1928. Synopsis of the scopelids in the North Atlantic. Preliminary review. Vidensk. Medd. Dansk Naturhist. Foren. Kjøbenhavn 86:49–69.

1932. Notes on scopelids from the Dana Expeditions. 1. Vidensk. Medd. Dansk Naturhist. Foren. Kjøbenhavn 94:125–146.

Wisner, R. L.

1976. The taxonomy and distribution of lanternfishes (family Myctophidae) of the eastern Pacific Ocean. NORDA Rep. 3, 229 p. Navy Ocean Res. Dev. Act., Bay St. Louis, MS.

Yamaguchi, M.

2000. Phylogenetic analyses of myctophid fishes using morphological characters: progress, problems, and future perspectives. Jpn. J. Ichthyol. 47:87–107.

Young, J. W., T. D. Lamb, and R. W. Bradford.

1996. Distribution and community structure of midwater fishes in relation to the subtropical convergence off eastern Tasmania, Australia. Mar. Biol. 126:571–584.

Zahuranec, B. J.

2000. Zoogeography and systematics of the lanternfishes of the genus *Nannobrachium* (Myctophidae: Lampanyctini). Smithson. Contrib. Zool. 607, 69 p. [Available from website.]

National Marine
Fisheries Service
NOAA

Fishery Bulletin
established in 1881

Spencer F. Baird
First U.S. Commissioner
of Fisheries and founder
of *Fishery Bulletin*

Collecting age and length data from recovered carcasses of filleted rockfish: a new data source for examination of life history characteristics

Kaila Fritch (contact author)[1]
Grant Waltz[1,2]
Melissa Monk[3]
Ellie Brauer[1]
Zachary Kucinski[1]
Chandler Skinner-Horne[1]
Dean Wendt[1]

Email address for contact author: k.raeanne99@gmail.com

[1] Biological Sciences Department
Center for Coastal Marine Sciences
California Polytechnic State University
1 Grand Avenue
San Luis Obispo, California 93407

[2] Oregon Department of Fish and Wildlife
17330 Southeast Evelyn Street
Clackamas, Oregon 97015

[3] Southwest Fisheries Science Center
National Marine Fisheries Service, NOAA
110 McAllister Way
Santa Cruz, California 95060

Abstract—In reports on stock assessments for rockfish species on the West Coast of the United States, the need for additional biological data to provide more accurate estimates of population abundance is commonly cited. Improvement of population estimates is important because those data are used to set catch quotas along this coast of the nation. The recreational charter boat fleet in the state of California has historically landed large amounts of rockfish species; however, vessels in this fleet discard carcasses once fillets have been removed from fish. These carcasses could be a valuable source of age, length, and sex data, with a standardized measurement method used to relate the post-fillet length of carcasses to the pre-fillet length. To determine the feasibility of a program to collect rockfish carcasses for biological data, specimens of 4 rockfish species were captured off the central coast of California and measured before and after filleting. Pre-fillet lengths were accurately predicted on the basis of post-fillet elongate length for blue (*Sebastes mystinus*), gopher (*S. carnatus*), copper (*S. caurinus*), and vermilion (*S. miniatus*) rockfish. A high percentage (87.5%) of the carcasses had identifiable gonads, a fortunate result because the availability of sex data on measured specimens is an important consideration for species with dimorphic growth. This new data source based on information from carcasses can be used to enhance the length-at-age and life history data available for stock assessments or other biological studies of rockfish populations.

Manuscript submitted 13 February 2024.
Manuscript accepted 6 June 2024.
Fish. Bull. 122:119–128 (2024).
Online publication date: 25 June 2024.
doi: 10.7755/FB.122.3.4

The views and opinions expressed or implied in this article are those of the author (or authors) and do not necessarily reflect the position of the National Marine Fisheries Service, NOAA.

The rockfish complex along the central coast of California is composed of 45 managed species that have a wide array of life histories and of preferred habitat and depth ranges. Rockfish species are generally long-lived and slow growing; therefore, effective management is crucial to maintenance of sustainable population levels (Love et al., 1990). An increased level of data on the West Coast rockfish stocks could enhance stock assessments and estimates of population abundance, which are used to set catch limits for rockfishes along the U.S. West Coast, including along the coasts of California, Oregon, and Washington. Stock assessments are important fisheries management tools used to provide resource managers with information needed to monitor and manage fish populations, but large amounts of data are required to run a full age-structured population model as part of an assessment (Hilborn and Walters, 1992; PFMC[1]). Stock assessment reports for West Coast rockfish populations commonly cite a need for additional biological information, such as length, age, abundance, and sex ratio data, to improve the estimates of population abundance derived through the stock assessment process (e.g., PFMC[2]).

Biological data can often be a limiting factor in the quality of a stock assessment, and a lack of biological data often results in reduced mandated harvest levels because of a precautionary management approach (Ralston et al., 2011). A rockfish stock assessment can fall into 1 of 3 categories: 1) data rich (full), 2) data moderate, or 3) data limited (Ralston et al., 2011). Many rockfish stocks are considered data limited or data moderate, and the availability of data can vary by state or region. Full stock assessments require the most data and include age-specific estimation of abundance and biomass as well as modeling of fish growth and mortality (PFMC[1]). Data-moderate assessments include length and abundance data that are used to create an estimate of stock status. Data-limited assessments lack an estimation of stock status and are used mainly to inform mandated harvest levels. Rockfish stocks that fall into the data-limited category or data-moderate category are subject to more conservative quota levels because of greater uncertainty in biomass estimates (Ralston et al., 2011).

---

[1] PFMC (Pacific Fishery Management Council). 2020. Terms of reference for the groundfish and coastal pelagic species stock assessment review process for 2021–2022, 38 p. Pac. Fish. Manag. Counc., Portland, OR. [Available from website.]

[2] PFMC (Pacific Fisheries Management Council). 2019. Gopher/black and yellow rockfish stock assessment review (STAR) panel report; Santa Cruz, 22–26 July, 15 p. Pac. Fish. Manag. Counc., Portland, OR. [Draft report.] [Available from website.]

Four socioeconomically valuable rockfish species with recent stock assessments and research recommendations identifying the need for additional data include the blue rockfish (*Sebastes mystinus*), gopher rockfish (*S. carnatus*), copper rockfish (*S. caurinus*), and vermilion rockfish (*S. miniatus*). The blue rockfish is the target of one of the most important recreational fisheries in California, and it is particularly key for the recreational charter boat fleet (a vessel in this fleet is hereafter referred to as a *party boat*), which accounted for 50% of total landings of blue rockfish off the coast of California over the past decade (Dick et al., 2018). The blue rockfish forms a species pair with the deacon rockfish (*S. diaconus*); these species are visually distinct but easily misidentified when morphology alone is used. Although work has helped to make it possible to more readily distinguish these species (Frable et al. 2015), the blue rockfish is particularly data limited prior to 2015 because all historic and some recent data are a mix of information on blue and deacon rockfish in unknown proportions (Dick et al., 2018). In the report on the latest stock assessment for the blue and deacon rockfish complex, it was noted that the estimate of the size of the blue rockfish population is imprecise, partly because of the lack of age data (Dick et al., 2018).

The gopher rockfish is another economically important species that is commonly encountered by the party boat fleet, particularly north of Point Conception in Southern California (Monk and He[3]). In 2011, Port San Luis, on the central coast of California, had the highest landings of gopher rockfish in California, a peak in a trend that has been elevated since 1990, with over 136,000 kg (over 300,000 lb) of gopher rockfish landed by the commercial fishery (Lisa Wise Consulting Inc.[4]). In the report on the most recent stock assessment for the complex that includes the gopher rockfish and the black-and-yellow rockfish (*S. chrysomelas*), a need for more age and length data was discussed (Monk and He[3]). This need exists in part because of historic misidentification between gopher and black-and-yellow rockfish; indeed, these species could not be differentiated in catch data before 1995 (Monk and He[3]).

Copper rockfish also have been an important part of both recreational and commercial fisheries; however, this species is considered data moderate, because of the lack of length, age, and length- or age-at-maturity data that could be used to determine stock status (Cope et al., 2015; Wetzel et al., 2021). Prior to 2013, no stock assessments had been conducted for copper rockfish, although this species is considered to be the most vulnerable rockfish species found off the West Coast (Cope et al., 2015). Therefore, accurate catch and biological data are especially vital for this species.

The vermilion rockfish is another species that has been historically important in the recreational fishery, given its desirability as a brightly colored, large species (Monk et al., 2021). Yet, the most recent stock assessment report cites a need for more biological data, including better indices of abundance, and biological sampling (Monk et al., 2021). This need is due in part to the morphological similarities between vermilion and sunset rockfish (*S. crocotulus*). These similarities have resulted in all historical and recent recreational and commercial catches of sunset and vermilion rockfish being recorded as catches of vermilion rockfish, limiting the available data (Monk et al., 2021). Because of differences in size composition and population structure between vermilion rockfish found in Northern and Southern California, separate stock assessments are provided for each of these regions. Although Northern California represents a larger portion of the coastline of California, very little biological data is available for this species in this region (Monk et al., 2021).

For all 4 species—the blue rockfish, gopher rockfish, copper rockfish, and vermilion rockfish—there is a lack of biological data throughout their ranges, and for all except the copper rockfish, this lack of data is in part due to morphological similarities with other species. Filling these data gaps is a critical need for the management of these socioeconomically valuable species.

One underutilized source of biological data are carcasses of rockfish that have been retained aboard party boats after captured fish have been filleted. The party boat fleet emerged in 1920 in California and has since become one of the largest recreational fleets in the world, with rockfish species among the most desirable targets (Young, 1969; Hill and Schneider[5]). Generally, the fillets collected aboard a party boat are taken home by the angler, and the carcasses are discarded at sea. These carcasses could be a valuable source of length, age, and sex data for the catch of the party boat sector of the recreational fleet. Many rockfish species have sex-specific growth patterns; therefore, for the length-at-age and sex information from carcasses of filleted rockfish to be useful, accurate estimates of prefillet length and sex must be obtainable from the carcasses of filleted fish (Love et al., 2002). The issue is that fish carcass length, with fillets removed, is different from whole fish length, and no information is available currently about how the length of a carcass of a filleted rockfish relates to the pre-filleted length. Information on this relationship is needed before accurate length-at-age data can be obtained from carcasses of filleted rockfish, particularly because carcass lengths likely would be combined with pre-fillet lengths from other data sources (e.g., commercial fleets) in a stock assessment and because standardization of length types is critical.

---

[3] Monk, M. H., and X. He. 2019. The combined status of gopher (*Sebastes carnatus*) and black-and-yellow rockfishes (*Sebastes chrysomelas*) in U.S. waters off California in 2019, 175 p. Agenda item H.5, attach. 11. Pac. Fish. Manag. Counc., Portland, OR. [Available from website.]

[4] Lisa Wise Consulting Inc. 2018. Port San Luis commercial fishing industry: economic impact report, 26 p. Lisa Wise Consult., San Luis Obispo, CA. [Available from website.]

[5] Hill, K. T., and N. Schneider. 1999. Historical logbook databases from California's commercial passenger fishing vessel (partyboat) fishery, 1936–1997. Scripps Inst. Oceanogr., SIO Ref. Ser. 99-19, 58 p. [Available from website.]

The idea of back-calculation, using a set of measurements on a fish to infer the total length at another time, is not new to fisheries science (Francis, 1990). In a few studies, back-calculations of total length and length at age have been done by using fish bones (Wise et al., 1980; Hansel et al., 1988), spine radii (Landa et al., 2015), headless fish carcasses (Gordon, 1994), and carcasses of filleted fish (Barnes et al., 2015; Barnes and Starr, 2018). There are currently no studies focused on the relationship between carcass length of filleted fish and total length of pre-filleted fish for the West Coast rockfish stocks. Investigating this relationship, as well as obtaining age data from otoliths, may help in the development of tools that can be applied on a statewide scale to help resource managers understand the state of the recreational fisheries that target rockfish species on the West Coast.

In order to address the unknowns regarding the potential of collecting data for stock assessments from rockfish carcasses sourced from party boats, we focused this study on 3 questions: 1) can a protocol be developed to standardize the measurement of carcasses of filleted fish, 2) what percentage of carcasses have identifiable gonads, and 3) can this method be used to develop a linear regression equation for accurate estimation of pre-fillet length from carcasses of filleted fish? The information from this study can be used by fishery managers to establish a carcass collection program aimed at enhancing the amount of length-at-age and life history data available for stock assessments or other studies of rockfish populations.

Materials and methods

Data for this study were collected primarily by onboard observers of the party boat fleet operating in waters off the central coast of California. The observers were part of a program administered by the California Polytechnic State University in collaboration with the party boat fleet in San Luis Obispo County, California, to gather rockfish fishery data (Stephens et al., 2006). Program observers on regularly operating party boat trips record the location, time, length, and fate of individuals of different fish species that are caught by recreational anglers. These observers follow the same method used for the onboard observer sampling of the California Recreational Fisheries Survey of the California Department of Fish and Wildlife. The primary difference is that, in the university program protocol, retained and discarded fish are measured, and in the California Department of Fish and Wildlife onboard protocol, only retained, not discarded, fish are measured. The data from the university program have been used in the development of indices of abundance and length composition data sets for a number of nearshore rockfish species (e.g., Dick et al., 2018; Monk and He[3]).

In addition to sourcing fish through the Observer Program of the California Polytechnic State University, we conducted several research trips from ports in California, with collections occurring from Half Moon Bay to the Channel Islands. The majority of specimens used in this study were collected from San Luis Obispo County. This county has 2 main ports that support commercial and recreational fisheries: a southern port, Port San Luis, and a northern port, Morro Bay (Fig. 1). Rockfish were collected

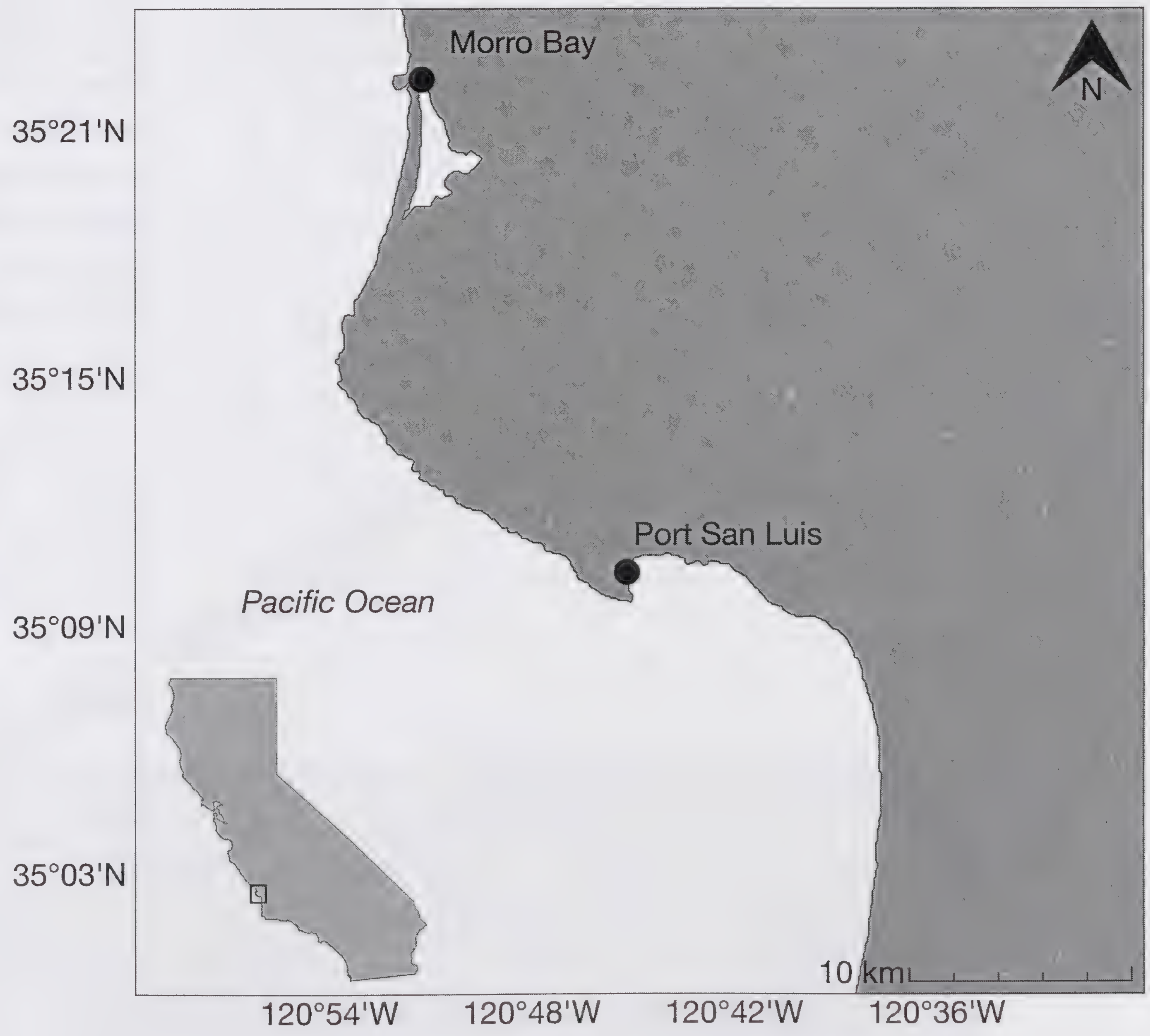

Figure 1

Map of the study region in San Luis Obispo County, California, showing the 2 harbors from which the charter boat trips involved in this study originated: Morro Bay and Port San Luis. The majority of the carcasses of filleted blue (*Sebastes mystinus*), gopher (*S. carnatus*), copper (*S. caurinus*), and vermilion (*S. miniatus*) rockfish used in this study were collected by observers aboard party boats during December 2017–February 2022.

from December 2017 through February 2022. These specimens were caught by using hook-and-line fishing methods with a variety of tackle. Processing of fish was done either onboard the fishing vessel by the boat crew or in a laboratory facility at the California Polytechnic State University by scientific staff within 2 d of being caught. Fish processing included species identification, measuring fork length to the nearest millimeter (from the tip of the snout to the end of the splayed caudal fin on a measuring board), filleting, otolith extraction, sex determination, and measuring post-fillet carcass length by using the procedures described in the next section. The adjustments between pre-fillet and post-fillet lengths developed in this study are intended to be applicable to rockfish that fall within the size distributions used in this study (Table 1). If the models developed in this study are to be applied with a data set for fish with a larger or different size distribution, the models must be adjusted to reflect the correct size distribution.

The most robust measurement technique was determined early on in this study by using a preliminary data set containing fish lengths collected by using different possible techniques to measure a carcass of a filleted fish. A standardized protocol was needed so that it would be possible to develop a reliable length regression equation based on a consistent relationship between post-fillet and pre-fillet lengths. We developed measurement protocols using 29 blue rockfish, individuals of one of the most common species in the study area, to test 3 possible post-fillet measurements: short, natural, and elongate (Fig. 2). All of these measurements were taken on a measuring board like the measurement for standard fork length. The post-fillet short length was taken from the tip of the snout to the end of the splayed caudal fin, with the head of the fish pointed down, the spine of the fish flexed as much as naturally possible, and the carcass kept flat on the board. The post-fillet natural length was taken from the tip of the snout to the end of the splayed caudal fin, with the fish laid on the board in a way believed to be the natural position of a fish with intact fillets. The post-fillet elongate length was taken from the tip of the snout to the end of the splayed caudal fin, with the spine of the carcass hyperextended to the point where the carcass could not be reasonably extended farther. Linear regression was used to describe the relationship between each of the post-fillet measurements and the pre-fillet length.

A sub-study was conducted to determine if there were differences in the relationship of post-fillet length to pre-fillet length due to the varied levels of experience of the scientists from whom length measurements were obtained. Once the measurement methods were developed, it was important to test whether measurements taken with these protocols could be consistent regardless of who took the measurement and their experience. A plot was created to test whether level of experience (novice versus experienced laboratory staff) had an effect on the relationship between post-fillet elongate length and pre-fillet length. This analysis was conducted only for gopher rockfish because there were not enough samples of the other 3 species. Although this test was done for only 1 species, the results are considered representative of what would be expected for all rockfish species included in this study, given their similar body morphologies.

Table 1

The distributions of fork lengths of blue (*Sebastes mystinus*), gopher (*S. carnatus*), copper (*S. caurinus*), and vermilion (*S. miniatus*) rockfish collected through the Observer Program of the California Polytechnic State University and during research trips in waters off the central coast of California from December 2017 through February 2022.

	Fork length (cm)		
Species	Minimum	Maximum	Average
Blue rockfish	14.30	40.70	27.09
Gopher rockfish	18.20	32.90	26.79
Copper rockfish	25.00	47.40	35.65
Vermilion rockfish	15.50	52.00	35.91

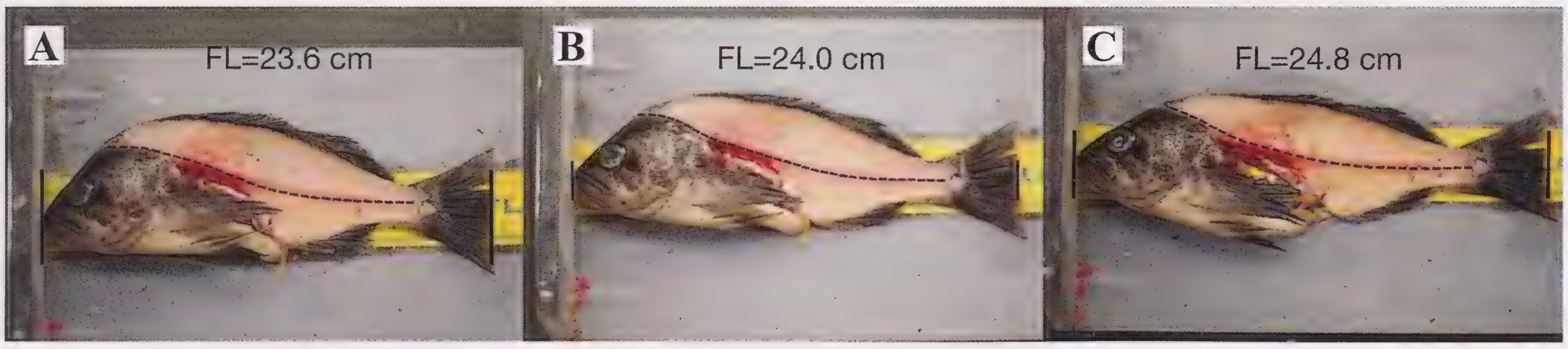

Figure 2

Photographs depicting the differences between 3 methods of measuring the fork length (FL) of carcasses of filleted rockfish: post-fillet (**A**) short, (**B**) natural, and (**C**) elongate measurements. The black dashed line follows the spine of the fish. The filleted blue rockfish (*Sebastes mystinus*) shown in these panels was caught in February 2018 in waters off central California.

We conducted a second sub-study to investigate if sex could be determined from fish filleted by the party boat crew during a regular trip with paying customers; the crew was asked to fillet fish as they normally would. Carcasses of filleted vermilion rockfish were collected on 2 party boat trips out of San Luis Obispo County. After the fish were filleted by crew members, their carcasses were analyzed to determine the fraction of carcasses that had intact and identifiable gonads. Having a high proportion of fish carcasses for which sex could be determined was critical to the efficacy of this study, if the results are to enhance information on sex-specific growth patterns. The identity of the individual processor (vessel crew member who filleted fish) was recorded for a subset of these vermilion rockfish, to test for a potential processor effect on the ratio of intact gonads to missing gonads. This test was important because the variable of processor cannot be controlled in the field. The data from this test were analyzed by using logistic generalized linear regression, with *processor* as the predictor variable and *intact or missing gonad* as the response variable. To determine whether the relationship between length and intact gonad was significant ($P<0.05$), logistic regression was used, with *length* as the predictor variable and *intact or missing gonad* as the response variable.

Individual regression analyses were conducted by using each of the different measurement methods as the predictor variables and *pre-fillet length* as the response variable for the 4 species noted previously: blue rockfish, copper rockfish, gopher rockfish, and vermilion rockfish. The regression equations obtained for each species were used to calculate pre-fillet length, and the calculated pre-fillet length values were compared to the actual pre-fillet length values. We also tested whether sex was a significant factor in these equations. For each species, outliers identified by using residuals-versus-fitted, normal quantile-quantile (Q-Q), and Cook's distance plots were excluded from analyses. All analyses for this study were conducted by using RStudio (vers. 2021.09.0; RStudio, 2021), the tidyverse collection of R packages (vers. 2.0.0; Wickham et al., 2019), and the R package ggpmisc (vers. 0.5.5; Aphalo et al., 2023).

Results

We found that the post-fillet short length was the weakest predictor of pre-fillet length for blue rockfish (Fig. 3; coefficient of multiple determination [R^2]=0.987, $P<0.001$, residual standard error [Σ]=0.503). The post-fillet natural length was a strong predictor of the pre-fillet length, but the original pre-fillet length was both over- and underestimated with it (Fig. 3; $R^2=0.993$, $P<0.001$, $\Sigma=0.366$). Although the natural length was a better predictor of pre-fillet length, there was more room for variability in measurement (Fig. 3). Post-fillet elongate length was also a strong predictor of pre-fillet length and was the most practical method for collecting consistent measurements, as pre-fillet length was consistently overestimated with it and it was the easiest method to implement (Fig. 3; $R^2=0.992$, $P<0.001$, $\Sigma=0.390$). Once it was determined that post-fillet elongate length was the most practical

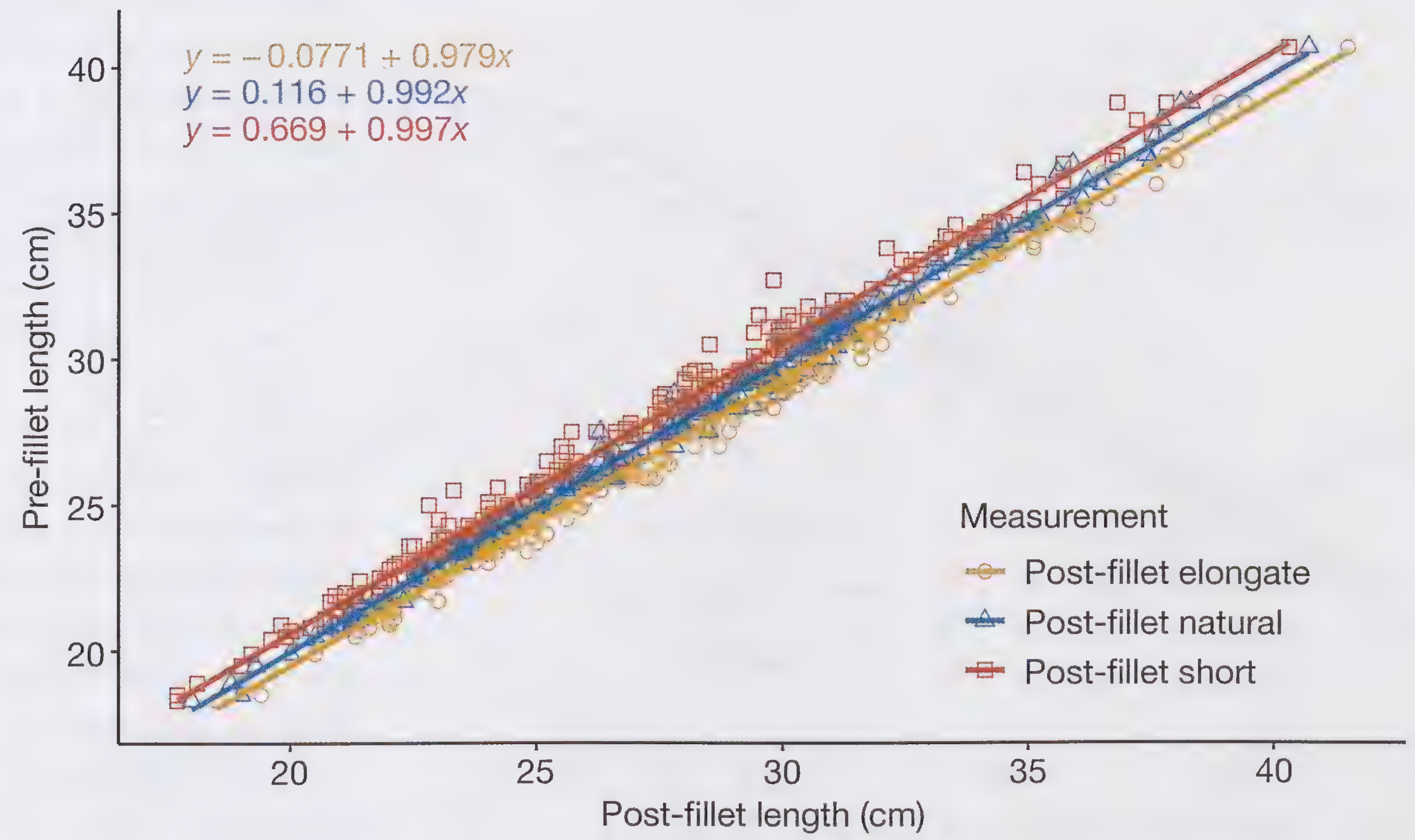

Figure 3

Comparison of the post-fillet elongate (coefficient of multiple determination [R^2]=0.992, $P<0.001$), post-fillet natural ($R^2=0.993$, $P<0.001$), and post-fillet short length measurements ($R^2=0.987$, $P<0.001$) to the pre-fillet length for carcasses of filleted blue rockfish (*Sebastes mystinus*) collected from December 2017 through August 2019 during charter boat trips in waters off central California. The linear regression equation is given for each type of measurement.

measurement, only the post-fillet elongate measurement method was used in the rest of the study.

Trained scientific staff and students in a college fisheries course at the California Polytechnic State University measured the pre-fillet and post-fillet elongate lengths of 94 gopher rockfish. The variance in measurements between trained staff and untrained students was not statistically significant ($F=1.06$, $P=0.849$); however, the untrained students tended to under-measure the post-fillet elongate length compared to what the trained staff did (Fig. 4).

For the second sub-study, 72 vermilion rockfish were collected and filleted by 2 party boat crew members. The carcasses of 87.5% of these fish had identifiable gonads, and the sex of all carcasses with intact gonads was identifiable. The ratio of intact to missing gonads (18:6, sample size=24) was not substantially different between the 2 crew members filleting fish (note that we were able to track the identity of the crew member who did the filleting for only 24 fish). However, there were not enough samples obtained from the second crew member to statistically compare the data to determine whether the person doing the filleting had a significant effect on whether fish had identifiable gonads. Length was a significant predictor of intact gonads remaining after filleting, with a positive relationship between increasing length and intact gonads ($Z=2.767$, estimate of the length coefficient=0.245, standard error of the estimate=0.0887, $P=0.0057$). In comparisons of pre-fillet length, 45.0% of the fish with lengths <40 cm had identifiable gonads and 95.0% of the fish with lengths ≥ 40 cm had identifiable gonads.

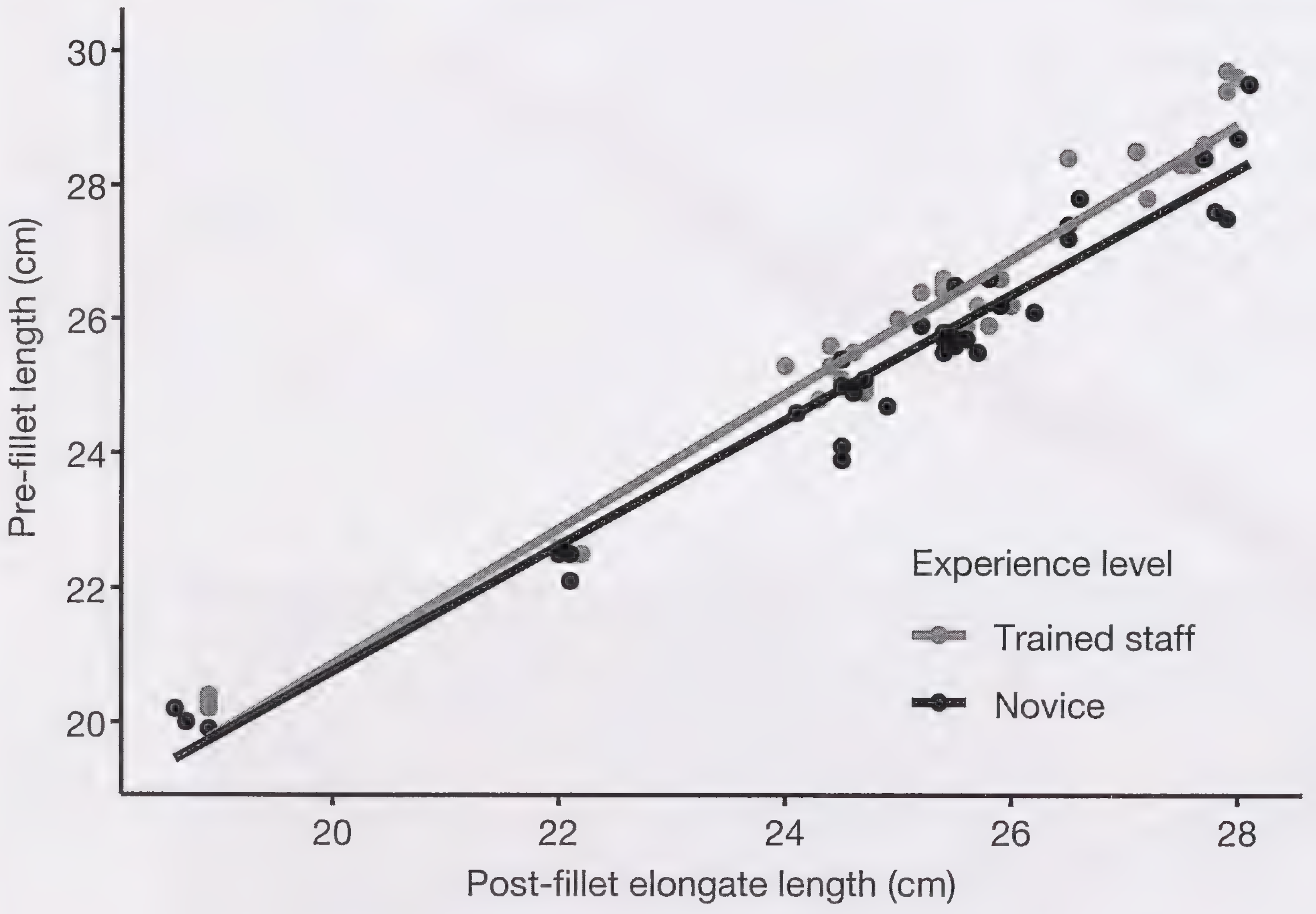

Figure 4

Plot of the pre-fillet lengths and post-fillet elongate lengths of carcasses of gopher rockfish (*Sebastes carnatus*) measured by trained staff and novice students of California Polytechnic State University. Fish were caught and filleted and their carcasses collected during charter boat trips taken between December 2017 and February 2022 in waters off central California.

We developed a linear regression equation for each of the 4 rockfish species, with data collected by measuring the carcasses of filleted rockfish with the post-fillet elongate length measurement method. For each species, a statistically significant relationship was found between post-fillet elongate length and pre-fillet length (Table 2, Fig. 5). Sex was not a significant factor in the linear regression equations.

Discussion

Information about length at age for catches of rockfish species from the party boat fleet on the West Coast is extremely limited, but Schroeder and Love (2002) suggested that the recreational sector can potentially have as large of an effect on fish populations as the commercial sector. The results of our study indicate the feasibility of collecting age and sex information from carcasses to create a new data source of biological information for rockfish species. In San Luis Obispo County, a single party boat can carry between 20 and 50 anglers, depending on the vessel, and the daily bag limit is 10 rockfish per angler per day, with varying species-specific sub-bag limits depending on current management measures. Assuming that 1 vessel carries an average of 30 anglers and each angler catches half of their daily limit, that is 150 carcasses per day per boat. There are approximately 16 party boats in San Luis Obispo County, and the rockfish season is about 270 d (Lisa Wise Consulting Inc.[4]). Therefore, even by a conservative estimate, hundreds of thousands of rockfish carcasses are discarded each rockfish season by the party boat fleet that operates in San Luis Obispo County.

This study is not the first to note the value of obtaining pre-fillet lengths from carcasses of filleted fish. Barnes et al. (2015) used a similar method to create an equation relating the filleted length of California halibut (*Paralichthys californicus*) back to the original pre-fillet length; this equation was used again in a later study (Barnes and Starr, 2018). In both studies, the equation was used to increase the amount of available data because some of the fish from which some of the data were gathered for these studies were from recreational anglers in the form of carcasses of filleted fish (Barnes et al., 2015; Barnes and Starr, 2018). The results of these studies highlight the importance of developing equations to relate the carcass length of filleted fish to their pre-fillet length.

Prior to this study, no research had assessed how the carcass length of a filleted rockfish relates to its pre-fillet fork length. We determined that the carcass of a filleted rockfish can be contorted into 3

Table 2

Results from the linear regression used to estimate the pre-fillet length for carcasses of filleted blue (*Sebastes mystinus*), gopher (*S. carnatus*), copper (*S. caurinus*), and vermilion (*S. miniatus*) rockfish collected and measured during charter boat trips in waters off central California from December 2017 through February 2022. Post-fillet elongate length, measured from the tip of the snout to the end of the splayed caudal fin with the spine of the carcass hyperextended, was used to calculate pre-fillet length. In the regression equations, post-fillet elongate length is used as the predictor value, and pre-fillet length is used as the response value. a=the slope of the line; b=the y-intercept; R^2=coefficient of multiple determination.

	Sample size		Linear regression equation				
Species	Males	Females	a	b	R^2	P	Residual
Blue rockfish	148	242	0.98	−0.09	0.99	<0.001	0.38
Gopher rockfish	90	105	0.96	0.52	0.97	<0.001	0.49
Copper rockfish	32	40	0.99	−0.55	0.99	<0.001	0.46
Vermilion rockfish	50	78	1.00	−0.44	0.99	<0.001	0.48

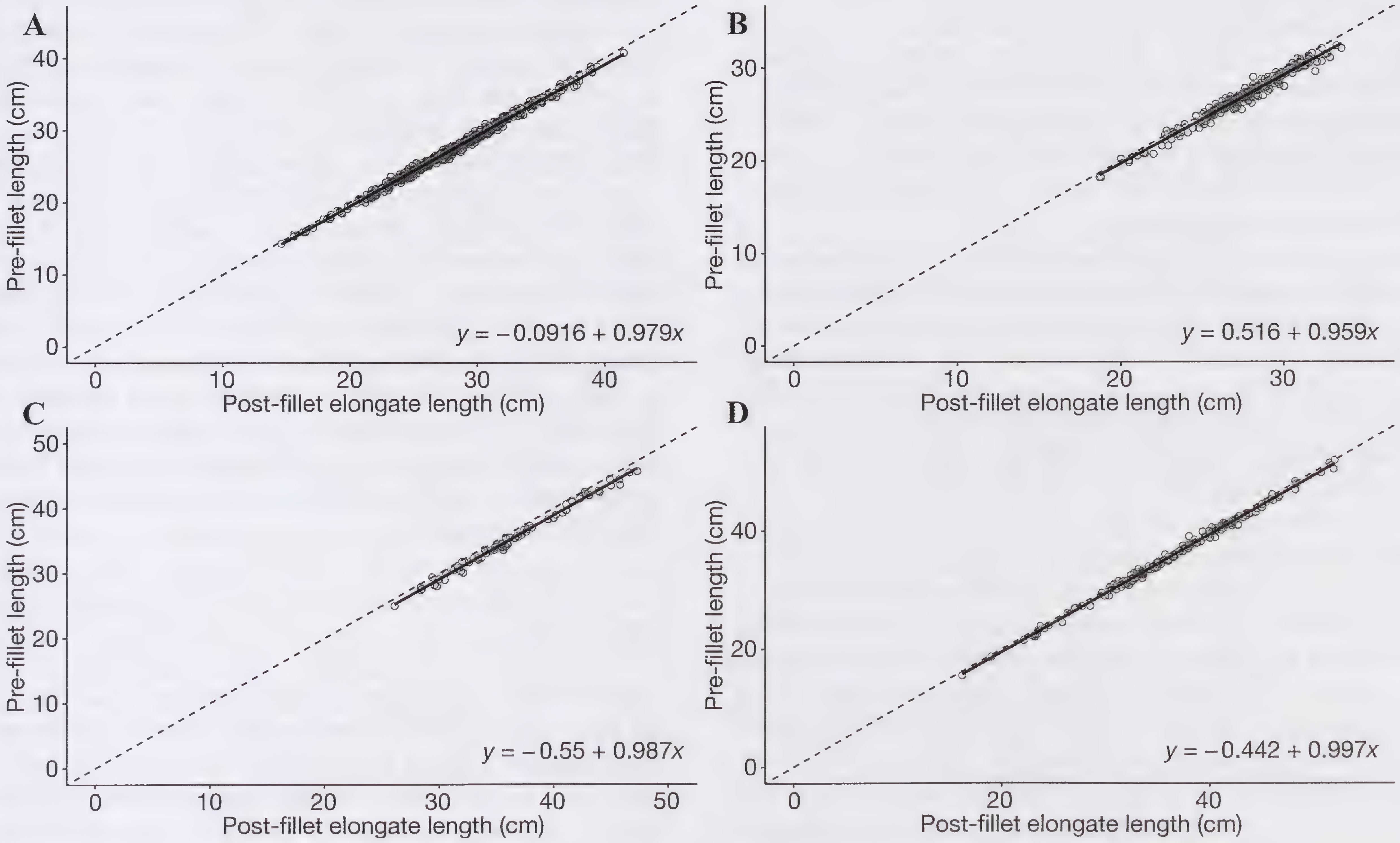

Figure 5

Plots of linear regression depicting the relationship between the post-fillet elongate length and pre-fillet length for carcasses of filleted (**A**) blue rockfish (*Sebastes mystinus*) (coefficient of multiple determination [R^2]=0.99, P<0.001, sample size [n]=404), (**B**) gopher rockfish (*S. carnatus*) (R^2=0.97, P<0.001, n=197), (**C**) copper rockfish (*S. caurinus*) (R^2=0.99, P<0.001, n=72), and (**D**) vermilion rockfish (*S. miniatus*) (R^2=0.99, P<0.001, n=134) collected during charter boat trips taken from December 2017 through February 2022 in waters off central California. The dashed diagonal line indicates 1:1 equivalence. The linear regression equation is given for each species.

different positions: post-fillet short, post-fillet natural, and post-fillet elongate. We found that post-fillet short length and post-fillet natural length were less precise than post-fillet elongate length and were prone to subjectivity depending on the scientists measuring the fish. When taking the post-fillet short measurement, scientists can arbitrarily shorten the carcass of a filleted fish, by compressing the spine, until they feel it is sufficiently short. Because there is no natural stopping point, the subjectivity in the shortening of a carcass leaves too much room for variability in length measurements. For the post-fillet natural method, determining the "natural" position of the fish was also subjective, and the use of this method led to less consistency in the relationship between pre-fillet length and post-fillet natural length than the use of the other methods. Post-fillet elongate length was determined to be less prone to variability due to measurer judgment because, fish to fish, the backbone could be hyperextended only a small and relatively consistent amount. Use of this method resulted in post-fillet lengths that were consistently longer than the pre-fillet length. Results of the regression analyses indicate strong relationships between all 3 post-fillet measurements and pre-fillet length. However, post-fillet elongate length was the most consistent measurement, providing precise measurements that could be used to calculate accurate estimates of pre-fillet length.

The degree of training did not affect the variance of post-fillet elongate lengths; however, the untrained students tended to under-measure post-fillet elongate length. Understanding this trend is important because, if this method is to be implemented on a statewide level, scientists measuring fish must be able to get similar measurements regardless of their level of training.

Preliminary data from assessment of the presence of identifiable gonads in filleted vermilion rockfish indicate that the majority of carcasses had identifiable gonads remaining. The fish that did not have identifiable gonads were typically smaller than 40 cm in pre-fillet length. These initial data indicate that the relationship between the percentage of carcasses with identifiable gonads and the person filleting the fish was not significant. Consideration of this relationship is important in implementing a carcass collection program, given that fish will likely be filleted by a number of different deckhands. Variability in the percentage of fish with intact gonads among the sets of fish filleted by different crew members could compromise the value of the gonad data if not enough carcasses had intact gonads available to identify the sex of fish. More data on how the individual doing the filleting affects the intactness of gonads are needed for vermilion rockfish and for any other rockfish species before carcass collection programs can be implemented. The collection of samples throughout the period of this study required close collaboration with recreational anglers and the party boat industry. Productive collaboration with industry partners will undergird the success of future programs.

It was determined that pre-fillet lengths could be accurately predicted from precise measurements of post-fillet elongate length for blue, gopher, copper, and vermilion rockfish. These data, combined with age estimates from analysis of otoliths and sex data from carcasses of filleted fish, hold great potential to generate a large amount of biological data that can be used in stock assessments. The methods outlined in this study can be used, for other species of rockfish, to implement a comprehensive program with the party boat fleet in California aimed at enhancing the amount of length-at-age and life history data available for stock assessments or other estimates of rockfish populations. Collaborative networks with available staff are in place and could make it possible for fish with fillet-only measurements to be processed immediately or to be frozen for processing later. Because our technique enables the calculation of the pre-fillet length, otoliths in fish carcasses can become another valuable source of biological data for stock assessments.

Our study results indicate the power of collaborative fisheries programs that involve scientists working directly with industry partners to produce data for fisheries management; of course, this study is not the first with findings that indicate the effectiveness of such programs (Wendt and Starr, 2009; Feeney et al., 2010; Yochum et al., 2011; Mason et al., 2020; Johnston et al., 2024). The Observer Program of the California Polytechnic State University has longstanding relationships with recreational anglers and party boat companies and crews in San Luis Obispo County (Stephens et al., 2006). These relationships were leveraged when developing the methods used in this study, and we found that party boat crews and recreational anglers generally were eager to help and curious about the data being collected. It is expected that the working relationship of the Observer Program with the community of anglers in San Luis Obispo County could provide a framework for other entities looking to establish such collaboration in other places. Cooperative relationships are critical to the success of any study designed to collect information from party boats. Anglers aboard party boats from Alaska to Baja California, Mexico, regularly catch rockfish, and the protocol described herein may allow researchers to add a significant amount of data that can be used in stock assessments and other efforts to estimate the abundance of rockfish populations.

Conclusions

Accurate and precise age, length, and sex data are critical components of stock assessments. Three measurement methods were tested to determine if there was a way to obtain a standardized post-fillet measurement from a carcass of a filleted rockfish. It was found that gonads can be identified, and sex was determined from the majority of carcasses of filleted fish. We also tested whether these data can be used to develop linear regression equations that allow the accurate calculation of pre-fillet length based on the measured post-fillet length of a fish carcass. The results of this study indicate that post-fillet elongate length is an easily incorporated and accurate predictor of pre-fillet length. Together with information from otoliths and gonads extracted from carcasses of filleted fish, the length information that can be collected through the protocol established in this study could form an extensive set of valuable length-frequency and life history data for historically data-poor or data-limited rockfish populations. The information from this study can be used by staff of government agencies, such as NOAA or the California Department of Fish and Wildlife, to determine the feasibility of establishing a program for collecting carcasses from the party boat fleet in California to enhance the amount of length-at-age and life history data available for stock assessments or other efforts to estimate abundance of rockfish populations.

Resumen

En los informes sobre las evaluaciones de las poblaciones de las especies de peces de roca de la costa oeste de Estados Unidos, se menciona con frecuencia la necesidad de disponer de datos biológicos adicionales que proporcionen estimaciones más precisas de la abundancia de la población. La mejora de las estimaciones de población es importante porque esos datos se utilizan para fijar las cuotas de capturas en esta costa del país. La flota de embarcaciones recreativas de alquiler del estado de California ha desembarcado históricamente grandes cantidades de especies de peces de roca; sin embargo, las embarcaciones de esta flota descartan los restos una vez extraídos los filetes de los peces. Estos restos podrían ser una valiosa fuente de datos sobre edad, longitud y sexo, si se utilizara un método de medición estandarizado para relacionar la talla posterior y previa al fileteado de los restos de peces. Para determinar la viabilidad de un programa de recolecta de restos de peces de roca para obtener datos biológicos, se capturaron especímenes de 4 especies de peces de roca en la costa central de California y se midieron antes y después del fileteado. Se estimaron con exactitud las longitudes previas al fileteo con base en la longitud estirada después del fileteo para el rocote azul (*Sebastes mystinus*), rocote amarillo (*S. carnatus*), rocote cobrizo (*S. caurinus*) y rocote bermejo (*S. miniatus*). Un alto porcentaje (87.5%) de los restos tenían gónadas identificables, un resultado afortunado porque la disponibilidad de datos sobre el sexo en los especímenes medidos es una consideración importante para las especies con crecimiento dimórfico. Esta nueva fuente de datos basada en la información procedente de los restos de los peces puede utilizarse para mejorar los datos sobre la talla a la edad y ciclo de vida, disponibles para las evaluaciones de poblaciones u otros estudios biológicos de las poblaciones de peces de roca.

Acknowledgments

We are grateful for the following individuals and groups for assisting with this project: J. Felton, I. Robbins, and members of the Dean E. Wendt Laboratory; members of Moss Landing Marine Laboratories and the National Marine Fisheries Service; Patriot Sportfishing, Stardust Sportfishing, Virg's Landing, and Morro Bay Landing and the crews of F/V *Patriot*, F/V *Avenger*, F/V *Fiesta*, F/V *Rita G*, F/V *Phenix*, F/V *Flying Fish*, F/V *Endeavor*, F/V *Huli Cat*, and F/V *Coral Sea*; and J. O'Leary, C. White, and students in the Fisheries Science and Resource Management class at California Polytechnic State University.

Literature cited

Aphalo, P. J., K. Slowikowski, and S. Mouksassi.
2023. ggpmisc: miscellaneous extensions to 'ggplot.' R package, vers. 0.5.5. [Available from website, accessed December 2023.]

Barnes, C. L., and R. M. Starr.
2018. Reproductive tactics of California halibut (*Paralichthys californicus*): combining spawning season, interspawning interval, and batch fecundity to estimate annual reproductive output for a multiple-batch spawning fish. CalCOFI Rep. 59:102–114.

Barnes, C. L., R. M. Starr, and P. N. Reilly.
2015. Growth, mortality, and reproductive seasonality of California halibut (*Paralichthys californicus*): a biogeographic approach. CalCOFI Rep. 56:110–118.

Cope, J., E. J. Dick, A. MacCall, M. Monk, B. Soper, and C. Wetzel.
2015. Data-moderate stock assessments for brown, China, copper, sharpchin, stripetail, and yellowtail rockfishes and English and rex soles in 2013, 247 p. Pac. Fish. Manag. Counc., Portland, OR. [Available from website.]

Dick, E. J., A. Berger, J. Bizzarro, K. Bosley, J. Cope, J. Field, L. Gilbert-Horvath, N. Grunloh, M. Ivens-Duran, R. Miller, et al.
2018. The combined status of blue and deacon rockfishes in U.S. waters off California and Oregon in 2017, 309 p. Pac. Fish. Manag. Counc., Portland, OR. [Available from website.]

Feeney, R. G., K. J. La Valley, and M. Hall-Arber.
2010. Assessing stakeholder perspectives on the impacts of a decade of collaborative fisheries research in the Gulf of Maine and Georges Bank. Mar. Coast. Fish. 2:205–216.

Frable, B. W., D. W. Wagman, T. N. Frierson, A. Aguilar, and B. L. Sidlauskas.
2015. A new species of *Sebastes* (Scorpaeniformes: Sebastidae) from the northeastern Pacific, with a redescription of the blue rockfish, *S. mystinus* (Jordan and Gilbert, 1881). Fish. Bull. 113:355–377.

Francis, R. I. C. C.
1990. Back-calculation of fish length: a critical review. J. Fish Biol. 36:883–902.

Gordon, D. A.
1994. Lingcod fishery and fishery monitoring in Southeast Alaska. Alsk. Fish. Res. Bull. 1(2):140–152.

Hansel, H. C., S. D. Duke, P. T. Lofy, and G. A. Gray.
1988. Use of diagnostic bones to identify and estimate original lengths of ingested prey fishes. Trans. Am. Fish. Soc. 117:55–62.

Hilborn, R., and C. J. Walters.
1992. Quantitative fisheries stock assessment: choice, dynamics and uncertainty, 570 p. Springer, Dordrecht, Netherlands.

Johnston, E. M., G. T. Waltz, R. Kosaka, E. M. Brauer, S. L. Ziegler, E. T. Jarvis Mason, H. S. Glanz, L. Zaragoza, A. N. Kellum, R. O. Brooks, et al.
2024. Participation in collaborative fisheries research improves the perceptions of recreational anglers towards marine protected areas. Front. Mar. Sci. 11:1330498.

Landa, J., E. Rodriguez-Marin, P. L. Luque, M. Ruiz, and P. Quelle.
2015. Growth of bluefin tuna (*Thunnus thynnus*) in the North-eastern Atlantic and Mediterranean based on back-calculation of dorsal fin spine annuli. Fish. Res. 170:190–198.

Love, M. S., P. Morris, M. McCrae, and R. Collins.
1990. Life history aspects of 19 rockfish species (Scorpaenidae: *Sebastes*) from the southern California Bight. NOAA Tech. Rep. NMFS 87, 38 p.

Love, M. S., M. Yoklavich, and L. Thorsteinson.
2002. The rockfishes of the northeast Pacific, 405 p. Univ. Calif. Press, Berkeley, CA.

Mason, E. T., A. N. Kellum, J. A. Chiu, G. T. Waltz, S. Murray, D. E. Wendt, R. M. Starr, and B. X. Semmens.
2020. Long-term participation in collaborative fisheries research improves angler opinions on marine protected areas. PeerJ 8:e10146.

Monk, M. H., E. J. Dick, J. C. Field, E. M. Saas, and T. L. Rogers.
2021. The status of vermilion rockfish (*Sebastes miniatus*) and sunset rockfish (*Sebastes crocotulus*) in U.S. waters off the coast of California north of Point Conception in 2021, 205 p. Pac. Fish. Manag. Counc., Portland, OR. [Available from website.]

Ralston, S., A. E. Punt, O. S. Hamel, J. D. DeVore, and R. J. Conser.
2011. A meta-analytic approach to quantifying scientific uncertainty in stock assessments. Fish. Bull. 109:217–231.

RStudio.
2021. RStudio: integrated development environment for R. RStudio Inc., Boston, MA. [Available from website, accessed September 2021.]

Schroeder, D. M., and M. S. Love.
2002. Recreational fishing and marine fish populations in California. CalCOFI Rep. 43:182–190.

Stephens, J., D. Wendt, D. Wilson-Vandenberg, J. Carroll, R. Nakamura, E. Nakada, S. Rienecke, and J. Wilson.
2006. Rockfish resources of the south central California coast: analysis of the resource from partyboat data, 1980–2005. CalCOFI Rep. 47:140–155.

Wendt, D. E., and R. M. Starr.
2009. Collaborative research: an effective way to collect data for stock assessments and evaluate marine protected areas in California. Mar. Coast. Fish. 1:315–324.

Wetzel, C. R., B. J. Langseth, J. M. Cope, and J. E. Budrick.
2021. The status of copper rockfish (*Sebastes caurinus*) in U.S. waters off the coast of California north of Point Conception in 2021 using catch and length data, 148 p. Pac. Fish. Manag. Counc., Portland, OR. [Available from website.]

Wickham, H., M. Averick, J. Bryan, W. Chang, L. D'Agostino McGowan, R. François, G. Grolemund, A. Hayes, L. Henry, J. Hester, et al.
2019. Welcome to the tidyverse. J. Open Source Softw. 4(43):1686.

Wise, H. M.
1980. The use of fish vertebrae in scats for estimating prey size of otters and mink. J. Zool. 192:25–31.

Yochum, N., R. M. Starr, and D. E. Wendt.
2011. Utilizing fishermen knowledge and expertise: keys to success for collaborative fisheries research. Fisheries 36:593–605.

Young, P. H.
1969. The California partyboat fishery 1947–1967. Calif. Dep. Fish Game, Fish Bull. 145, 62 p.

Fishery Bulletin

Guidelines for authors

Contributions published in *Fishery Bulletin* describe original research in marine fishery science, fishery engineering and economics, and marine environmental and ecological sciences (including modeling). Preference will be given to manuscripts that examine processes and underlying patterns. Descriptive reports, surveys, and observational papers may occasionally be published but should appeal to an audience outside the locale in which the study was conducted.

Although all contributions are subject to peer review, responsibility for the contents of papers rests upon the authors and not on the editor or publisher. *Submission of an article implies that the article is original and is not being considered for publication elsewhere.*

All submissions are subject to a double-blind review to remove the identity of author and reviewer during the review process.

Plagiarism and double publication are considered serious breaches of publication ethics. To verify the originality of the research in papers and to identify possible previous publication, manuscripts may be screened with plagiarism-detection software.

Manuscripts must be written in English; authors whose native language is not English are strongly advised to have their manuscripts checked by English-speaking colleagues before submission.

Artificial intelligence (AI), machine learning, or similar algorithmic tools should not be used to write or generate scientific content, including text, tables, and figures, for manuscripts submitted to *Fishery Bulletin*. Although some authors may use such tools to improve the readability or syntax of their manuscript, it must be done with extreme caution, and authors must review and edit the result. If such a tool is used, authors must declare the name of the tool, where it was used, and the purpose for which it was used in an "Artificial intelligence declaration" section after the "Acknowledgments" section. Authors remain accountable for all elements of their manuscript and should state that they take full responsibility for the content of their manuscript in the AI declaration.

Once a paper has been accepted for publication, online publication takes approximately 2 weeks.

There is no cost for publication in *Fishery Bulletin*.

Types of manuscripts accepted by the journal

Articles generally range from 20 to 30 double-spaced typed pages (12-point font) and describe an original contribution to fisheries science, engineering, or economics. Tables and figures are not included in this page count, but the number of figures should not exceed 1 figure for every 4 pages of text. Articles contain the following divisions: abstract, introduction, methods, results, discussion, and conclusions.

Notes are generally less than 10 double-spaced typed pages (12-point font), including the Literature cited section. Like articles, notes describe an original contribution to fisheries science. They follow a format similar to that for articles: abstract, introduction, methods, results, and discussion, but the results and discussion sections may be combined and a conclusions section should not be included. They should include no more than 2 figures or tables (2 of each would be too many). They are distinguished from full articles in that they report a noteworthy new observation or discovery—such as the first report of a new species, a unique finding, condition, or event that expands our knowledge of fisheries science, engineering, or economics—and do not require a lengthy discussion. Manuscripts on range extensions will not be considered.

Companion articles should be submitted together and are published together as a scientific contribution. Both articles should address a closely related topic and may be articles that result from a workshop or conference.

Review articles of exceptional quality may be considered occasionally for publication on a case-by-case basis. They address a timely topic that is relevant to aspects of fisheries science. They should include an abstract, but the format of the article, per se, will be up to the author. Please contact the scientific editor to discuss your ideas regarding a potential review article before embarking on such a project.

Perspective essays generally are less than 5 double-spaced typed pages (12-point font) and provide clarification of misused terms or misunderstood topics in fisheries science. Essays are accepted at the discretion of the scientific editor. Opinion pieces on policy will not be considered. They should include an abstract and a list of the literature cited, but no other sections should divide the article. Please contact the scientific editor to discuss your idea before making a submission.

Preparation of manuscript

Title page should include authors' full names, affiliations, mailing addresses, and the senior author's email address.

Abstract should be limited to 200 words (one-half typed page), state the main scope of the research, and emphasize the authors' conclusions and relevant findings. Do not review the methods of the study or list the contents of the paper. Because abstracts are circulated by abstracting agencies, it is important that they represent the research clearly and concisely.

General text must be typed in 12-point Times New Roman font throughout. A brief introduction should convey the broad significance of the paper; the remainder of the paper should be divided into the following sections: Materials and methods, Results, Discussion, Conclusions, and Acknowledgments. Headings within each section must be short, reflect a logical sequence, and follow the rules of subdivision (i.e., there can be no subdivision without at least 2 subheadings). The entire text should be intelligible to interdisciplinary readers; therefore, all acronyms, abbreviations, and technical terms should be written out in full and defined the first time they are mentioned. Abbreviations should be used sparingly because they are not carried over to indexing databases and slow readability for those readers outside a discipline. They should never be used for the main subject (e.g., species or method) of a paper.

For general style, follow the U.S. Government Publishing Office *Style Manual* (2016, available at website) and *Scientific Style and Format: the CSE Manual for Authors, Editors, and Publishers* (2014, 8th ed.) published by the Council of Science Editors. For scientific nomenclature, use the current edition of the American Fisheries Society's (AFS) *Common and Scientific Names of Fishes from the United States, Canada, and Mexico* and its companion volumes (*Crustaceans, Mollusks, Cnidaria and Ctenophora*, and *World Fishes Important to North Americans*). For species not found in the previously mentioned AFS publications and for more recent changes in nomenclature, use the Integrated Taxonomic Information System (ITIS, available at website), or, secondarily, the California Academy of Sciences *Catalog of Fishes* (available at website) for species names not included in ITIS. Common (vernacular) names of species should be lowercase. Citations must be given for the identification of specimens. For example, "Fish species were identified according to Collette and Klein-MacPhee (2002); sponges were identified according to Stone et al. (2011)."

Dates should be written as follows: 11 November 2018. Measurements should be expressed in metric units, for example, "58 metric tons (t);" if other units of measurement are used, please make this fact explicit to the reader. Use numerals, not words, to express whole and decimal numbers in the general text, tables, and figure captions (except at the beginning of a sentence). For example, "We considered 3 hypotheses. We collected 7 samples in this location." Use American spelling. Refrain from using the shorthand slash (/), an ambiguous symbol, in the general text.

Cite all software, special equipment, and chemical solutions used in the study within parentheses in the general text, including the version number, company name, and the city and state (or nation) of the company headquarters, for example, "SAS, vers. 9.4 (SAS Institute Inc., Cary, NC)."

Word usage and grammar that may be useful are the following:

- *Aging*
  For our journal, the word *aging* is used to mean both age determination and the aging process (senescence). Authors should make clear which meaning is intended where ambiguity may arise.

- *Fish and fishes*
  The plural of the word fish (a collective noun that implies individuals without regard to species) is *fish*.
  Example: The *fish* were collected by trawl net.
  Example: The numbers of *fish* collected that season were less than the numbers from previous years.

  The plural for *fish species* is *fishes* (a contrived plural used by taxonomists to mean several or more *fish species*) or one can use *fish species* (which is preferred in this journal for clarity across disciplines).
  Example: The *fishes* of Puget Sound [biodiversity is implied] or
  Example: The *fish species* of Puget Sound [preferred plural for clarity across disciplines].

- *Crab and crabs, squid and squids, etc.*
  The plural of the word *crab* (i.e., many individuals without regard to species) is *crab*.
  Example: The crab were sorted by weight.
  Example: Many red king *crab* were dying [Many individuals of one species of crab.]

  The plural of *crab species* is *crabs* (a word used by taxonomists) or *crab species* (the latter is preferred in this journal for clarity).
  Example: These *crabs* were selected for treatment. [Different crab species are implied.]
  Example: These *crab species* were selected for treatment. [Preferred word choice for clarity.]
  Example: Snow *crabs* are found throughout the North Pacific Ocean and Bering Sea. [There are 2 species of snow crab; therefore the word *crabs* can be used here.]
  Example: *Two species* of snow *crab* are found throughout the North Pacific Ocean and Bering Sea. [Preferred usage for clarity.]
  Example: Three crabs were selected for treatment. [3 species of crab are implied.]
  Example: Three crab species were selected for treatment. [Preferred word choice for clarity.]

- We use *fisherman* and *fishermen*, not *fisher* and *fishers*, in this journal. One can always use crew member, vessel operator, and angler (the latter for recreational fishing).

- *The definite article with common names of species*
  When the singular common name of a species represents the entire class or group to which it belongs, use the definite article.
  Example: Only one species of the genus *Salmo* is found in the Atlantic Ocean—*the* Atlantic salmon (*Salmo salar*).
  Example: The sonic emissions of *the* bottlenose dolphin are complex.

  For plural common names, this rule does not apply.
  Example: Chinook salmon are found throughout the Pacific Ocean.
  Example: Bottlenose dolphins are found in temperate and tropical waters.

- *Sex*
  For the meaning of male and female, use the word *sex*, not *gender*. Do not write, "fish were sexed." Write, "sex was determined."

- *Participles*
  As adjectives, participles must modify a specific noun or pronoun.
  Example: Using mark-recapture methods, these scientists determined the size of the population. [Correct. The participle *using* modifies the word *scientists*.]
  Example: These scientists, based on the collected data, concluded that the mortality rate of these fish had increased. [Incorrect. The scientists were not based on the collected data.]
  Example: These scientists concluded, on the basis of collected data, that the mortality rate of these fish had increased. [Correct. The offending participle has been eliminated and an adverbial phrase modifies the verb *concluded*.]

Equations and mathematical symbols should be set from a standard mathematical program (MathType or Equation Editor). Equations formatted in LaTex are not acceptable. For mathematical symbols in the general text (α, χ^2, π, $\pm$, etc.), use the symbols provided by the MS Word program and italicize all variables, except those variables represented by Greek letters and the superscript and subscript parts of variables and expressions. Do not use photo mode when creating these symbols in the general text, and do not cut and paste equations, letters, or symbols from a different software program.

Number equations (if there are more than one) for future reference by scientists; place the number within parentheses at the end of the first line of the equation.

Literature cited section comprises published works and those accepted for publication (in press) in peer-reviewed journals. Follow the name and year system for citation format in this section (i.e., citations should be listed alphabetically by the authors' last names, and then by year if there is more than one citation by the same author. A list of abbreviations for citing journal titles can be found on our website.

Authors are responsible for the accuracy and completeness of all citations. Avoid the use of multiple citations when a single citation sufficiently supports a statement; cite the work that first reported the information that supports a statement, not all of the subsequent works. Literature citation format: Authors (last name, followed by initials for first name and, if given, middle name of first author; then list names of additional authors with initials before last names). Year. Title of article. Abbreviated title of the journal in which it was published. Always include either the range of page numbers (for a journal article) or a total number of pages (for a book or other type of publication). List a sequence of citations in the general text chronologically, for example, "(Smith, 1932; Green, 1998; Smith and Jones, 2015)."

Acknowledgments should be no more than 6 lines of text. Only those who have contributed in an outstanding way should be acknowledged by name. For recognition of other persons or groups, use a general term, such as *crew*, *observers*, or *research coordinators*, and do not include names with these terms.

Digital object identifier (doi) code ensures that a publication has a permanent location online. A doi link (which may include a doi code) should be included at the end of citations of published literature. Authors are responsible for submitting accurate doi links. Faulty links will be deleted at the page-proof stage.

Footnotes are used for all documents that have not been formally peer reviewed and for observations and personal communications, but these types of references should be cited sparingly in manuscripts submitted to the journal.

All reference documents, administrative reports, internal reports, progress reports, project reports, contract reports, personal observations, personal communications, unpublished data, manuscripts in review, and council meeting notes are footnoted in 10-point font and placed at the bottom of the page on which they are first cited. Footnote format is the same as that for formal literature citations. A link to the online source (e.g., [Available from http://www... , accessed July 2017.]), or the mailing address of the agency or department holding the document, should be provided so that readers may obtain a copy of the document.

Tables are often overused in scientific papers; it is seldom necessary to present all the data associated with a study. Tables should not be excessive in size and must be cited in numerical order in the text. Headings should be short but ample enough to allow the table to be intelligible on its own.

All abbreviations and unusual symbols must be explained in the table legend. Other incidental comments may be footnoted with numeral footnote markers. Use asterisks only to indicate significance in statistical data. Do not put a table legend on a page separate from the table; place the legend above the table. *Do not submit tables in photo mode.*

- Note probability with a capital, italic *P*.
- Provide a zero before all decimal points for values less than one (e.g., 0.07).
- Round all values to 2 decimal points.
- Use a comma in numbers of 5 digits or more (e.g., 13,000 but 3000).

Figures must be cited in numerical order in the text. Graphics should aid in the comprehension of the text, but they should be limited to presenting patterns rather than raw data. The number of figures should not exceed 1 figure for every 4 pages of text.

Figure legends should explain all symbols and abbreviations seen in the figure and should be double spaced on a separate page at the end of the manuscript.

Line art and halftone figures should be saved at resolutions >600 dots per inch (dpi) and >300 dpi, respectively. Color is allowed in figures to show morphological differences among species (for species identification), to show stain reactions, to show gradations (such as those of temperature and salinity within maps), and to distinguish between numerous lines and symbols in graphs. Figures approved for color should be saved in CMYK format.

All figures must be submitted as PDF, TIFF, or EPS files.

- Capitalize only the first letter of the first word and proper nouns in all labels within figures.
- Do not use overly large font sizes for labels in maps and for axis labels in graphs.
- Use the same point size for all labels, except for panel labels (e.g., **A**), which should be slightly larger than other labels (e.g., 11 point versus 8 point).
- Use a sans serif font for all labels. Panel labels (e.g., **A**), however, should be in Times New Roman font.
- Do not use bold fonts or bold lines in figures. Do not use italic fonts. Exceptions include use of italic fonts for labels of bodies of water in maps and a bold font for panel labels (e.g., **A**).
- Do not place outline rules around graphs.
- Do not include vertical and horizontal lines in the background of graphs. Ticks for values on the x-axis and y-axis will suffice.
- Place a north arrow and label degrees latitude and longitude (e.g., 170°E) in all maps. If scale of map requires more than degrees, use degrees minutes, not decimal degrees.
- Place panel labels (e.g., **A**, **B**, **C**) within the upper-left area of each graph or photo in a multi-panel figure, from left to right, then top to bottom. If the letter is not visible against a dark background, put a white box behind it. Do not use white labels.
- Avoid placing labels vertically or diagonally. Y-axis labels can be vertical. Words in horizontal labels can be stacked vertically to fit.
- Use symbols, shading, or patterns (not clip art) in maps and graphs.
- For scale bars in maps, use kilometers. Use the label *km* or *kilometers* (lowercased).

Supplementary materials that are considered essential, but are too large or impractical for inclusion in a paper (e.g., metadata, figures, tables, videos, and websites), may be provided at the end of an article. These materials are subject to the editorial standards of the journal. A URL to the supplementary material and a brief explanation for including such material should be sent at the time of initial submission of the paper to the journal.

- **Metadata, figures, and tables** should be submitted in standard digital format (MS Word or PDF file) and should be cited in the general text, for example, as "... was determined (Suppl. Table 3, Suppl. Fig. 1)."
- **Websites** should be cited with a URL in the general text.
- **Videos** must not be larger than 30 MB to allow a swift technical response for viewing the video. Authors should consider whether a short video uniquely captures what text alone cannot capture for the understanding of a process or behavior under examination in the article. Supply an online link to the location of the video.

Copyright law does not apply to *Fishery Bulletin*, which falls within the public domain. However, if an author reproduces any part of an article from *Fishery Bulletin*, reference to source is considered correct form (e.g., Source: Fish. Bull. 117:105).

Failure to follow these guidelines and failure to correspond with editors in a timely manner will delay publication of a manuscript.

Submission of manuscript

Submit a manuscript online at the ScholarOne Manuscripts website for *Fishery Bulletin*. Commerce Department authors must provide proof of internal clearance of their manuscripts with either a completed and signed NOAA Form 25-700 or a copy of the clearance email from the Research Publication Tracking System. For further details on electronic submission, please contact the associate editor, Cara Mayo, at

cara.mayo@noaa.gov.

When requested, the text and tables should be submitted in MS Word format. Each figure should be sent as a separate PDF, TIFF, or EPS file. Send a copy of a figure in the original software if conversion to any of these formats yields a degraded version of the figure.

Questions? If you have questions regarding these guidelines, please contact the managing editor, Kathryn Dennis, at

kathryn.dennis@noaa.gov.

Questions regarding manuscripts under review should be addressed to Associate Editor Cara Mayo.

Fishery Bulletin

Subscription form

Superintendent of Documents **Publications** Order Form

*5178

☐ YES, please send me the following publications:

____ Subscriptions to *Fishery Bulletin*
for $32.00 per year ($44.80 foreign)

The total cost of my order is $ ________ . Prices include regular domestic postage and handling and are subject to change.

(Company or Personal Name) (Please type or print)

(Additional address/attention line)

(Street address)

(City, State, ZIP Code)

(Daytime phone including area code)

(Purchase Order No.)

Charge your order.

IT'S EASY!

VISA

MasterCard

Please Choose Method of Payment:

☐ Check payable to the Superintendent of Documents

☐ GPO Deposit Account ☐☐☐☐☐☐☐–☐

☐ VISA or MasterCard Account

☐☐☐☐☐☐☐☐☐☐☐☐☐☐☐☐☐☐☐☐

☐☐☐☐ (Credit card expiration date)

To fax your orders (202) 512-2104

(Authorizing Signature)

Mail to: Superintendent of Documents
P.O. Box 979050, St. Louis, Missouri 63197
Tel. no. (U.S. callers): 866-512-1800
Tel. no. (International callers): 1-202-512-1800

Thank you for your order!

Also available online at
https://bookstore.gpo.gov/products/fishery-bulletin
email: ContactCenter@gpo.gov

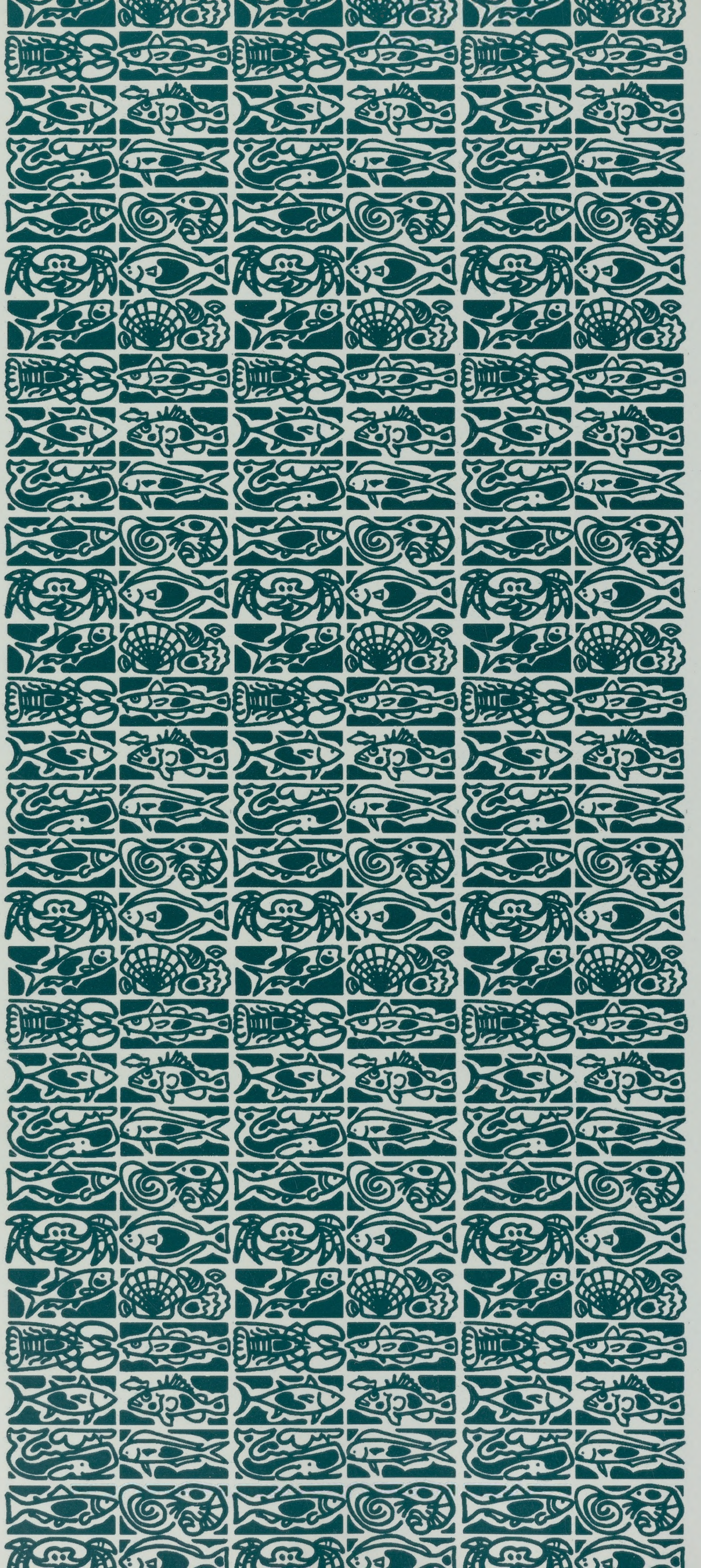

SMITHSONIAN LIBRARIES
3 9088 02066 7960